CR-152160
(D. Koenig)

[redacted]

(NASA-CR-152160) A CORRELATION METHOD TO PREDICT THE SURFACE PRESSURE DISTRIBUTION ON AN INFINITE PLATE FROM WHICH A JET IS ISSUING (Nielsen Engineering and Research, Inc.) 121 p HC A06/MF A01 CSCL 01A G3/02

N81-21019

Unclas
21122

NIELSEN ENGINEERING AND RESEARCH, INC.

OFFICES: 510 CLYDE AVENUE / MOUNTAIN VIEW, CALIFORNIA 94043 / TELEPHONE (415) 968-9457

COPY NO. 25

A CORRELATION METHOD TO PREDICT THE SURFACE PRESSURE DISTRIBUTION ON AN INFINITE PLATE FROM WHICH A JET IS ISSUING

By

Stanley C. Perkins, Jr.
and
Michael R. Mendenhall

NEAR TR 160

May 1978

Prepared under Contract No. NAS2-9509

by

NIELSEN ENGINEERING & RESEARCH, INC.
Mountain View, California

for

NATIONAL AERONAUTICS AND SPACE ADMINISTRATION
Ames Research Center

1. Report No.	2. Government Accession No.	3. Recipient's Catalog No.
NASA CR-152,160		

4. Title and Subtitle	5. Report Date
A Correlation Method to Predict the Surface Pressure Distribution on an Infinite Plate from which a Jet is Issuing	May 1978
	6. Performing Organization Code 409/C
7. Author(s) Stanley C. Perkins, Jr. and Michael R. Mendenhall	8. Performing Organization Report No. NEAR TR-160
	10. Work Unit No.
9. Performing Organization Name and Address Nielsen Engineering & Research, Inc. 510 Clyde Avenue Mountain View, California 94043	11. Contract or Grant No. NAS2-9509
	13. Type of Report and Period Covered Contractor Report
12. Sponsoring Agency Name and Address NASA Ames Research Center Moffett Field, California 94035	14. Sponsoring Agency Code

15. Supplementary Notes

Ames Technical Monitors, David G. Koenig and Donald L. Ciffone

16. Abstract

A correlation method to predict pressures induced on an infinite plate by a jet issuing from the plate into a subsonic free stream has been developed. The complete method consists of an analytical method which models the blockage and entrainment properties of the jet and a correlation which accounts for the effects of separation. The method has been developed for jet velocity ratios up to ten and for radial distances up to five diameters from the jet. Correlation curves and data comparisons are presented for jets issuing normally from a flat plate with velocity ratios one to twelve. Also, a list of references which deal with jets in a crossflow is presented in the Appendix.

17. Key Words (Suggested by Author(s))	18. Distribution Statement
Subsonic crossflow Jet in a crossflow Pressure distribution V/STOL	Unclassified-Unlimited

19. Security Classif. (of this report)	20. Security Classif. (of this page)	21. No. of Pages	22. Price*
Unclassified	Unclassified	117	

*For sale by the National Technical Information Service, Springfield, Virginia 22161

TABLE OF CONTENTS

PRECEDING PAGE BLANK NOT FILMED

A CORRELATION METHOD TO PREDICT THE SURFACE PRESSURE DISTRIBUTION ON AN INFINITE PLATE FROM WHICH A JET IS ISSUING

Stanley C. Perkins, Jr. and Michael R. Mendenhall
Nielsen Engineering & Research, Inc.

SUMMARY

A correlation method to predict pressures induced on an infinite plate by a jet issuing from the plate into a subsonic free stream has been developed. The complete method consists of an analytical method which models the blockage and entrainment properties of the jet and a correlation which accounts for viscous effects. The method has been developed for jet velocity ratios up to ten and for radial distances up to five diameters from the jet. Correlation curves and data comparisons are presented for jets issuing normally from a flat plate with velocity ratios one to twelve. Also, a list of references which deal with jets in a crossflow is presented in the Appendix.

INTRODUCTION

During the past several years there has been an increased interest in V/STOL configurations which utilize lift jet engines mounted in wings and/or the fuselage. While these configurations usually exhibit improved lift characteristics, the interaction of the jet and the free stream can result in undesirable aerodynamic loading characteristics influencing lift and stability. This situation arises during transition from hovering to horizontal flight, when the configuration has attained some forward speed but must still rely on the jet for lift. Investigation of the effects of a lift jet on the pressure distribution on an infinite flat plate, as presented in this report, is a first step in understanding the jet/wing and jet/fuselage interference problem.

Experimental investigations on jet interference effects on an infinite flat plate (refs. 1-5) have shown that the jet produces a region of positive pressure upstream of the jet and regions of negative pressure downstream and to each side of the jet. The negative pressure field has been found to intensify as the jet velocity ratio is increased. Oil film tests, such as those done by Mosher (ref. 5), show a strong viscous region immediately downstream of the jet. It is in this viscous dominated region that pressures on the plate are difficult to predict.

In recent years, several theoretical and empirical methods to predict jet induced pressures on a flat plate have been developed. One of the most successful of these methods is that of Dietz (ref. 6) which utilizes a sink-vortex pair representation of the jet. Data comparisons are good in the regions ahead and to the side of the jet, but poor in the region behind the jet. This method requires knowledge of certain vortex properties, such as vortex strength, spacing, and core size, which can only be obtained from detailed velocity measurements in the jet plume. Another method is the sink-doublet-vortex pair method of Yeh (ref. 7). This method accounts for jet entrainment using a sink distribution, jet blockage using a doublet distribution, and the formation of the vortex pair. Data comparisons are good in regions ahead of the jet and fair to poor for the regions to the side and behind the jet. Other recent methods include a vortex lattice method (ref. 8), a finite-element potential flow method (ref. 9), and a method which utilizes matched asymptotic expansions (ref. 10). Data comparisons using these methods are for the most part good upstream of the jet and poor to the side and downstream of the jet.

Accurate prediction of the pressure distribution on the plate in the viscous region of the jet was not obtained by any of the aforementioned methods. Since purely analytic methods have not been successful in predicting the viscous effects of the jet, an empirical approach is suggested.

The pressure prediction method presented in this report consists of an analytical model and an empirical correlation factor to account for viscous effects. The analytical model utilizes the sink distribution of reference 7 to represent entrainment effects and a distribution of vortex quadrilateral panels on the jet boundary to represent blockage effects. The jet boundary and position are determined from empirical observations. The viscous correction factor is obtained from a correlation of the difference between analytically predicted surface pressures and measured results.

The development of the correlation factors for jets issuing normal to flat plates is presented in this report, and predicted pressure distributions are compared with experimental data from several sources. Also included are normal-force and pitching-moment coefficients on finite plates for selected jet velocity ratios. Recommendations for improving the present correlation method are also discussed.

SYMBOLS

A_i	area of sector or segment of circular flat plate, see figure 18
A_{max}	total area of circular flat plate, πr_{max}^2
a	half width of a quadrilateral vortex ring, see sketch 1
b	half-width of the jet mixing region, see figure 1; also half-height of a quadrilateral vortex ring, see sketch 1
C_m	pitching-moment coefficient, $-\frac{1}{r_{max}A_{max}}\sum_{i=1}^{n} C_{p_i}A_i x_{m_i}$, see figure 18
C_n	normal-force coefficient, $-\frac{1}{A_{max}}\sum_{i=1}^{n} C_{p_i}A_i$, see figure 18
C_p	pressure coefficient, $\frac{p - p_\infty}{q_\infty}$
C_{p_i}	pressure coefficient at area centroid of sector or segment of circular flat plate
D	jet diameter at the exit plane, see figure 1
$\vec{F}_m$	influence coefficient for velocity at a point induced by a vortex quadrilateral, equation (6)
L	length of jet initial region
ℓ	distance from leading edge of plate to center of jet
M_j	Mach number of jet at the exit plane
m	jet velocity ratio, V_j/V_∞
$\vec{n}$	unit normal at a point, see figure 3
p	static pressure
Q_a	sink intensity, volume per unit time
q_a	local sink intensity, volume per unit time
q_a'	nondimensional sink intensity, $q_a/V_\infty D$
q_∞	dynamic pressure, $\frac{1}{2}\rho V_\infty^2$
Re_D	Reynolds number based on jet diameter at the exit plane, $\rho_\infty V_\infty D/\mu_\infty$

Re_ℓ	Reynolds number based on distance from leading edge of plate to center of jet, $\rho_\infty V_\infty \ell/\mu_\infty$
r	radial distance along the plate from the center of the jet to any field point on the plate
r_a	vector from a sink to each field point, $\sqrt{(x_j - x_a)^2 + (y_j - y_a)^2 + (z_j - z_a)^2}$
r_{max}	radius of the circular plate (used in normal force and pitching moment calculations), see figure 18
$(r/D)_{max}$	maximum radial position at which data is recorded
r_o	jet radius at the exit plane
s_a	curve length of the jet axis
$\vec{s}$	vector defining magnitude and direction of one side of a vortex ring, see sketch 2
t	local jet width in X-Y plane, see figure 1
$\vec{U}$	velocity vector induced by a vortex element, equation (8)
U_x, U_y, U_z	velocity components due to entrainment as determined in the jet coordinate system
u, v, w	velocity components in the X, Y, and Z directions, respectively
V_j	jet velocity at the exit plane
V_m	local centerline velocity of the jet
$\vec{V}_\Gamma$	velocity induced by a series of vortex quadrilaterals, equation (6)
V_∞	constant free-stream velocity
X, Y, Z	plate coordinate system fixed at the center of the jet exit plane, positive X is upstream
x_a, y_a, z_a	coordinates of the jet axis in the jet coordinate system
x_j, y_j, z_j	jet coordinate system fixed at center of the jet exit plane, positive x_j is downstream
x_{m_i}	local moment arm of area A_i, see figure 18
z_a'	normalized vertical coordinate of jet axis, z_a/D

SYMBOLS (Concluded)

α	local slope of jet centerline; dz_j/dx_j, $\alpha = \delta_j$ at exit plane, see figure 1
β	polar angle, measured clockwise from the positive X-axis in the plate X-Y plane, see figure 1
Γ_m	strength of a vortex quadrilateral
$(\Delta C_p)_{viscous}$	correlation increment of pressure coefficient
δ_j	initial inclination angle of jet centerline, measured from the positive X-axis in the X-Z plane, $\delta_j = 90° - \theta$; see figure 1
θ	initial inclination angle of jet centerline, measured from the positive z_j axis in the x_j-y_j plane, $\theta = 0°$ for a jet issuing normal to the free stream, see figure 1
μ_∞	absolute viscosity of free stream
ρ_∞	free-stream density
σ	fraction of length of one side of a vortex ring, see sketch 2
ϕ	potential as determined in the jet coordinate system

<u>Subscripts</u>

a	jet centerline quantity
max	maximum value
∞	free-stream quantity

APPROACH

Figure 1 shows a sketch of an expanding jet of initial velocity V_j emerging from an infinite plate at initial inclination angle θ into a subsonic crossflow of velocity V_∞. It has been observed that the jet centerline path depends on the jet velocity ratio V_j/V_∞ and inclination angle θ, and the jet expansion rate depends on V_j/V_∞. The overall effect of the jet on the plate is to produce a region of positive pressures upstream of the jet and a region of negative pressures laterally and downstream of the jet. This region of influence of the jet generally extends no further than five jet diameters from the center of the jet.

Most theoretical pressure results tend to compare well with data in the region $0° \leq \beta < 90°$, where viscous effects are small. The more successful methods may give good results up to $\beta = 120°$, but downstream of this angle the viscous effects are strong and present theoretical methods cannot predict plate pressures accurately.

One approach to the problem of predicting pressures in a viscous region is to correlate the pressure difference between analytical results without viscous effects and available data. Assuming such a correlation can be made, the pressure coefficient at each point on the plate can be expressed as:

$$C_p = C_p\Big|_{\text{potential}} + \Delta C_p\Big|_{\text{viscous}} \tag{1}$$

where $\Delta C_p\Big|_{\text{viscous}}$ is the correlation result which represents viscous effects. The potential portion of the above equation is calculated using the Bernoulli equation in the following form

$$C_p = 1 - \left(\frac{V_\infty + u}{V_\infty}\right)^2 - \left(\frac{v}{V_\infty}\right)^2 \tag{2}$$

Details of the jet model and the pressure correlation are presented in the following sections.

Jet Model

Details concerning the specification of the jet centerline path, the blockage and entrainment models, and the spreading rate of the jet are presented in the following sections.

Centerline shape.- The path of the jet centerline is specified using the empirical relation developed by Margason (ref. 11). This relation was obtained by correlating results from several experimental tests and is given as:

$$\frac{x_j}{D} = \frac{1}{4\sin^2\delta_j}\left(\frac{V_\infty}{V_j}\right)^2\left(\frac{z_j}{D}\right)^3 + \frac{z_j}{D}\cot\delta_j \tag{3}$$

The centerline shape given by equation (3) compared well with jet wake vapor flow visualization data for several different velocity ratios throughout the inclination angle range of interest ($0° \leq \delta_j \leq 90°$), and it also is in good agreement with other methods. Figure 1 shows a sketch of the jet exhausting from the plate at inclination angle δ_j in the jet coordinate system. Figure 2 shows centerline shapes for velocity ratios 2.2, 3.9, 6.1 and 10.0 as given by equation (3) with $\delta_j = 90°$.

Blockage model.- A jet exhausting from an infinite plate into a subsonic free stream has been observed to exhibit a displacement effect as if the jet boundary were behaving as a solid surface, particularly near the surface of the plate. Some discussion of this phenomenon is presented in references 7 and 10. The effect of the solid jet boundary is obtained by representing the specified wake surface by a series of vortex quadrilateral panels on which a boundary condition of flow tangency is enforced. A description of the vortex quadrilateral panel blockage model follows.

The boundary of the jet wake, specified by the centerline path and the wake radius along the centerline, is divided into length segments as illustrated in figure 3. Each length segment is further divided into a number of circumferential segments. A slice through the wake, normal to the centerline, shows the circular cross section wake to be represented by a series of straight segments. The control point on each panel is located at the centroid of the panel, and the vector $\vec{n}$ is the unit normal to the panel, positive when directed outward. The boundary condition satisfied at each control point is

$$\vec{V} \cdot \vec{n} = 0 \tag{4}$$

where

$$\vec{V} = \vec{V}_\infty + \vec{V}_\Gamma \tag{5}$$

The second term of equation (5), $\vec{V}_\Gamma$, is the velocity induced at a panel control point by all vortex quadrilateral panels making up the blockage model. This term can be written as

$$\vec{V}_\Gamma = \sum_{m=1}^{M} \frac{\Gamma_m}{4\pi} \vec{F}_m \tag{6}$$

Thus equation (4) at each control point becomes

$$\vec{n} \cdot \sum_{m=1}^{M} \frac{\Gamma_m}{4\pi} \vec{F}_m = - \vec{V}_\infty \cdot \vec{n} \tag{7}$$

which is a set of M linear simultaneous equations in terms of the M unknown vortex quadrilateral strengths, Γ_m. Note that $\vec{F}_m$ is the influence coefficient for the velocity induced at a control point by the quadrilateral vortex ring Γ_m.

The velocity vector, at a field point, induced by a single quadrilateral vortex ring is described in reference 12. The equations are reproduced here for convenience. Consider a single quadrilateral vortex ring as shown in sketch 1.

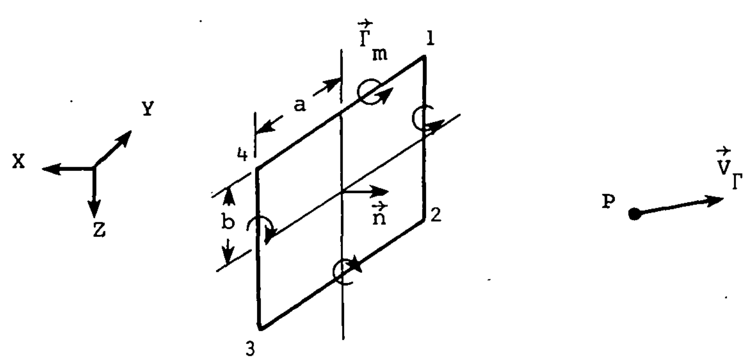

Sketch 1.- Quadrilateral vortex ring

According to the sign convention chosen for the jet model, a positive Γ_m is indicated in the above sketch. Consider now the contribution of side

1-2 to the velocity at point P. Sketch 2, also from reference 12, illustrates a single side of the vortex ring and identifies the parameters required for the derivation of the velocity equations.

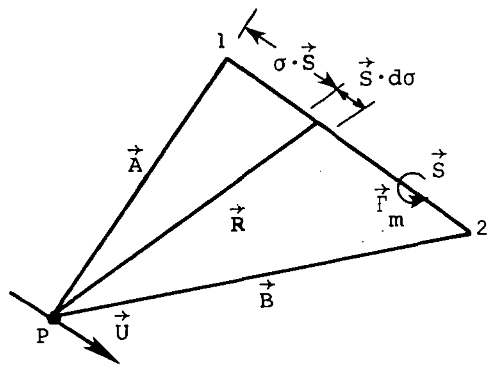

Sketch 2.- Vortex element

The velocity vector at point P is

$$\vec{U} = \frac{1}{4\pi} \int_{\vec{A}}^{\vec{B}} \frac{\vec{R} \times \Gamma \overrightarrow{dS}}{|\vec{R}|^3} \tag{8}$$

where Γ is the density of vorticity per unit length.

$$\vec{R} = \vec{A} + \sigma\vec{S} \tag{9}$$

$$\overrightarrow{dS} = \vec{S} d\sigma \tag{10}$$

$$\vec{U} = u\vec{i} + v\vec{j} + w\vec{k} \tag{11}$$

The resultant velocity at point P, from equation (7), is

$$\vec{U} = \frac{\Gamma_m}{4\pi} \frac{\vec{A} \times \vec{B}}{(\vec{A} \times \vec{B}) \cdot (\vec{A} \times \vec{B})} \left[|\vec{A}| + |\vec{B}| \right] \left[1 - \frac{\vec{A} \cdot \vec{B}}{|\vec{A}| \ |\vec{B}|} \right] \tag{12}$$

as developed in reference 12. Let

$$\left. \begin{aligned} \vec{A} &= (X_1 - X_P)\vec{i} + (Y_1 - Y_P)\vec{j} + (Z_1 - Z_P)\vec{k} \\ \vec{B} &= (X_2 - X_P)\vec{i} + (Y_2 - Y_P)\vec{j} + (Z_2 - Z_P)\vec{k} \end{aligned} \right\} \tag{13}$$

The total velocity at P, $\vec{V}_\Gamma$, induced by a single quadrilateral vortex ring is obtained by summing the contribution from equation (8) for the four sides of the ring. A summation over all the panels representing the jet surface will result in the velocity induced at a point, P, by the complete blockage model.

As with all finite panel methods, the representation of the flow around a solid body is better the further the point of interest is from the body. For practical problems of interest in this work, that is, flow around circular cross section jets with small diameters compared to their length, a good rule of thumb is that the point of interest should not be nearer to the surface than one panel width. This has been verified for the flow around a cylinder. The present blockage model was used to represent a long, straight cylinder ($L/D \simeq 10$) with varying numbers of panels on its circumference. The induced velocity in the plane normal to the cylinder axis was compared with the exact potential flow around a two-dimensional cylinder. Considering a minimum of six and a maximum of twenty panels around the cylinder, the panel method was in excellent agreement with the exact results so long as the comparisons were made farther than one panel width from the surface. All results presented in this report were obtained using twenty panels around the circumference unless otherwise noted.

The predicted flow fields are insensitive to the length of the panel so long as the panel aspect ratio (height/width) is within reasonable limits. In the region where the flow field is to be calculated, the panel aspect ratio is specified to be between one and four. On extreme portions of the surface which are a large distance from the flow field points, the panel aspect ratio can be much larger without affecting predicted results.

Entrainment model.- A jet exhausting from an infinite plate into a subsonic free stream will entrain air from the free stream and accelerate it in the direction of the jet. The induced flow external to the jet boundary can be represented in potential theory by sinks distributed along the jet axis. One approach to this method of modeling entrainment was developed by Yeh (ref. 7) and is described herein.

The potential of a three-dimensional sink is given as:

$$\phi = \frac{1}{4\pi} \frac{Q_a}{r_a} \tag{14}$$

where Q_a is the sink intensity and r_a is the vector from the sink to each field point. If the sink distribution lies on the jet axis, the potential can be found by integrating a variable sink intensity over the length of the semi-infinitely-long jet axis. The expression for the potential becomes

$$\phi(x_j, y_j, z_j) = \frac{1}{4\pi} \int_0^\infty \frac{q_a ds_a}{\left[(x_j - x_a)^2 + (y_j - y_a)^2 + (z_j - z_a)^2\right]^{1/2}} \tag{15}$$

where q_a is the local sink intensity and s_a is the curve length along the jet axis. In order to obtain velocity components, the potential is differentiated with respect to each coordinate direction. These expressions are

$$U_x = -\frac{1}{4\pi} \int_0^\infty \frac{(x_j - x_a) q_a ds_a}{\left[(x_j - x_a)^2 + (y_j - y_a)^2 + (z_j - z_a)^2\right]^{3/2}} \tag{16}$$

$$U_y = -\frac{1}{4\pi} \int_0^\infty \frac{(y_j - y_a) q_a ds_a}{\left[(x_j - x_a)^2 + (y_j - y_a)^2 + (z_j - z_a)^2\right]^{3/2}} \tag{17}$$

$$U_z = -\frac{1}{4\pi} \int_0^\infty \frac{(z_j - z_a) q_a ds_a}{\left[(x_j - x_a)^2 + (y_j - y_a)^2 + (z_j - z_a)^2\right]^{3/2}} \tag{18}$$

where U_x, U_y, and U_z are the velocity components in the x_j, y_j, and z_j directions, respectively.

Yeh describes the deflected jet in a crossflow as being mainly characterized by two opposed lateral vortices which increase in intensity along the jet. The local sink intensity, according to Keffer's findings (ref. 13), increases gradually with the growth of the vortex formation to a maximum in the main region (which Yeh defines as: $z_a/D \geq 0.35\ V_j/V_\infty$) and then decreases in the region where there is no relative axial velocity between the jet and the free-stream flow. Yeh approximates this sink distribution by assuming an equation of the form:

$$q_a' = \frac{q_a}{V_\infty D} = ae^{bz_a' - c(z_a')^2} \tag{19}$$

where a, b, and c are functions of V_j/V_∞ and z_a' and are defined as follows:

$$a = (q_a')_{z_a'=0} \tag{20}$$

$$b = 2c(z_a')_{q_a'=(q_a')_{max}} \tag{21}$$

$$c = \frac{\ell n\left(\frac{(q_a')_{max}}{a}\right)}{(z_a')^2_{q_a'=(q_a')_{max}}} \tag{22}$$

By use of empirical correlation, Yeh arrives at the following expressions for a, $(q_a')_{max}$, and $(z_a')_{q_a'=(q_a')_{max}}$.

$$a \approx 0.3096(V_j/V_\infty) - 0.0094(V_j/V_\infty)^2 - 0.6752 \tag{23}$$

$$(q_a')_{max} \approx 0.0106(V_j/V_\infty)^2 + 0.4323(V_j/V_\infty) - 0.7971 \tag{24}$$

$$(z_a')_{q_a'=(q_a')_{max}} = 2.24(V_j/V_\infty) - 3.615 \tag{25}$$

Substituting these coefficients into equation (19) for q_a', an expression for the local sink intensity as a function of z_a is obtained. Since the induced velocities are obtained by integrating equations (16), (17), and (18) along the jet axis, and since the distance along the axis is a function of z_a, equation (3) for the jet centerline must be used in conjunction with these integrals to obtain U_x, U_y, and U_z. The expressions for the induced velocities due to entrainment at field point (x_j, y_j, z_j) on the plate, in nondimensional form, become:

$$\frac{U_x}{V_\infty} = -\frac{1}{4\pi}\int_0^\infty \frac{\left(\frac{x_j}{D} - \frac{x_a}{D}\right)\frac{q_a}{V_\infty D}\,d\left(\frac{s_a}{D}\right)}{\left(\frac{r_a}{D}\right)^3} \tag{26}$$

$$\frac{U_y}{V_\infty} = -\frac{1}{4\pi}\int_0^\infty \frac{\left(\frac{y_j}{D} - \frac{y_a}{D}\right)\frac{q_a}{V_\infty D}\,d\left(\frac{s_a}{D}\right)}{\left(\frac{r_a}{D}\right)^3} \tag{27}$$

$$\frac{U_z}{V_\infty} = -\frac{1}{4\pi}\int_0^\infty \frac{\left(\frac{z_j}{D} - \frac{z_a}{D}\right)\frac{q_a}{V_\infty D}\,d\left(\frac{s_a}{D}\right)}{\left(\frac{r_a}{D}\right)^3} \tag{28}$$

where

$$\frac{r_a}{D} = \left[\left(\frac{x_j}{D} - \frac{x_a}{D}\right)^2 + \left(\frac{y_j}{D} - \frac{y_a}{D}\right)^2 + \left(\frac{z_j}{D} - \frac{z_a}{D}\right)^2\right]^{1/2} \tag{29}$$

In order for U_z to be zero in the X-Y plane to satisfy the no-flow condition at the plate, the entrainment model is imaged below the Z = 0 plane. The effect of this imaging is to double the X-component and Y-component of the induced velocities in the Z = 0 plane and cancel the Z-component of velocity. It is also noted here that the X-component of induced velocity in the jet coordinate system is of opposite sign when expressed in the body (plate) coordinate system (X,Y,Z).

The integral which defines the potential for a distribution of sinks along the jet axis, given by equation (15), does not have an analytical solution and must be solved numerically. Since, for all practical purposes, the integration cannot be carried out to infinity, it must be determined how far along the jet the integral should be evaluated in order to obtain an accurate solution. The effect of jet length on the blockage results was discussed in a previous section, and it was noted that a jet length of 20 initial jet radii produced consistent results. To determine the effect of increasing this upper integration limit on the entrainment results, a constant radius jet at $V_j/V_\infty = 8.0$ was modeled. A comparison of predicted pressure coefficients obtained using upper integration limits of 20 and 40 initial jet radii are shown in figure 4 for $\beta = 0°$, 30°, 90°, and 180°. The small differences in the theoretical solutions in figure 4 represent differences due to the entrainment solution, since the blockage results for both cases are virtually identical. Increasing the length of the jet centerline beyond 20 initial jet radii increases computation time without effecting much change in the final results. Consequently, 20 initial jet radii is the upper integration limit for all results presented in this report.

Spreading rate.- As a circular jet exhausts from an infinite plate into a subsonic crossflow velocity, the jet interaction with the free-stream velocity causes the boundary to expand or spread with increasing distance along the jet. Some knowledge of the extent of the jet boundary is important in predicting the displacement or blockage effect of the jet. In actuality, the jet expands and its cross section distorts into a kidney shape as shown in sketch 3. The distortion of the jet and its roll-up into a pair of vortices is described in references 14, 15, 16, and 17.

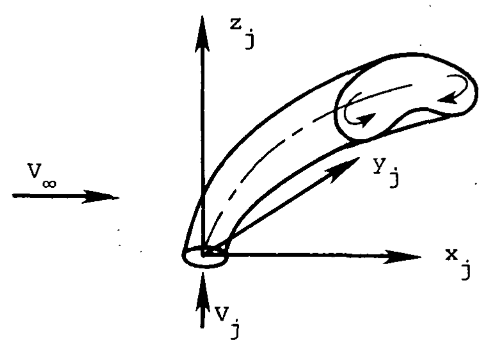

Sketch 3.- Jet Cross Section

This condition occurs near the end of the potential core of the jet. The modeling of the vortex pair is very important if flow field velocities in the vicinity of the downstream portion of the jet are desired, but for purposes of calculating the pressure distribution on the plate near the jet, the displacement effect is more important. For this reason, the authors have chosen to neglect the formation of the vortex pair in the model presented in this report.

Numerous investigators have studied the spreading rates of jets in a crossflow using both experimental and analytical methods. The results in references 13 and 18 will be used to calculate the required spreading rates in the following manner. Bowley and Sucec, in reference 18, assume the jet to be a co-flowing jet in a crossflow velocity $V_\infty \cos \alpha$. They also assumed the crossflow velocity to be a shear layer velocity with a specified profile; however, for purposes of the present work, the crossflow velocity will be assumed uniform. Reference 18 relies heavily on Abramovich's results for a jet in a crossflow (ref. 19). Treating the jet as a planar jet of local thickness t, the spreading rate in the x_j-z_j plane is determined using Abramovich's results for plane turbulent jets with a co-flowing external stream. The spreading rate for the initial region, which extends from the jet exit plane to the end of the potential core, is determined from the expression

$$\frac{1}{2}\frac{dt}{ds_a} = (0.584 - 0.134\ m)\frac{db}{ds_a} \tag{30}$$

where

$$m = \frac{V_\infty \cos\alpha}{V_j} \tag{31}$$

$$\frac{db}{ds_a} = 0.27\left(\frac{1 - m}{1 + m}\right) \tag{32}$$

The expression for the main region, where $b = t/2$, is

$$\frac{1}{2}\frac{dt}{ds_a} = 0.22\left[\frac{V_m - V_\infty \cos\alpha}{V_m + V_\infty \cos\alpha}\right] \tag{33}$$

The above expressions were developed for rectangular shaped jets. Even though the present model has been limited to circular cross section jets, it was assumed that the dt/ds_a from equations (30) and (33) could be used to represent the spreading jet boundary. This assumption is best in the region near the plate where the jet has not had the opportunity to spread a large amount, and the spreading model will deteriorate at large distances from the plate. However, at large distances from the plate, the displacement effect on the plate and the induced pressure on the plate will be small. The effect of this assumption will be seen in the comparisons with data presented in a later section of this report.

The differential equations, (30) and (33), which describe the spreading rates cannot be solved analytically; therefore, an approximate solution is obtained as follows. The equations are of the form:

$$\Delta\left(\frac{t}{D}\right) = C(s_a)\Delta\left(\frac{s_a}{D}\right) \tag{34}$$

where D is the initial jet diameter and $C(s_a)$ is a coefficient which is a function of distance along the jet axis. Calculating $C(s_a)$, which represents the slope of the curve, at various positions along the jet centerline and assuming $t/D = 1.0$ at $L/D = 0$ (since the jet is axisymmetric) an approximate expansion curve is determined for each velocity ratio.

In order to determine the spreading rate in the main region, it is necessary to know the distribution of V_m, the local centerline velocity of the jet. Keffer and Baines (ref. 13) present experimental results of $[(V_m - V_\infty)/(V_j - V_\infty)]$ vs s_a/D for velocity ratios of 4.0, 6.0, and 8.0. Using these results, the value of V_m at various positions along the jet axis, and therefore the local slope $C(s_a)$, is determined for each jet velocity ratio case. The local slope is used to determine the growth rate in the main region.

Since the length of the initial region is a factor in determining the spreading rate of the jet, some considerations for the choice of initial region length are in order. From reference 19, a jet flowing into a quiescent region will have an initial region length of approximately five jet diameters. As shown in reference 17, the presence of a crossflow decreases the length of the initial region; however there is some disagreement between investigators as to the variation of initial region length with crossflow velocity ratio. The following systematic study of the effect of initial region length was carried out.

Assuming initial region lengths of 0, 3, and 5 jet diameters, spreading rate curves were calculated for two jet velocity ratios, $V_j/V_\infty = 4$ and 8. These expansion curves are shown in figure 5. Using these expansion curves to determine the jet boundary for the blockage model, and including the entrainment model, pressure distributions are predicted on the plate in the region upstream of the jet where the viscous effects should be smallest. These results are compared with experimental data from reference 4 in figures 6 and 7. The results obtained using an initial region of 5 jet diameters are not shown because they are nearly identical to those obtained using the initial region of 3 jet diameters. The V_j/V_∞ results in figure 6 indicate that, at $\beta = 60°$, an initial region of 3 jet diameters produces better agreement with data than the results obtained with no initial region. The predicted pressure distributions at $\beta = 0°$ and 30° are not sensitive to the length of the initial region. The same trends are evident at the higher jet velocity condition shown in figure 7, although the agreement between the measured and predicted pressure distributions at $\beta = 60°$ is not as good as in the previous figure. Even though the length of the initial region varies with jet velocity ratio, the small effect of this length on the predicted pressure distributions in the upstream region of the jet indicate that a constant initial region length will suffice for the present model. For all calculations in this report, the initial region is assumed to be 3 jet diameters in length.

Since the data from which V_m is obtained in reference 13 is only for $V_j/V_\infty = 4.0$, 6.0, and 8.0, it is necessary to develop an approximate method for determining the expansion rate in the main region for other jet velocity ratios. A plot of $(t/D)_{max}$ vs V_j/V_∞, where $(t/D)_{max}$ is the value of t/D at $s_a/D = 10$, is shown in figure 8. Assuming that $(t/D)_{max} \rightarrow 1.0$ as $V_j/V_\infty \rightarrow 0$, a curve is faired through this point and the values of $(t/D)_{max}$ obtained for $V_j/V_\infty = 4.0$, 6.0, and 8.0. To obtain a spreading rate for arbitrary V_j/V_∞, the initial expansion can be obtained using equation (30) for the initial region and $(t/D)_{max}$ is read from figure 8. The remainder of the curve can be constructed by interpolation or extrapolation of the known curves. A series of expansion rate curves is presented in figure 9. These curves are used to determine the blockage model for the predicted results presented in this report.

Correlation

The purpose of the correlation is to isolate the viscous effects of the jet on the plate. It is expected that the predicted potential pressure distribution away from the jet and within the range $0° \leq \beta \leq 60°$ will be in good agreement with experiment. The predicted pressures near the jet and within the range $60° \leq \beta \leq 180°$ will likely be in poor agreement with experiment due to viscous effects. Assuming that the measured pressure distribution is given by a potential part, which consists of blockage and entrainment contributions, plus a viscous part, the viscous part can be determined by a differencing technique. This expression is given as

$$\Delta C_p\Big|_{viscous} = C_p\Big|_{experiment} - C_p\Big|_{potential} \tag{35}$$

Correlating this quantity as a function of jet velocity ratio and position on the plate, the predicted pressure on a plate induced by a jet exhausting from the plate into a crossflow is given by

$$C_p = C_p\Big|_{potential} + \Delta C_p\Big|_{viscous} \tag{36}$$

The success of this correlation, as with any correlation, is dependent on the quantity of data available and how well these data compare with one another. In regions where multiple sets of data are in good agreement with one another, the correlation method results should compare well with these and other data. In region where the data sets are in poor agreement, it is impossible to obtain a correlation which will provide good results with all data.

In comparing data sets with the same velocity ratio, it is necessary to note that other parameters, such as jet size, jet Mach number, initial jet mean velocity profile, jet turbulence level, free-stream Mach number, and Reynolds number based on run length (Re_ℓ) are seldom the same for any two data sets. Although it is felt that the velocity ratio is the dominant parameter in determining the pressure on the plate, these other parameters may indeed have secondary effects. An example of such effects was investigated by Vogler (ref. 1) and involves varying free-stream and jet velocities for constant jet velocity ratios. Results for $V_j/V_\infty = 2.5$ at $\beta = 0°$ and $60°$ are shown in figure 10. The effects of the free-stream velocity on the plate pressures vary from being negligible for $r/D < 2.0$ at $\beta = 0°$ to producing a difference in C_p of 0.12 at $\beta = 60°$ for $r/D = 0.60$. Although results of this type would indicate a need for investigating such effects, very little data are available. In most experimental investigations, the jet velocity ratio is the primary effect studied. The correlation presented in this report is based on jet velocity ratio only, without consideration of the other flow parameters.

The references used to develop the correlation are listed in Table I along with pertinent experimental parameters. These parameters are jet velocity ratio (V_j/V_∞), initial inclination angle (θ), jet Mach number (M_j), Reynolds numbers based on initial jet diameter and run length (Re_D and Re_ℓ, respectively), ratio of the run length to the initial jet diameter (ℓ/D), and the ratio of the maximum radial station at which data was taken to the initial jet diameter $(r/D)_{max}$. Also included is a column which indicates the manner in which the data is presented in each report. The large ranges of the various parameters is an indication of the difficulty encountered in trying to correlate these data. As can be seen from the table, it was impossible to find two sets of data for which the range of experimental parameters was identical. Given adequate data, the correlation could include any of the aforementioned parameters; however, in the absence of these data, the correlation developed in this study is based only on the jet velocity ratio.

The correlation curves presented in this report were obtained in the following manner. First, theoretical results were obtained using the blockage model alone for $V_j/V_\infty < 2.35$ and the blockage plus entrainment model for $V_j/V_\infty \geq 2.35$. The $V_j/V_\infty = 2.35$ limit value is built into Yeh's entrainment model equations, and is the lowest jet velocity ratio for which the entrainment equations can be used. It is well known that blockage effects are dominant at low velocity ratios, while the entrainment effects are dominant at high velocity ratios. The velocity ratio at which entrainment effects begin to influence the pressure distribution on the plate is not known, but comparisons with data from reference 4, such as those shown in figure 11(a), indicate that the blockage model alone is sufficient for low jet velocity ratios. Data comparisons using the blockage model alone and blockage plus entrainment model for $V_j/V_\infty = 3.9$ and 8.0 are shown in figures 11(b) and (c), respectively. The $V_j/V_\infty = 3.9$ data comparisons indicate that while some entrainment is needed to improve theoretical results, the present entrainment model is providing "too much" entrainment at this particular V_j/V_∞. Figure 11(c) shows a large entrainment effect at $V_j/V_\infty = 8.0$ which improves the blockage alone results and shows excellent agreement with data at $\beta = 0°$ and $30°$. As a result of similar data comparisons throughout the jet velocity ratio range and because of the limits of the entrainment model, it was decided to use the blockage model alone in the low jet velocity ratio range ($1.0 \leq V_j/V_\infty \leq 2.35$) and the blockage plus entrainment model in the medium to high jet velocity ratio range ($2.35 \leq V_j/V_\infty \leq 10.0$).

After calculating theoretical pressure coefficients at chosen β and r/D stations for each V_j/V_∞, a $(\Delta C_p)_{viscous}$ is obtained by comparing these results with experimental data. In cases where more than one data set exists for a particular V_j/V_∞, $(\Delta C_p)_{viscous}$ is found by averaging the correlation values obtained from each data set. By determining a $(\Delta C_p)_{viscous}$ for each $(\beta, r/D)$ pair, a data base is set up which consists of a $(\Delta C_p)_{viscous}$ array for each jet velocity ratio. Linear interpolation is used to determine correlation values at any V_j/V_∞, β, and r/D values for which correlation curves have not been determined. These results are described in the following section.

RESULTS

Correlation curves are presented in figure 12 for jet velocity ratios 1.0, 1.67, 2.2, 3.33, 3.9, 5.0, 6.1, 8.0, 10.0, and 12.0. The correlation values were determined at β = 0°, 30°, 60°, 90°, 120°, 150°, and 180° and r/D = 0.75, 1.0, 1.5, 2.0, 3.0, and 5.0. The correlation curves for V_j/V_∞ = 1.0, 1.67, 2.2, and 6.0 were determined using only one data set each as other data at these velocity ratios are unavailable. All other correlation curves were obtained using two or more independent sets of data.

The results shown in figure 12 exhibit some variations in form, as would be expected considering the nature of the data used to develop these results. There is a systematic variation of $(\Delta C_p)_{viscous}$ at each velocity ratio; however, the actual shape of each correlation curve changes somewhat with changing velocity ratio. The correlation factors are presented as a function of β for constant radius values because the systematic nature of the $(\Delta C_p)_{viscous}$ values is more obvious than when presented as a function of radius for constant β values.

Some effort was made to further correlate the factors of figure 12 by attempting to collapse all the curves at a given velocity ratio onto a single curve. This would have simplified the use of the correlation factors, and it would also have smoothed the curves. Unfortunately, this effort was not successful. It proved impossible to find a common normalizing parameter which was applicable for all velocity ratios. As a result of this investigation, the correlating factors were maintained in data base form as shown in figure 12. Any required factor can be obtained by interpolating between curves at a given velocity ratio and interpolating between velocity ratios.

The pressure prediction method, made up of the blockage model, the entrainment model, and the viscous correction factor, will now be applied to a range of flow conditions for which data are available for comparison. Unfortunately, the available data are the same data used to develop the viscous correlation factors, thus the quality of the agreement in reality depends on the degree of agreement between different sets of data. It would be more useful to compare the prediction method with independent data, but adequate additional data are not available at the present time.

Data comparisons of C_p vs r/D at β = constant for V_j/V_∞ = 3.33, 3.9, 5.0, 8.0 and 10.0 are presented in figures 13 through 17, respectively. In figure 13, predicted pressure distributions with and without the correlation correction are included to illustrate the effect of the correction factor at various positions around the jet. The uncorrected results are not shown in figures 14 through 17. Data comparisons are not presented for V_j/V_∞ = 1.0, 1.67, 2.2 or 6.1, since the correlation curves for each of these jet velocity ratios were determined using only a single data set. The predicted results were determined for $0.75 \leq r/D \leq 5.0$ and for β = 0°, 30°, 60°, 90°, 120°, 150°, and 180°.

As can be seen from these figures, varying degrees of success were obtained using the data correlation prediction method. As mentioned above, the success is dependent on how well the various sets of data agree with one another. In regions where the data sets are in good agreement with one another, the prediction method results agree well with all experimental results. In general, comparisons with data are in good agreement over a wide range of flow conditions.

A special note is made here with respect to the V_j/V_∞ = 3.33 correlation results in figure 13. It was felt that the experimental results from reference 3 should not be used in determining correlation factors since they do not follow trends seen in other experimental data. For example, the C_p value at β = 0° and 180° approaches zero within 2 jet diameters, which is a phenomenon that is not found in any other experimental data in this V_j/V_∞ range. Also, the behavior at β = 30° is unlike that seen for other data in this jet velocity ratio range. That is to say, other experimental results show a slight peak in the C_p value between r/D = 0 and 2, while the reference 3 data shows a smooth curve. As a result of these inconsistencies with respect to other data, it was decided to use reference 1 for the V_j/V_∞ = 3.33 correlation. Data from reference 3 is included in the data comparisons to show the behavior of these data.

An interesting means of comparing measured and predicted results is to compare the total force and distribution of force on a finite plate with the jet at its center. The normal force is obtained by integrating pressures on a circular finite plate whose diameter is dependent on the location of the outermost data points. The circle is divided into sectors and segments, as shown in figure 18(a), and the pressure coefficient at the area centroid of each of these pieces is used to determine a force on each piece. These forces are summed to obtain a total normal force, and moments are taken about the Y-axis to obtain a pitching moment. The positive sense of the normal force and pitching moment is shown in figure 18(b). The measured and predicted force and moment coefficients are compared in figure 19.

A circular plate with a radius of 5.5 jet diameters was used to obtain results for the reference 1 and 4 data comparisons. A smaller plate with a radius of 4.25 jet diameters was used for the reference 5 comparisons. The good agreement for both normal force and pitching moment coefficients indicate that, while the correlation method pressure distribution results are not in perfect agreement with experiment, the method can give accurate integrated force and moment results.

All of the correlations and comparisons made thus far have been for a jet exhausting normal to a plate ($\theta = 0°$). There is a practical interest in having the capability of predicting the jet induced pressure distribution on a plate from which the jet is exhausting at some arbitrary angle ($\theta \neq 0°$). Unfortunately, adequate data do not exist to develop a set of correlation factors for other jet inclination angles. The following investigation was made to determine the possibility of using the existing correlation factors for $\theta = 0°$ to predict the pressure distribution for other jet inclination angles.

In reference 20, pressure distribution data are available for a wide range of jet inclination angles ($0° \leq \theta \leq 60°$) for a jet velocity ratio of 12. The correlation curves for $V_j/V_\infty = 12$ are used to predict the pressure distributions which are compared with data for a jet exhausting normal to the plate (figure 20). Two sets of data, from references 5 and 20, are presented in this figure and the agreement between both sets of data and the predicted curves is generally very good.

Next, these same correlation factors are applied to the predicted results for the jet exhausting at an inclination angle of 30°. These results are compared with the experimental data from reference 20 in figure 21. The agreement in this figure is not as good as that obtained for normal jets ($\theta = 0°$) in previous comparisons. The results of figure 21 indicate that separate correlation curves are needed for each jet inclination angle.

CONCLUDING REMARKS

A correlation method was developed to include viscous effects in the predicted pressures on an infinite plat plate from which a jet is issuing into a subsonic crossflow. Correlation values of viscous induced pressure coefficients were defined as the difference between pressures predicted by a potential model and those obtained from experimental data. Jet blockage and entrainment effects were accounted for in the potential model using a vortex quadrilateral panel model and a sink distribution model, respectively. The viscous effects of the jet were represented by the correlation values.

Comparisons of measured and predicted plate pressures in the vicinity of normal jets ($\theta = 0°$) over a wide range of jet velocity ratios were generally good. Data comparisons of normal force and pitching moment on a finite plate were also in good agreement.

The correlation method did not work well when it was applied to flow conditions which were outside the range of the data used to obtain the correlation factors. For example, the application of correlation factors corresponding to a normal jet ($\theta = 0°$) to a condition with a nonzero jet inclination angle proved to be unsatisfactory. It is possible to interpolate for velocity ratio and plate position, but the correlation factors must correspond to the correct jet inclination angle.

The success of the method described in this report for jets exhausting from infinite flat plates indicates that it is possible to extend the method to other configurations, with the one requirement that ample data be available to determine the correlation factors. For example, the method could be extended to include jets exhausting from finite plates or from curved shapes like a fuselage or pod.

RECOMMENDATIONS

The correlation method described in this report could be improved and made more general in several areas. The first improvement to the method as it exists now would be the infusion of additional data at the same flow conditions used to determine the present correlation factors. This would verify the factors and give additional confidence in their application to pressure prediction in the vicinity of jets exhausting from a plate.

If additional data were available which had a systematic variation including jet inclination angle, jet Mach number, and plate Reynolds number, these parameters could be included in the correlation curves.

Finally, it is noted that while some care may be taken in the design of wind tunnel experiments to control jet turbulence level and mean velocity profile, these quantities are generally not measured. For purposes of this kind of prediction work, it would be desirable to have flow field measurements in and around the jet to define its flow properties, location, and spreading as well as induced surface pressure measurements.

NIELSEN ENGINEERING & RESEARCH, INC.
Mountain View, California
May, 1978

APPENDIX A

JET-IN-A-CROSSFLOW BIBLIOGRAPHY

A literature search was instigated to determine the available data reports and predictive methods for subsonic jets issuing from an infinite plate into a subsonic crossflow. In the course of the search, reports related to the V/STOL problem, but not directly related to the specified subject, were discovered. These reports included information on jets ejecting into a supersonic crossflow, jets ejecting from wings and fuselages, jets ejecting from complete aircraft models, and confined jets in a crossflow. Confined jets are defined as jets whose vertical or lateral movement is restricted by wind tunnel walls. These references, though not specifically related to the subject of current interest, are important for an overview of the total subject of jet induced aerodynamics. Since these additional references may be useful in future work, they are retained in the bibliography; however, the bibliography should not be considered to be complete in these additional areas.

The appendix is presented in the following format. Each reference is given an identification number, and the references are listed chronologically in order of the year of publication. Table A-I is a cross index of the reference number and its year of publication. Table A-II defines the symbols and abbreviations used in this Appendix.

Table A-III classifies the references, whose numbers are given in column 1, as to the type of report (GENERAL CATEGORY) and types of subject matter treated or type of data obtained (SUBJECTS TREATED). The type of report is divided into three general categories: DATA, THEORETICAL or EMPIRICAL METHOD, and REVIEW, SUMMARY, or SURVEY REPORT. DATA reports are those which present original experimental data. THEORETICAL or EMPIRICAL METHODS are reports which present predictive methods dealing with some aspect of the jet in a crossflow problem. REVIEW, SUMMARY, or SURVEY REPORTS are those reports which synthesize or analyze previously available information. The GENERAL CATEGORY section is followed by two columns which indicate the model investigated and the free-stream Mach number range. The models are presented in the form A/B, where A represents the general configuration investigated and B is the location of the fan or jet. For example, the symbol W in this column indicates a wing alone was investigated in the given reference. The fact that this symbol is not followed by a slash (/) indicates that the jet or fan is in the wing. The designation WB/F indicates that a wing-body configuration with a fan or jet in the fuselage was investigated. The M_∞ RANGE column indicates whether the free-stream Mach number range of the given reference is in the subsonic (SUB) or supersonic (SUP) regime. The SUBJECTS TREATED category is divided into eight columns. A cross mark (X) in any one of these columns indicates that particular subject was investigated in some fashion in the given reference.

The Appendix is set up for use in the following manner. First, determine the reference number of interest from Table A-III. Second, look up the year of publication in Table A-I; and finally, locate the reference in the chronological listing at the end of the Appendix.

TABLE A-I.- CROSS INDEX FOR REFERENCES

Ref. No.	Year	Ref. No.	Year	Ref. No.	Year	Ref. No.	Year	Ref. No.	Year	Ref. No.	Year
1	'71	31	'65	61	'71	91	'66	121	'72	151	'63
2	74	32	65	62	61	92	68	122	73	152	70
3	64	33	67	63	61	93	61	123	73	153	75
4	68	34	63	64	67	94	50	124	73		
5	67	35	73	65	69	95	69	125	73		
6	72	36	72	66	76	96	77	126	69		
7	61	37	71	67	76	97	65	127	64		
8	63	38	68	68	76	98	67	128	74		
9	66	39	75	69	76	99	67	129	73		
10	70	40	75	70	76	100	73	130	75		
11	64	41	74	71	76	101	71	131	74		
12	63	42	73	72	63	102	75	132	68		
13	61	43	77	73	61	103	76	133	75		
14	67	44	73	74	66	104	72	134	75		
15	65	45	65	75	48	105	72	135	74		
16	68	46	62	76	50	106	74	136	75		
17	63	47	69	77	68	107	73	137	75		
18	64	48	69	78	70	108	49	138	74		
19	61	49	65	79	66	109	66	139	68		
20	62	50	70	80	66	110	73	140	68		
21	61	51	66	81	67	111	72	141	67		
22	59	52	77	82	64	112	72	142	69		
23	70	53	76	83	69	113	71	143	64		
24	66	54	74	84	66	114	70	144	70		
25	67	55	73	85	69	115	70	145	77		
26	69	56	67	86	74	116	70	146	67		
27	62	57	73	87	67	117	70	147	69		
28	67	58	64	88	75	118	71	148	66		
29	65	59	74	89	75	119	72	149	77		
30	67	60	71	90	70	120	73	150	76		

TABLE A-II.- MODEL SYMBOLS AND ASSOCIATED CONFIGURATIONS USED IN TABLE II

Symbol	Configuration or Subject Treated
A	Arbitrary body
CON	Confined jet
F	Fuselage
FAN	Lift fan hardware investigation
LIT	Literature survey
N	Nozzle
O	Other
P	Engine pod
PL	Flat plate
W	Wing
WB	Wing-body
WBT	Wing-body-tail

TABLE A-III.- CLASSIFICATION TABLE

Reference Number	General Category: Data	General Category: Theoretical or Empirical Method	General Category: Review, Summary, or Survey Report	Model	M_∞ Range	Subjects Treated: Jet Trajectory	Subjects Treated: Jet Entrainment	Subjects Treated: Jet Pressures	Subjects Treated: Velocity Fields	Subjects Treated: Plate or Body Pressures	Subjects Treated: Force and Moment Measurement	Subjects Treated: Comparison of Theory and Data	Subjects Treated: Temp. Fields, Turbulence, Vorticity, Other
1		x		W	SUB	x				x			
2	x			W					x				x
3		x		W/None					x	x	x		
4		x		W						x	x	x	
5		x		W						x	x	x	
6			x	A						x		x	
7	x			WB/F						x	x		
8	x			WB/W						x	x		
9	x			WBT/F							x		
10			x	WB									
11	x			WB/W							x		
12	x			WB/F						x	x		
13			x	WB/F							x		
14	x			WB/W							x		
15	x			WB/W						x	x		
16	x			N		x				x		x	
17	x			PL						x			
18	x			WB/F							x		
19	x			PL							x		
20	x			WB/F							x		
21			x	WB/W, F							x		
22	x			W							x		
23	x			WB/W							x		
24(a)	x			WBT/W, P							x		
24(b)			x	WBT/W, F							x		
24(c)	x			WB/F						x			
24(d)	x			WBT/W, P									

TABLE A-III.- Continued.

Reference Number	General Category: Data	General Category: Theoretical or Empirical Method	General Category: Review, Summary, or Survey Report	Model	M_∞ Range	Subjects Treated: Jet Trajectory	Jet Entrainment	Jet Pressures	Velocity Fields	Plate or Body Pressures	Force and Moment Measurement	Comparison of Theory and Data	Temp. Fields, Turbulence, Vorticity, Other
25	x			FAN	SUB								x
26(a)			x	PL,WB,WBT		x				x	x		x
26(b)		x		PL					x				x
26(c)		x		N		x							
26(d)	x			PL		x			x	x			
26(e)			x	F, PL						x			
26(f)		x		PL			x				x	x	
26(g)		x		PL		x						x	
26(h)		x		PL		x							
26(i)		x		PL						x			
26(j)		x		PL		x							
26(k)		x		W								x	x
26(ℓ)		x		W		x				x	x	x	
26(m)		x		PL						x		x	
26(n)		x		PL					x				
26(o)		x		PL		x	x						
27		x		W		x					x		
28		x		W						x	x	x	
29	x			PL						x			
30	x	x		W						x		x	
31		x		W							x	x	
32	x			PL		x		x					
33	x			W									x
34	x			WBT/F,W							x		
35	x			WB/F						x			
36	x			PL,F						x			

TABLE A-III.- Continued.

	General Category				Subjects Treated								
Reference Number	Data	Theoretical or Empirical Method	Review, Summary, or Survey Report	Model	M_∞ Range	Jet Trajectory	Jet Entrainment	Jet Pressures	Velocity Fields	Plate or Body Pressures	Force and Moment Measurement	Comparison of Theory and Data	Temp. Fields, Turbulence, Vorticity, Other
37	x			PL	SUB	x							
38	x			PL		x	x						
39	x			PL						x			
40		x	x	PL		x			x				x
41		x	x	PL		x			x				x
42	x			W						x	x		
43	x			N					x				x
44	x			W					x	x	x		
45	x			W						x	x		
46	x			W						x			x
47		x		W					x			x	x
48		x		W					x				x
49	x			W							x		x
50		x		W					x				x
51			x	PL, F		x				x	x	x	
52		x		W					x	x			x
53		x		PL		x						x	
54	x			PL (CON)		x							x
55		x		PL		x			x			x	
56	x			WBT/W, P							x		
57	x	x		PL (CON)		x						x	x
58		x		A					x		x		
59		x		PL		x			x				
60	x			WBT/P							x		
61	x			PL					x				x
62	x			PL, W	SUP					x			

TABLE A-III.- Continued.

Reference Number	General Category: Data	General Category: Theoretical or Empirical Method	General Category: Review, Summary, or Survey Report	Model	M_∞ Range	Subjects Treated: Jet Trajectory	Subjects Treated: Jet Entrainment	Subjects Treated: Jet Pressures	Subjects Treated: Velocity Fields	Subjects Treated: Plate or Body Pressures	Subjects Treated: Force and Moment Measurement	Subjects Treated: Comparison of Theory and Data	Subjects Treated: Temp. Fields, Turbulence, Vorticity, Other
63	x			PL	SUP					x			
64		x		PL	SUB	x							
65	x			W						x	x		
66			x	WB/F, P, W					x	x	x	x	
67	x			PL					x				x
68	x			PL					x				x
69			x										
70		x		O									x
71		x		WBT/F							x	x	
72	x	x		PL		x	x						x
73	x			PL			x						
74			x	PL, WB/F, W						x	x		
75	x			PL (CON)		x		x					
76	x			PL (CON)		x			x	x			
77	x			WBT/F		x					x		
78		x		PL						x		x	
79	x			WB/F							x		
80	x			PL, WB/F						x	x	x	
81	x			WB/W						x	x		
82	x			W						x			
83	x	x		PL			x		x	x		x	
84	x			PL						x			
85	x			WBT/F							x		
86	x			WB/F, P						x			
87 (a)			x	WBT/W, F							x		
87 (b)	x	x		PL							x		

TABLE A-III.- Continued.

Reference Number	General Category: Data	General Category: Theoretical or Empirical Method	General Category: Review, Summary, or Survey Report	Model	M_∞ Range	Subjects Treated: Jet Trajectory	Jet Entrainment	Jet Pressures	Velocity Fields	Plate or Body Pressures	Force and Moment Measurement	Comparison of Theory and Data	Temp. Fields, Turbulence, Vorticity, Other
88		x		PL	SUB	x			x			x	x
89			x	WBT/F,W					x		x		
90			x	PL		x			x	x	x	x	
91		x		PL		x				x		x	
92			x	WBT/F,P		x					x		
93	x			WB/P							x		
94	x			PL		x		x	x				x
95		x		PL		x							
96	x			N		x			x				
97		x		N		x							
98	x	x		N		x						x	
99		x	x	PL		x							
100		x		PL		x							
101		x		PL									x
102	x			PL		x			x	x			x
103	x			N		x			x			x	
104	x			PL						x			
105	x			PL		x		x	x				
106	x			N					x				x
107	x			N					x				x
108	x			PL(CON)					x			x	
109		x		PL	SUP	x							
110	x	x		PL	SUB	x			x			x	x
111	x			PL		x			x				x
112		x		N		x						x	
113		x		PL		x			x	x			

TABLE A-III.- Continued.

Reference Number	General Category: Data	General Category: Theoretical or Empirical Method	General Category: Review, Summary, or Survey Report	Model	M_∞ Range	Subjects Treated: Jet Trajectory	Subjects Treated: Jet Entrainment	Subjects Treated: Jet Pressures	Subjects Treated: Velocity Fields	Subjects Treated: Plate or Body Pressures	Subjects Treated: Force and Moment Measurement	Subjects Treated: Comparison of Theory and Data	Subjects Treated: Temp. Fields, Turbulence, Vorticity, Other
114	x			PL	SUB	x				x			
115	x			PL						x			
116	x			PL					x	x			
117	x			PL						x			
118	x			W				x					x
119	x			W						x	x		
120		x		PL					x	x		x	
121		x		PL		x	x			x			
122		x		PL				x				x	
123	x			PL		x				x			
124	x			N		x							x
125			x	W									x
126		x		PL		x						x	
127			x	WBT/W,F									x
128(a)		x		PL		x				x		x	
128(b)			x	LIT									x
129		x		PL						x		x	
130		x		PL		x			x			x	x
131	x			O		x							
132	x			PL	SUP					x			
133		x		PL	SUB		x			x		x	
134	x			F		x			x	x			
135		x		N		x	x					x	
136(a)	x			N					x			x	
136(b)	x			N		x							x
136(c)	x			N			x						

TABLE A-III.- Concluded.

Reference Number	General Category: Data	General Category: Theoretical or Empirical Method	General Category: Review, Summary, or Survey Report	Model	M_∞ Range	Subjects Treated: Jet Trajectory	Subjects Treated: Jet Entrainment	Subjects Treated: Jet Pressures	Subjects Treated: Velocity Fields	Subjects Treated: Plate or Body Pressures	Subjects Treated: Force and Moment Measurement	Subjects Treated: Comparison of Theory and Data	Subjects Treated: Temp. Fields, Turbulence, Vorticity, Other
136(d)	x			F,WB/F	SUB					x	x		
136(e)	x			N,F						x			
137		x		PL						x		x	
138		x		N		x			x			x	
139	x			F				x					
140		x		PL,F	SUP					x		x	
141	x			PL	SUB, SUP					x			
142		x		N	SUB	x							
143		x		PL						x		x	
144	x			PL						x			
145	x			PL		x				x	x		
146			x	LIT									x
147		x		F,PL	SUB, SUP				x	x			
148	x			PL	SUB				x	x			
149	x			WBT/P							x		
150	x			F,PL						x	x		
151		x		N,O	SUB, SUP			x	x			x	x
152	x			PL	SUB					x			
153	x			W					x				x

1948

75. Callaghan, E. E. and Ruggeri, R. S.: Investigation of the Penetration of an Air-Jet Directed Perpendicularly to an Air Stream. NACA TN 1615, June 1948.

1949

108. Callaghan, E. E. and Bowden, D. T.: Investigation of Flow Coefficient of Circular, Square and Elliptical Orifices at High Pressure Ratios. NACA TN 1947, Sep. 1949.

1950

76. Ruggeri, R. S., Callaghan, E. E., and Bowden, D. T.: Penetration of Air Jets Issuing from Circular, Square and Elliptical Orifices Directed Perpendicularly to an Air Stream. NACA TN 2019, Feb. 1950.

94. Cousin, S. and Uberoi, M. S.: Further Experiments on the Flow and Heat Transfer in a Heated Turbulent Air Jet. NACA Rept. 998, 1950.

1959

22. Hickey, D. H. and Ellis, D. R.: Wind Tunnel Tests of a Semispan Wing with a Fan Rotating in the Plane of the Wing. NASA TN D-88, Oct. 1959.

7. Aoyagi, K., Hickey, D. H. and deSavigny, R. A.: Aerodynamic Characteristics of a Large-Scale Model with a High Disk-Loading Lifting Fan Mounted in the Fuselage. NASA TN D-775, Oct. 1961.

13. Maki, R. L. and Hickey, D. H.: Aerodynamics of a Fan-in-Fuselage Model. NASA TN D-789, May 1961.

19. Vogler, R. D.: Effects of Various Arrangements of Slotted and Round Jet Exits on the Lift and Pitching-Moment Characteristics of a Rectangular-Base Model at Zero Forward Speed. NASA TN D-660, Feb. 1961.

21. Spreeman, K. P.: Induced Interference Effects on Jet and Buried-Fan VTOL configurations in Transition. NASA TN D-731, Mar. 1961.

62. Cubbison, R. W., Anderson, B. H. and Ward, J. J.: Surface Pressure Distributions with a Sonic Jet Normal to Adjacent Flat Surfaces at Mach 2.92 to 6.4. NASA TN D-580, 1961.

63. Janos, J. J.: Loads Induced on a Flat-Plate Wing by an Air Jet Exhausting Perpendicularly Through the Wing and Normal to a Free-Stream Flow of Mach Number 2.0. NASA TN D-649, 1961.

73. Ricou, F. P. and Spalding, D. B.: Measurements of Entrainment by Axisymmetrical Turbulent Jets. J. Fluid Mech., vol. 11, part I, Aug. 1961, pp. 21-32.

93. Spreeman, K. P.: Investigation of Interference of a Deflected Jet with Free Stream and Ground on Aerodynamic Characteristics of a Semispan Delta-Wing VTOL Model. NASA TN D-915, Aug. 1961.

1962

20. Otis, J. H., Jr.: Induced Interference Effects on a Four-Jet VTOL Configuration with Various Wing Planforms in the Transition Speed Range. NASA TN D-1400, Sept. 1962.

27. Wooler, P. T.: Lift and Moment Forces Due to a Jet Ejected From the Lower Surface of a Wing. Aero-Research Rept. No. 8, Nov. 1962.

46. Gregory, N., Raymer, W. G., and Love, E. M.: The Effect of Forward Speed on the Inlet Flow Distribution and Performance of a Lifting Fan Installed in a Wing. NPL Aero. Rept. 1018, June 1962.

1963

8. Hickey, D. H. and Hall, L. P.: Aerodynamic Characteristics of a Large-Scale Model with Two High Disk-Loading Fans Mounted in the Wing. NASA TN D-1650, Feb. 1963.

12. deSavigny, R. A. and Hickey, D. H.: Aerodynamic Characteristics in Ground Effect of a Large-Scale Model with a High Disk-Loading Lifting Fan Mounted in the Fuselage. NASA TN D-1557, Jan. 1963.

17. Vogler, R. D.: Surface Pressure Distributions Induced on a Flat Plate by a Cold Air Jet Issuing Perpendicularly from the Plate and Normal to a Low-Speed Free-Stream Flow. NASA TN D-1629, Mar. 1963.

34. Goldsmith, R. H. and Hickey, D. H.: Characteristics of Aircraft with Lifting-Fan Propulsion Systems for V/STOL. IAS Paper No. 63-27, Jan. 1963.

72. Keffer, J. F. and Baines, W. D.: The Round Turbulent Jet in a Cross-wind. J. Fluid Mech., vol. 15, part 4, Apr. 1963, pp. 481-497.

151. Abramovich, G. N.: The Theory of Turbulent Jets. M.I.T. Press, 1963.

1964

3. Rubbert, P. E.: Theoretical Characteristics of Arbitrary Wings by a Non-Planar Vortex Lattice Method. Boeing Rept. No. D6-9244, Feb. 1964.

11. Kirk, J. V., Hickey, D. H., and Hall, L. P.: Aerodynamic Characteristics of a Full-Scale Fan-in-Wing Model Including Results in Ground Effect with Nose-Fan Pitch Control. NASA TN D-2368, July 1964.

18. Vogler, R. D.: Interference Effects of Single and Multiple Round or Slotted Jets on a VTOL Model in Transition. NASA TN D-2380, Aug. 1964.

58. Hess, J. L. and Smith, A. M. O.: Calculation of Nonlifting Potential Flow About Arbitrary Three-Dimensional Bodies. J. Ship Res., vol. 8, no. 2, Sept. 1964.

82. Peake, D. J.: The Pressures on a Surface Surrounding a Jet Issuing Normal to a Mainstream. Aero. Rept. LR-410, National Research Council of Canada, Nov. 1964.

127. Hirsch, D. L.: VTOL at Northrop. The Status of Flight Control Research and Development. NOR-64-292, Nov. 1964.

143. Wygnanski, I.: The Flow Induced by Two-Dimensional and Axisymmetric Turbulent Jets Issuing Normally from an Infinite Plane Surface. Aeronaut. Quart., vol. 15, Nov. 1964.

1965

15. Davenport, E. E. and Kuhn, R. E.: Wind-Tunnel-Wall Effects and Scale Effects on a VTOL Configuration with a Fan Mounted in the Fuselage. NASA TN D-2560, Jan. 1965.

29. Bradbury, L. J. S. and Wood, M. N.: The Static Pressure Distribution Around a Circular Jet Exhausting Normally from a Plane Wall into an Airstream. Aeronaut. Res. Council C.P. No. 882, Aug. 1965.

31. Monical, R. E.: A Method of Representing Fan-Wing Combinations for Three-Dimensional Potential Flow Solutions. J. Aircraft, vol. 2, no. 6, Nov.-Dec. 1965, pp. 527-530.

32. Jordinson, R.: Flow in a Jet Directed Normal to the Wind. ARC R&M 3074, Aug. 1965.

45. Schaub, U. W.: Experimental Studies of VTOL Fan-in-Wing Inlets. Agard No. 103. Aerodynamics of Power Plant Installation, Part II, Oct. 1965.

49. Schaub, U. W. and Bassett, R. W.: Analysis of the Performance of a Highly Loaded 12-Inch VTOL Z-Axis, Fan-in-Wing Model at Zero Forward Speed. NRC No. 8829, Sept. 1965.

97. Vakhlamov, S. V.: Computation of the Trajectory of a Jet in a Drifting Flow. FTD-TT-65-1977, June 1966.

1966

9. Kirk, J. V. and Hickey, D. H.: Full-Scale Wind-Tunnel Investigation of a VTOL Aircraft with a Jet-Ejector System for Lift Augmentation. NASA TN D-3725, Nov. 1966.

24. NASA SP-116, NASA Conference on V/STOL and STOL Aircraft held at Ames Research Center, Moffett Field, CA, Apr. 4-5, 1966.

    (a) Hickey, D. H., Kirk, J. V., and Hall, L. P.: Aerodynamic Characteristics of a V/STOL Transport Model with Lift and Lift-Cruise Fan Power Plants. Paper No. 7, pp. 81-96.

    (b) Margason, R. J.: Jet-Induced Effects in Transition Flight. Paper No. 13, pp. 177-189.

    (c) Tolhurst, W. H., Jr. and Kelly, M. W.: Characteristics of Two Large-Scale Jet-Lift Propulsion Systems. Paper No. 15, pp. 205-228.

    (d) Cook, W. L. and Hickey, D. H.: Comparison of Wind-Tunnel and Flight-Test Aerodynamic Data in the Transition-Flight Speed Range for Five V/STOL Aircraft. Paper No. 26, pp. 447-467.

51. Lee, C. C.: A Review of Research on the Interaction of a Jet with an External Stream. Brown Eng. Co. TN R-184, Mar. 1966.

74. Williams, J. and Wood, M. N.: Aerodynamic Interface Effects with Jet-Lift V/STOL Aircraft Under Static and Forward Speed Conditions. RAE TR-66403, Dec. 1966.

79. Vogler, R. D.: Ground Effects on Single-and Multiple-Jet VTOL Models at Transition Speeds over Stationary and Moving Ground Planes. NASA TN D-3213, Jan. 1966.

80. Gentry, G. L. and Margason, R. J.: Jet-Induced Lift Losses on VTOL Configuration Hovering in and out of Ground Effect. NASA TN D-3166, Feb. 1966.

84. Gelb, G. H. and Martin, W. A.: An Experimental Investigation of the Flow Field about a Subsonic Jet Exhausting Into a Quiescent and a Low Velocity Air Stream. Canadian Aeronaut. Space J., vol. 12, no. 8, Oct. 1966, pp. 333-342.

91. Shandorov, G. S.: Calculation of a Jet Axis in a Drifting Flow. NASA TT F-10638, Dec. 1966.

109. Schetz, J. A. and Billig, F. S.: Penetration of Gaseous Jets Injected into a Supersonic Stream. J. Spacecraft & Rockets, vol. 3, no. 11, Nov. 1966.

148. Reichenau, D. E. A.: Interference Effects of Cold and Hot Rocket Exhausts Issuing Normal to the Airsteam from a Flat Plate at Freestream Mach Numbers from 0.6 to 1.4. AEDC TR-66-127, June 1966.

5. Rubbert, P. E., Saaris, G. R., Scholey, M. B., Standen, N. M., and Wallace, R. E.: A General Method for Determining the Aerodynamic Characteristics of Fan-in-Wing Configuration. USAAVLABS Tech. Rept. 67-61A, vol. 1, 1967.

14. Kirk, J. V., Hodder, B. K., and Hall, L. P.: Large-Scale Wind-Tunnel Investigation of a V/STOL Transport Model with Wing-Mounted Lift Fans and Fuselage-Mounted Lift-Cruise Engines for Propulsion. NASA TN D-4233, Nov. 1967.

25. Przedpelski, Z. J.: Lift Fan Technology Studies. NASA CR-761, Apr. 1967.

28. Wooler, P. T.: On the Flow Past a Circular Jet Exhausting at Right Angles from a Flat Plate or Wing. J. Roy. Aeronaut. Soc., vol. 71, Mar. 1967, pp. 216-218.

30. Wooler, P. T., Burghart, G. H., and Gallagher, J. T.: The Pressure Distribution on a Rectangular Wing with a Jet Exhausting Normally into an Airstream. AIAA Paper No. 67-1, Jan. 1967; also J. Aircraft, vol. 4, no. 6, Nov.-Dec. 1967, pp. 537-543.

33. Schaub, U. W.: Fan-in-Wing Aerodynamics: Experimental Assessment of Several Inlet Geometries. AIAA Paper No. 67-746, Oct. 1967.

56. Hall, L. P., Hickey, D. H., and Kirk, J. V.: Aerodynamic Characteristics of a Large-Scale V/STOL Transport Model with Lift and Lift-Cruise Fans. NASA TN D-4092, Aug. 1967.

64. Pratte, B. D. and Baines, W. D.: Profiles of the Round Turbulent Jet in a Cross Flow. J. Hydraulics Div., Proceedings of the ASCE, vol. 92, no. HY6, Nov. 1967, pp. 53-64.

81. Spreeman, K. P.: Free-Stream Interference Effects on Effectiveness of Control Jets Near the Wing Tip of a VTOL Aircraft Model. NASA TN D-4084, Aug. 1967.

87. AGARD CP-22, AGARD Conference on Fluid Dynamics of Rotor and Fan Supported Aircraft at Subsonic Speeds held at Paris, France, Sept. 1967.

    (a) Hickey, D. H. and Cook, W. L.: Aerodynamics of V/STOL Aircraft Powered by Lift Fans. Paper No. 15.

    (b) Crowe, C. T. and Riesebieter, H.: An Analytic and Experimental Study of Jet Deflection in a Cross Flow. Paper No. 16.

1967 (Concluded)

98. Fan, L.: Turbulent Buoyant Jets into Stratified or Flowing Ambient Fluids. Rept. No. KH-R-15, Keck Hyd. Lab., Calif. Inst. Tech., June 1967.

99. Garner, J. E.: A Review of Jet Efflux Studies Applicable to V/STOL Aircraft. AEDC-TR-67-163, Sept. 1967.

141. Reichenau, D. E. A.: Interference Effects Produced by a Cold Jet Issuing Normally to the Airstream from a Flat Plate at Transonic Mach Numbers. AEDC TR-67-220, Oct. 1967.

146. Spring, D. J., Street, T. A., and Amick, J. L.: Transverse Jet Experiments and Theories - A Survey of the Literature. U. S. Army Missile Command Rept. No. RD-TR-67-4, June 1967.

1968

4. Rubbert, P. E. and Saaris, G. R.: A General Three-Dimensional Potential-Flow Method Applied to V/STOL Aerodynamics. Air Transportion Meeting, NY, Apr. 29 - May 2, 1968.

16. Margason, R. J.: The Path of a Jet Directed at Large Angles to a Subsonic Free Stream. NASA TN D-4919, Nov. 1968.

38. Platten, J. L. and Keffer, J. F.: Entrainment in Deflected Axisymmetric Jets at Various Angles to the Stream. UTME-TP 6808, June 1968.

77. Margason, R. J. and Gentry, G. L.: Aerodynamic Characteristics of a Five-Jet VTOL Configuration in the Transition Speed Range. NASA TN D-4812, Oct. 1968.

92. Margason, R. J.: A Discussion of V/STOL Propulsion Induced Effects on the Aircrafts' Aerodynamics. Notes for Lecture Presented at the U. of Tenn. Space Inst. Short Course on V/STOL, Nov. 1968.

132. Street, T. A. and Spring, D. J.: Experimental Investigation of a Transverse Jet Injecting from a Flat Plate into a Mach Number 5.0 Free Stream. U. S. Army Missile Command, Rept. No. RD-TM-68-6, Aug. 1968.

139. Spring, D. J. and Street, T. A.: Experimental Investigation of the Pressure Distributions Induced upon a Body of Revolution by Several Transverse Jets at Low Speeds. U. S. Army Missile Command Rept. No. RD-TM-68-7, Aug. 1968.

140. Cassel, L. A., Davis, J. G., and Engh, D. P.: Lateral Jet Control Effectiveness Prediction for Axisymmetric Missile Configurations. U. S. Army Missile Command Rept. No. RD-TR-68-5, June 1968.

1969

26. NASA SP-218, NASA Symposium on Analysis of a Jet in a Subsonic Crosswind held at Langley Research Center, Hampton, VA, Sept. 9-10, 1969.

    (a) Jet-Wake Characteristics and Their Induced Aerodynamic Effects on V/STOL Aircraft in Transition Flight. Margason, R. J. and Fearn, R. L.

    (b) The Physical Nature of the Subsonic Jet in a Cross-Stream. Keffer, J. F.

    (c) The Aerodynamics of the Lifting Jet in a Cross Flowing Stream. Hackett, J. E. and Miller, H. R.

    (d) Experimental Investigation of Pressures Induced on a Flat Plate by a Jet Issuing into a Subsonic Crosswind. McMahon, H. M. and Mosher, D. K.

    (e) Experimental Reaction Jet Effects at Subsonic Speeds. Street, T. A. and Spring, D. J.

    (f) A Blockage-Sink Representation of Jet Interference Effects for Noncircular Jet Orifices. Wu, J. C. and Wright, M. A.

    (g) Development of an Analytical Model for the Flow of a Jet into a Subsonic Crosswind. Wooler, P. T.

    (h) Numerical Treatment of Line Singularities for Modeling a Jet in a Low-Speed Cross Flow. Skifstad, J. G.

    (i) Analytic Descrption of Jet-Wake Cross Sections for a Jet Normal to a Subsonic Free Stream. Margason, R. J.

    (j) Cross Wing Effects of Trajectory and Cross Sections of Turbulent Jets. Braun, G. W. and McAllister, J. D.

    (k) A General Jet Efflux Simulation Model. Heltsley, F. L. and Kroeger, R. A.

    (l) Calculation of Jet Interference Effects on V/STOL Aircraft by a Nonplanar Potential Flow Method. Rubbert, P. E.

    (m) Inviscid Models for the Pressure Induced by a Jet Transverse to a Subsonic Stream. Rosen, R., Durando, N. A., and Cassel, L. A.

(n) The Use of Matched Asymptotic Expansions as an Approach to the Problem of the Jet in a Crossflow. Werner, J. E.

(o) Mass Entrainment of a Circular Jet in a Cross Flow. Fearn, R. L.

47. Stockman, N. O.: Potential Flow Solutions for Inlets of VTOL Lift Fans and Engines. Analytical Methods in Aircraft Aerodynamics. NASA SP-228, Oct. 28-30, 1969.

48. Stockman, N. O. and Lieblein, S.: Theoretical Analysis of Flow in VTOL Lift Fan Inlets Without Crossflow. NASA TN D-5065, Feb. 1969.

65. Carter, A.: Effects of Jet-Exhaust Location on the Longitudinal Aerodynamic Characteristics of a Jet V/STOL Model. NASA TN D-5333, July 1969.

83. Wu, J. C., Mosher, D. K., and Wright, M. A.: Experimental and Analytical Investigations of Jets Exhausting into a Deflecting Stream. AIAA Paper No. 69-223, Feb. 1969.

85. Winston, M. M.: Wind-Tunnel Data from a 0.16-Scale V/STOL with Direct-Lift and Lift-Cruise Jets. NASA TM X-1758, Mar. 1969.

95. Wooler, P. T.: Flow of a Circular Jet into a Cross Flow. J. Aircraft, vol. 6, no. 3, May-June 1969.

126. Bowley, W. W. and Sucec, J.: Trajectory and Spreading of a Turbulent Jet in the Presence of a Crossflow of Arbitrary Velocity Distribution. Presented at 14th Annual Gas Turbine Conference and Products Show, ASME Paper 69-GT-33, Mar. 1969.

142. Wygnanski, I.: Two-Dimensional Turbulent Jet in a Uniform Parallel Stream. AIAA Journal, vol. 7, no. 1, Jan. 1969.

147. Cassel, L. A., Durando, N. A., Bullard, C. W., and Kelso, J. M.: Jet Interaction Control Effectiveness for Subsonic and Supersonic Flight. MICOM Rept. No. RD-TR-69-21, Sept. 1969.

1970

10. Margason, R. J.: Review of Propulsion-Induced Effects on Aerodynamics of Jet/STOL Aircraft. NASA TN D-5617, Feb. 1970.

23. Hodder, B. K., Kirk, J. V., and Hall, L. P.: Aerodynamic Characteristics of a Large-Scale Model with a Lift Fan Mounted in a 5-Percent-Thick Triangular Wing, Including the Effects of BLC on the Lift-Fan Inlet. NASA TN D-7031, Dec. 1970.

50. Serdengecti, S. A. and Marble, F. E.: A Theory of Two-Dimensional Airfoils with Strong Inlet Flow on the Upper Surface. ARL 70-0139, Aug. 1970.

78. Rosen, R. and Cassel, L. A.: Secondary Jet Interaction with a Subsonic Mainstream. J. Aircraft, vol. 7, no. 1, Jan-Feb. 1970.

90. Skifstad, J. G.: Aerodynamics of Jets Pertinent to VTOL Aircraft. J. Aircraft, vol. 7, no. 3, May-June 1970.

114. Fricke, L. B., Wooler, P. T., and Ziegler, H.: A Wind Tunnel Investigation of Jets Exhausting into a Crossflow. AFFDL-TR-70-154, vol. I, Dec. 1970.

115. Fricke, L. B., Wooler, P. T., and Ziegler, H.: A Wind Tunnel Investigation of Jets Exhausting into a Crossflow. AFFDL-TR-70-154, vol. IV, Dec. 1970.

116. Mosher, D. K.: An Experimental Investigation of a Turbulent Jet in a Cross Flow. Georgia Inst. of Tech. Rept GIT-AER-70-715, Dec. 1970. (Ph.D. Thesis)

117. Fricke, L. B., Wooler, P. T., and Ziegler, H.: A Wind Tunnel Investigation of Jets Exhausting into a Crossflow. AFFDL-TR-70-154, vol. III, Dec. 1970.

144. Frick, L. B., Wooler, P. T., and Ziegler, H.: A Wind Tunnel Investigation of Jets Exhausting into a Crossflow. AFFDL-TR-70-154, vol. II, Dec. 1970.

152. Street, T. A.: An Experimental Investigation of a Transverse Jet Ejecting from a Flat Plate into a Subsonic Free Stream. U. S. Army Missile Command Rept. No. RD-TM-70-5, May 1970.

1971

1. Hu, G.: An Analysis of a Two-Dimensional Propulsion Wing. Stanford Univ., Mar. 1971. (Ph.D. Thesis)

37. Platten, J. L. and Keffer, J. F.: Deflected Turbulent Jet Flows. J. Appl. Mech., Dec. 1971, pp. 756-758.

60. Kirk, J. V., Hall, L. P., and Hodder, B. K.: Aerodynamics of Lift Fan Aircraft. NASA TM X-62086, Sept. 1971.

61. McMahon, H. M., Hester, D. D., and Palfrey, J. G.: Vortex Shedding from a Turbulent Jet in a Cross Wind. J. Fluid Mech., vol. 48, part 1, 1971, pp. 73-80.

101. Durando, N. A.: Vortices Induced in a Jet by Subsonic Crossflow. AIAA Journal, vol. 9, no. 2, Feb. 1971.

113. Hackett, J. E. and Miller, H. R.: A Theoretical Investigation of a Circular Lifting Jet in a Cross-Flowing Mainstream. AFFDL-TR-70-170, Jan. 1971.

118. Lieblein, S., Yuska, J. A., and Diedrich, J. H.: Wind Tunnel Tests of a Wing-Installed Model VTOL Lift Fan with Coaxial Drive Turbine. NASA TM X-67854, 1971.

1972

6. Rubbert, P. E. and Saaris, G. R.: Review and Evaluation of a Three-Dimensional Lifting Potential Flow Analysis Method for Arbitrary Configurations. Presented at AIAA 10th Aerospace Sciences Meeting, San Diego, CA, Jan. 17-19, 1972.

36. Ousterhout, D. S.: An Experimental Investigation of a Cold Jet Emitting from a Body of Revolution into a Subsonic Free Stream. NASA CR-2089, Aug. 1972.

104. Souillier, A.: Testing at S1.MA for Basic Investigations on Jet Interactions: Distributions of Pressure Around the Jet Orifice. NASA TT F-14066, Jan. 1972.

105. Souillier, A.: Testing at S1.MA for Basic Investigations on Jet Interactions: Distribution of Pressure and Velocities in the Jet using the Ideal Standard Nozzle (In Unheated State). NASA TT F-14072, Jan. 1972.

111. Kamotani, Y. and Greber, I.: Experiments on a Turbulent Jet in a Cross Flow. AIAA Journal, vol. 10, no. 11, Nov. 1972.

112. Hoult, D. F. and Weil, J. C.: "Turbulent Plume in a Laminar Cross Flow." Atmospheric Environment, vol. 6, 1972, pp. 513-531.

119. Yuska, J. A. and Diedrich, J. H.: Fan and Wing Force Data from Wind-Tunnel Investigation of a .38-meter (15-in.) Diameter VTOL Model Lift Fan Installed in a Two-Dimensional Wing. NASA TN D-6654, Mar. 1972.

121. Chang, H. S. and Werner, J. E.: Analysis of an Entrainment Model of the Jet in a Crossflow. NASA CR-132324, Nov. 1972.

1973

35. Viehweger, G.: Aerodynamic Interference Between Fuselage and Lifting Jets Emerging From Its Lower Part. AGARD-CP-135, Sept. 1973.

42. Mikvolowsky, W. and McMahon, H.: An Experimental Investigation of a Jet Issuing from a Wing in Crossflow. J. Aircraft, vol. 10, no. 9, Sept. 1973, pp. 546-553.

44. Lieblein, S., Yuska, J. A., and Diedrich, J. H.: Performance Characteristics of a Model VTOL Lift Fan in Crossflow. J. Aircraft, vol. 10, no. 3, Mar. 1973, pp. 131-136.

55. Campbell, J. F. and Schetz, J. A.: Analysis of the Injection of a Heated Turbulent Jet Into a Crossflow. NASA TR R-413, Dec. 1973.

57. Stoy, R. L. and Ben-Haim, Y.: Turbulent Jets in a Confined Crossflow. J. Fluid Eng., Dec. 1973, pp.551-556.

100. Wu, J.: Near-Field Trajectory of Turbulent Jets Discharged at Various Inclinations into a Uniform Crossflow. AIAA Journal, vol. 11, no. 11, Nov. 1973.

107. Harms, L.: Experimental Investigation of the Flow Field of a Hot Turbulent Jet with Lateral Flow. Part 2. NASA TT F-15706, Sept. 1973.

110. Campbell, J. F. and Schetz, J. A.: Flow Properties of Submerged Heated Effluents in a Waterway. AIAA Journal, vol. 11, no. 2, Feb. 1973.

120. Heltsley, F. L. and Parker, R. L., Jr.: Application of the Vortex Lattice Method to Represent a Jet Exhausting from a Flat Plate into a Crossflowing Stream. AEDC-TR-73-57, June 1973.

122. Ziegler, H. and Wooler, P. T.: Analysis of Stratified and Closely Spaced Jets Exhausting into a Crossflow. NASA CR-132297, Nov. 1973.

123. Shaw, C. S. and Margason, R. J.: An Experimental Investigation of a Highly Sonic Jet Ejecting from a Flat Plate into a Subsonic Crossflow. NASA TN D-7314, Dec. 1973.

124. Nece, R. E. and Littler, J. D.: Round Horizontal Thermal-Buoyant Jet in a Cross Flow. Charles W. Harris Hydraulics Lab. TR-34, June 1973.

125. Petty, J. S.: Final Report on Work Unit 08 (V/STOL Aerodynamics), ARL-73-0164, Nov. 1973.

129. Snel, H.: A Potential Flow Model for the Flow Field Induced by a Jet Exhausting into a Uniform Cross Flow. NLR TR 73048 U, Apr. 1973.

2. Camelier, I.: An Experimental Study of the Structures and Acoustic Field of a Jet in a Cross Stream. Stanford Univ., Dec. 1974, (Ph.D. Thesis).

41. Fearn, R. L. and Weston, R. P.: Vorticity Associated with a Jet in a Crossflow. AIAA Journal, vol. 12, no. 12, Dec. 1974, pp. 1666-1671.

54. Kamotani, Y. and Greber, I.: Experiments on Confined Turbulent Jets in Cross Flow. NASA CR-2392, Mar. 1974.

59. Chassaing, J., George, J., Claria, A., and Sananes, F.: Physical Characteristics of Subsonic Jets in a Cross-Stream. J. Fluid Mech., vol. 62, part 1, 1974, pp. 41-64.

86. Mineck, R. E. and Margason, R. J.: Pressure Distribution on a Vestored-Thrust V/STOL Fighter in the Transition-Speed Range. NASA TM X-2867, Mar. 1974.

106. Harms, L.: Experimental Investigation of the Flow Field of a Hot Turbulent Jet with Lateral Flow. Part 1. NASA TT F-15707, June 1974.

128. AGARD CP-143, AGARD Conference on V/STOL Aerodynamics held at Delft, Netherlands, Apr. 24-26, 1974.

(a) Snel, H.: A Method for the Calculation of the Flow Field Induced by a Jet Exhausting Perpendicularly into a Cross Flow. Paper No. 18.

(b) Ransom, E. C. P. and Wood, P. M.: A Literature Survey on Jets in Crossflow. Paper No. 26.

131. Carter, H. H. and Regier, R.: Three Dimensional Heated Surface Jet in a Cross Flow. John Hopkins Univ. TR 88, Nov. 1974.

135. Snel, H.: A Model for the Calculation of the Properties of a Jet in a Cross Flow. NLR-TR-74080-V, June 1974.

138. Endo, H.: A Working Hypothesis for Predicting the Path and Induced Velocity of a Jet Exhausting at a Large Angle into a Uniform Cross Flow. Japan Soc. for Aeronaut. and Space Sci., Transactions, vol. 17, no. 36, pp. 45-64.

1975

39. Fearn, R. L. and Weston, R. P.: Induced Pressure Distribution of a Jet in a Crossflow. NASA TN D-7916, June 1975.

40. Weston, R. P.: A Description of the Vortex Pair Associated with a Jet in a Crossflow. Navy Workshop on Prediction Methods for Jet V/STOL Propulsion Aerodynamics. July 28-31, 1975.

88. Chien, J. C. and Schetz, J. A.: Numerical Solution of the Three-Dimensional Navier-Stokes Equations with Applications to Channel Flows and a Buoyant Jet in a Cross Flow. J. Appl. Mech., vol. 42, Sept. 1975, pp. 575-579.

89. Winston, M. M., Weston, R. P., and Mineck, R. E.: Propulsion-Induced Interference Effects on Jet-Lift VTOL Aircraft. AIAA Paper No. 75-1215, Oct. 1975.

102. Sterland, P. R. and Hollingsworth, M. A.: An Experimental Study of Multiple Jets Directed Normally to a Cross-Flow. J. Mech. Eng. Sci., vol. 17, no. 3, June 1975.

130. Sellers, W. L., III: A Model for the Vortex Pair Associated with a Jet in a Cross Flow, NASA CR-136756, Mar. 1975.

133. Yeh, B. T.: Calculation of the Pressure Distribution Induced by a Jet on a Flat Plate. ESRO-TT-159, May 1975.

134. Graefe, H. J.: Analysis of the Flow Field of Cross-Blown Lifting Jets by Flow-Field Measurements. ESA TT-165, June 1975.

136. Practical Problems on Longitudinal and Cross-Blown Free Jets: The Simulation of Engine Jets in Wind Tunnels. Rept. on the Conference of the D.G.L.R. Technical Committee 2A1 on Fixed-Wing Aircraft held at Porz-Wahn, W. Germany, Dec. 6, 1973. ESA TT-206, Nov. 1975.

(a) Harms, L.: Investigation into the Flow Field of a Hot Jet in a Cross Flow.

(b) Graefe, H. J.: Measurements in the Outer Field of Jets Blown Across their Axis.

(c) Graefe, H. J.: The Injector Effect of Free Jets at High Mach Numbers.

(d) Viehweger, G.: Mutual Interference Between Propulsive Jets and Interference with the Fuselage, Wing, and the Ground.

1975 (Concluded)

(e) Viehweger, G.: An Attempt to Separate the Influence of the Injector Effect from the Displacement Effect of a Free Jet Blown Across its Axis.

137. Dietz, W. E., Jr.: A Method for Calculating the Induced Pressure Distribution Associated with a Jet in a Crossflow. NASA CR-146434, 1975.

153. Camelier, I., Karamcheti, K., and Hodder, B.: An Experimental Study of the Structures and Acoustic Field of a Jet in a Cross Stream. AIAA Paper No. 75-460, Mar. 1975.

1976

53. Sucec, J. and Bowley, W. W.: Prediction of the Trajectory of a Turbulent Jet Injected into a Crossflowing Stream. ASME Paper No. 76-FE-8, Mar. 1976.

66. Platzer, M. F. and Margason, R. J.: Prediction Methods for Jet V/STOL Propulsion Aerodynamics. AIAA Paper No. 76-932, Sept. 1976.

67. Morris, P. J.: Turbulence Measurements in Subsonic and Supersonic Axisymmetric Jets in a Parallel Stream. AIAA Journal, vol. 14, no. 10, Oct. 1976, pp. 1468-1475.

68. Antonia, R. A. and Bilger, R. W.: The Heated Round Jet in a Co-Flowing Stream. AIAA Journal, vol. 14, no. 11, Nov. 1976, pp. 1541-1547.

69. Rolls, L. S., Quigley, H. C., and Perkins, R. G., Jr.: Review of V/STOL Lift/Cruise Fan Technology. AIAA Paper No. 76-931, Sept. 1976.

70. Giesing, J. P.: Correction Factor Techniques for Improving Aerodynamic Prediction Methods. NASA CR-144967, May 1976.

71. Siclari, M. J., et al.: Development of Theoretical Models for Jet-Induced Effects on V/STOL Aircraft. J. Aircraft, vol. 13, no. 12, Dec. 1976, pp. 938-944.

103. Rudinger, G. and Moon, L. F.: Laser-Doppler Measurements in a Subsonic Jet Injected into a Subsonic Cross Flow. J. Fluid Eng., vol. 98, series I, no. 3, Sept. 1976.

150. Viehweger, G.: Flow Effects with Cross-Blown Lifting Jets of V/STOL Aircraft and their Reaction on Aerodynamical Forces and Moments of the Nacelle. NASA TM-75143, July 1976.

1977

43. Moussa, Z. M., Trischka, J. W., and Eskinazi, S.: The Near Field in the Mixing of a Round Jet with a Cross-stream. J. Fluid Mech., vol. 80, part 1, Apr. 1977, pp. 49-80.

52. Kotansky, D. R. and Bower, W. W.: Viscous Flowfields and Airframe Forces Induced by Two-Dimensional Lift Jets in Ground Effect. Rept. ONR-CR215-246-1, Mar. 1977.

96. Groesbeck, D. E., Huff, R. G., and von Glahn, U. H.: Comparison of Jet Mach Number Decay Data with a Correlation and Jet Spreading Contours for a Large Variety of Nozzles. NASA TN D-8423, June 1977.

145. Taylor, P.: An Investigation of an Inclined Jet in a Crosswind. Aeronaut. Quart., vol. XXVIII, part 1, Feb. 1977.

149. Bergeles, G., Gosman, A. D., and Launder, B. E.: Near-Field Character of a Jet Discharged through a Wall at 30° to a Mainstream. AIAA Journal, vol. 15, no. 4, Apr. 1977.

REFERENCES

1. Vogler, R. D.: Surface Pressure Distributions Induced on a Flat Plate by a Cold Air Jet Issuing Perpendicularly from the Plate and Normal to a Low-Speed Free-Stream Flow. NASA TN D-1629, Mar. 1963.

2. Bradbury, L. J. S. and Wood, M. N.: The Static Pressure Distribution Around a Circular Jet Exhausting Normally from a Plane Wall into an Airstream. Aeronaut. Res. Council C. P. No. 882, Aug. 1965.

3. Ousterhout, D. S.: An Experimental Investigation of a Cold Jet Emitting from a Body of Revolution into a Subsonic Free Stream. NASA CR-2089, Aug. 1972.

4. Fearn, R. L. and Weston, R. P.: Induced Pressure Distribution of a Jet in a Crossflow. NASA TN D-7916, June 1975.

5. Mosher, D. K.: An Experimental Investigation of a Turbulent Jet in a Cross Flow. Georgia Inst. of Tech. Rept. GIT-AER-70-715, Dec. 1970 (Ph.D. Thesis).

6. Dietz, W. E., Jr.: A Method for Calculating the Induced Pressure Distribution Associated with a Jet in a Crossflow. NASA CR-146434, 1975.

7. Yeh, B. T.: Calculation of the Pressure Distribution Induced by a Jet on a Flat Plate. ESRO-TT-159, May 1975.

8. Heltsley, F. L. and Parker, R. L., Jr.: Application of the Vortex Lattice Method to Represent a Jet Exhausting from a Flat Plate into a Crossflowing Stream. AEDC-TR-73-57, June 1973.

9. Hackett, J. E. and Miller, H. R.: A Theoretical Investigation of a Circular Lifting Jet in a Cross-Flowing Mainstream. AFFDL-TR-70-170, Jan. 1971.

10. Chang, H. S. and Werner, J. E.: Analysis of an Entrainment Model of the Jet in a Crossflow. NASA CR-132324, Nov. 1972.

11. Margason, R. J.: The Path of a Jet Directed at Large Angles to a Subsonic Free Stream. NASA TN D-4919, Nov. 1968.

12. Maskew, Brian: Calculation of the Three-Dimensional Potential Flow Around Lifting Nonplanar Wings and Wing-Bodies using a Surface Distribution of Quadrilateral Vortex Rings. Report TT-7009, Loughborough University of Technology, Sept. 1970.

13. Keffer, J. F. and Baines, W. D.: The Round Turbulent Jet in a Cross-Wind. J. Fluid Mech., Vol. 15, part 4, Apr. 1963, pp. 481-497.

REFERENCES (Concluded)

14. Fearn, R. L. and Weston, R. P.: Vorticity Associated with a Jet in a Crossflow. AIAA Journal, vol. 12, no. 12, Dec. 1974, pp. 1666-1671.

15. Kamotani, Y. and Greber, I.: Experiments on a Turbulent Jet in a Cross Flow. AIAA Journal, vol. 10, no. 11, Nov. 1972.

16. Pratte, B. D. and Baines, W. D.: Profiles of the Round Turbulent Jet in a Cross Flow. J. Hydraulics Div., Proceedings of the ASCE, vol. 92, no. HY6, Nov. 1967, pp. 53-64.

17. Camelier, I., Karamcheti, K., and Hodder, B.: An Experimental Study of the Structures and Acoustic Field of a Jet in a Cross Stream. AIAA Paper No. 75-460, Mar. 1975.

18. Bowley, W. W. and Sucec, J.: Trajectory and Spreading of a Turbulent Jet in the Presence of a Crossflow of Arbitrary Velocity Distribution. Presented at 14th Annual Gas Turbine Conference and Products Show, ASME Paper 69-GT-33, Mar. 1969.

19. Abramovich, G. N.: <u>The Theory of Turbulent Jets.</u> M.I.T. Press, 1963.

20. Taylor, P.: An Investigation of an Inclined Jet in a Crosswind. Aeronaut. Quart., Vol. XXVIII, part 1, Feb. 1977.

TABLE I.- REFERENCES USED TO DEVELOP CORRELATION METHOD

Ref. No.	V_j/V_∞	θ	M_j	Re_D ($\times 10^{-6}$)	Re_ℓ ($\times 10^{-6}$)	ℓ/D	$(r/D)_{max}$	Type of Data[1]
1	1.00	0°	0.18	0.106	2.125	20	10	G, C
	1.25	↓	0.18	0.085	1.700	↓	↓	↓
	1.25		0.45	0.213	4.250			
	1.67		0.18	0.064	1.275			
	1.67		0.45	0.159	3.188			
	2.50		0.18	0.043	0.850			
	2.50		0.45	0.106	2.125			
	3.33		0.45	0.080	1.590			
	5.00		0.91	0.106	2.125			G
2	2.00	0°	0.107	0.031	0.109	42	15	C
	4.00	↓	0.213	↓	↓	↓	↓	↓
	8.00		0.426					
3	2.38	0°	0.19	0.018	0.857	48	10	G, T
	2.85	↓	0.23	↓	↓	↓	↓	↓
	3.33		0.27					
4	2.20	0°	0.39	0.42	3.78	9	6	G, T, C
	2.80	↓	0.44	0.37	3.33	↓	↓	↓
	3.90		0.75	0.45	4.03			
	5.10		0.95	0.44	3.95			
	6.10		0.94	0.36	3.27			
	7.00		0.94	0.32	2.85			
	8.00		0.93	0.27	2.47			
	10.00		0.93	0.22	1.97			
5	4.0	0°	0.178	0.052	0.625	12	8	C
	8.0	↓	0.355	↓	↓	↓	↓	↓
	10.0		0.444					
20	12.0	0°	0.533	0.013	0.256	20	5	C, G
	↓	15°	↓	↓	↓	↓	↓	↓
		30°						
		45°						
		60°						

[1]Method of presentation of data:

C - pressure contours on plate

G - graphical data (C_p vs r/D for β = constant or C_p vs β for r/D = constant)

T - tabulated data

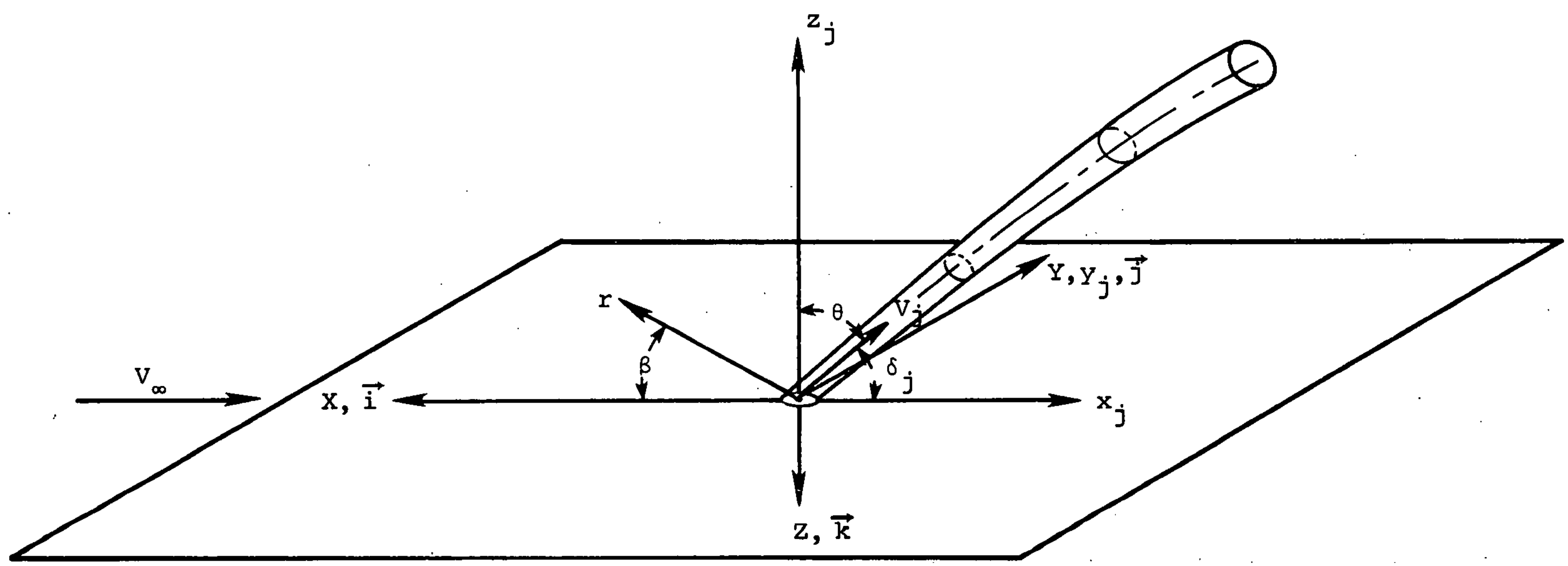

(a) Isometric view.

Figure 1.- Coordinate system for a jet issuing from a flat plate into a subsonic crossflow.

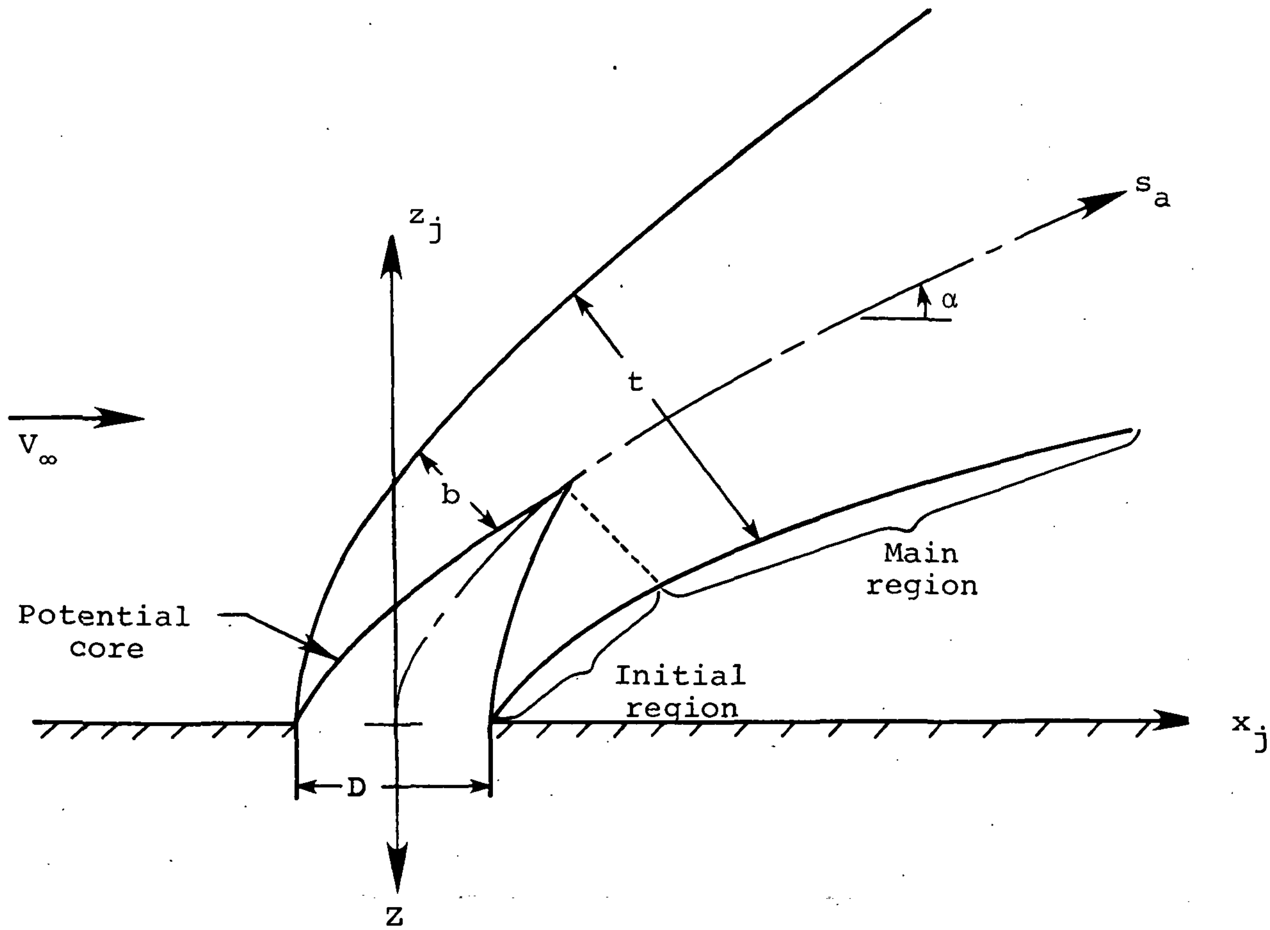

(b) Side view.

Figure 1.- Concluded.

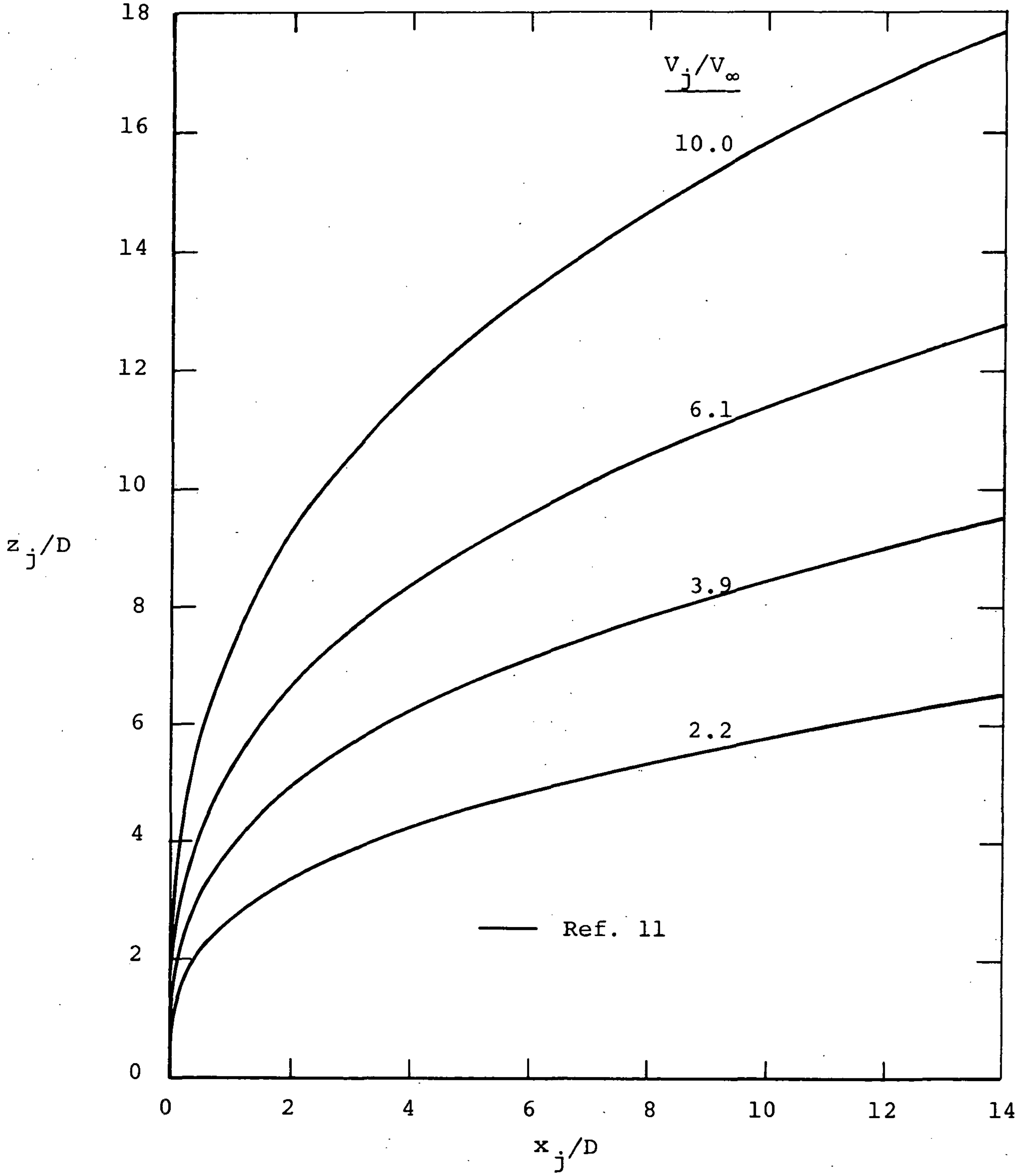

Figure 2.- Centerline shapes for a jet exhausting normal to a plate.

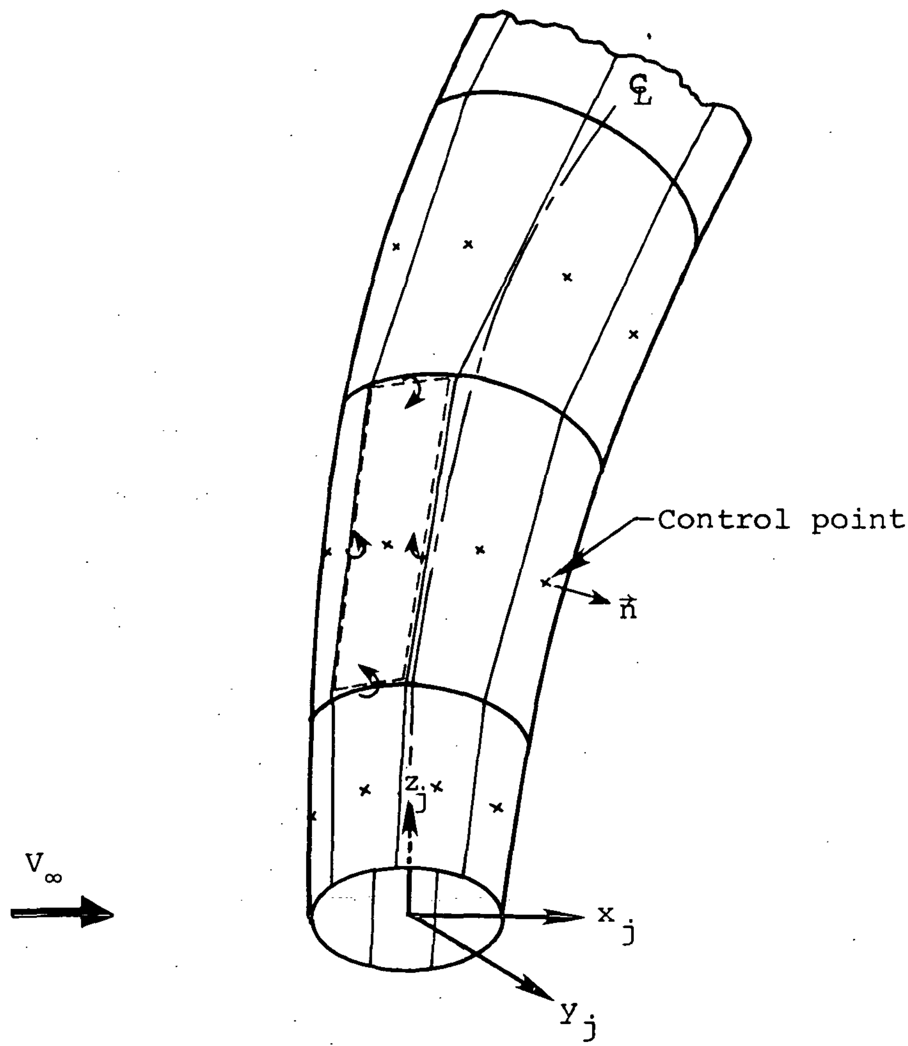

Figure 3.- Vortex quadrilaterals on wake surface.

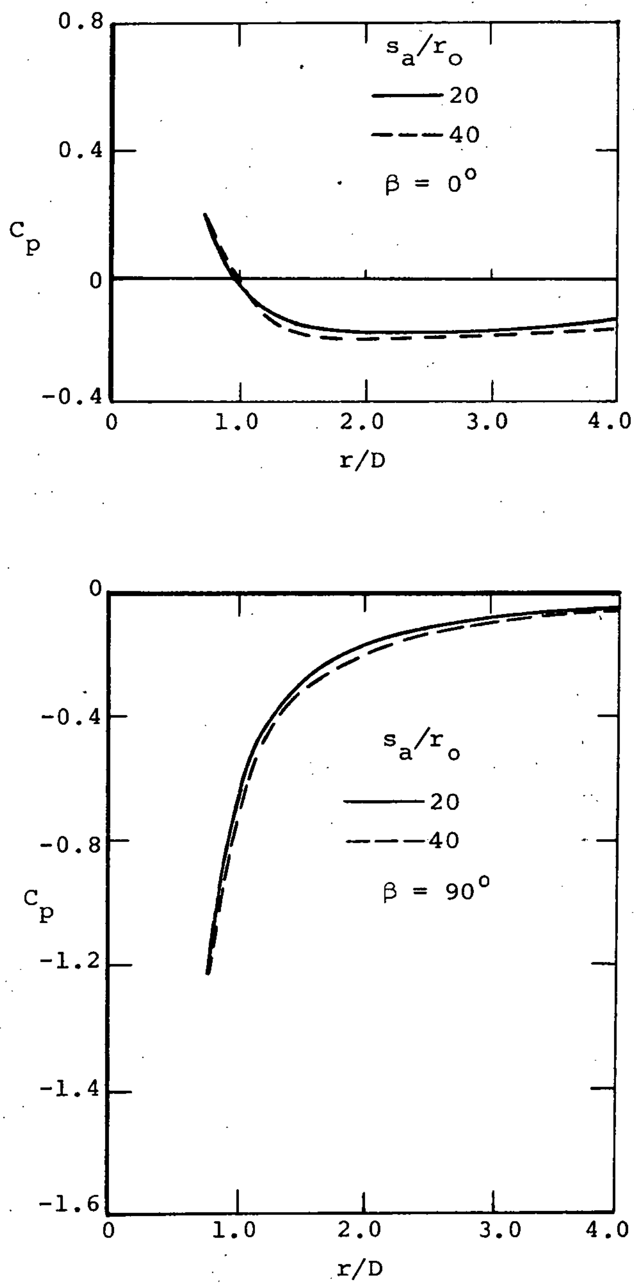

Figure 4.- Effect of the length of the entrainment model singularity distribution on the predicted flat plate pressure coefficient near a jet, $V_j/V_\infty = 8.0$, $\delta_j = 90°$.

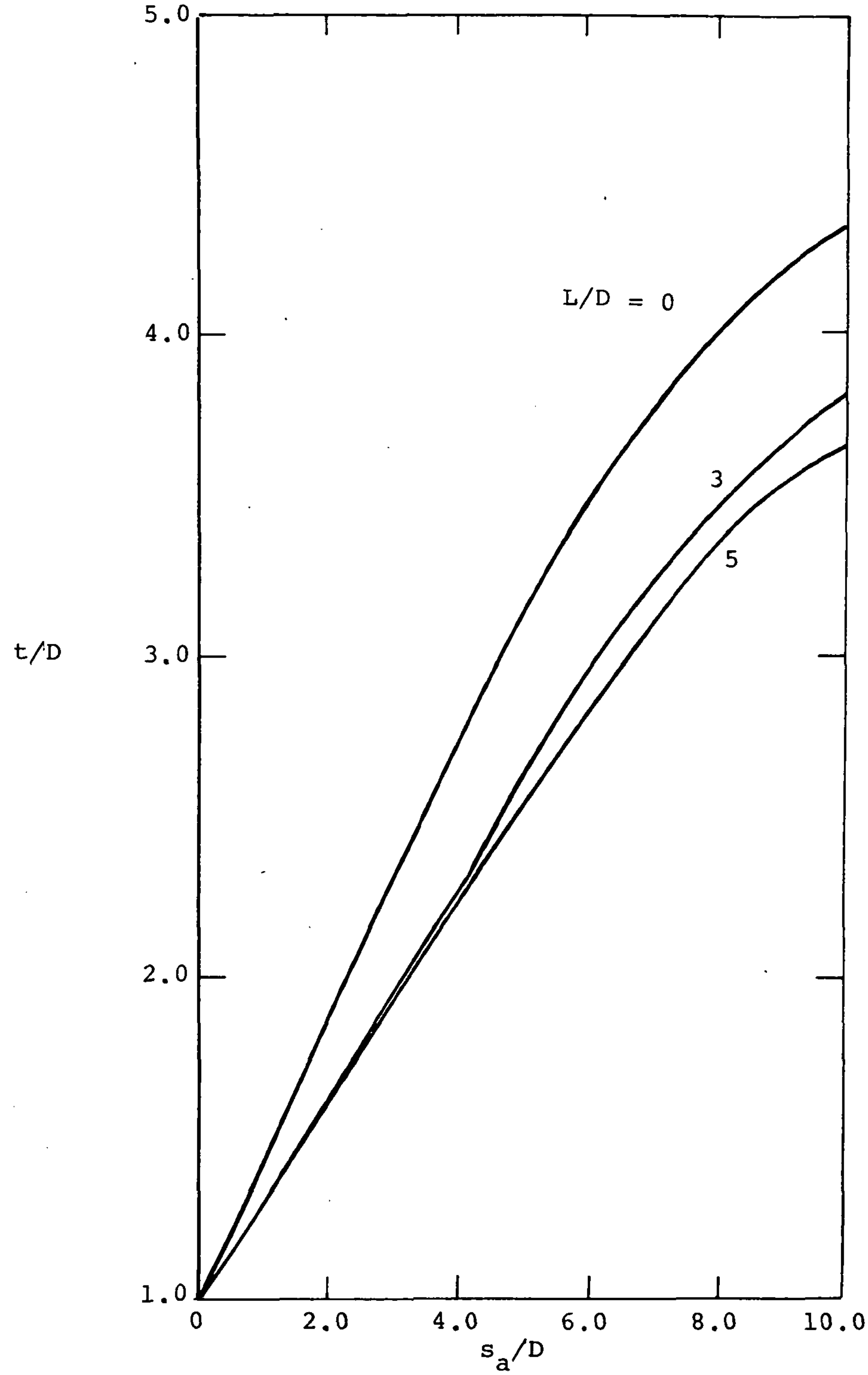

(a) $V_j/V_\infty = 4.0$.

Figure 5.- Effect of initial region length on predicted jet spreading rates.

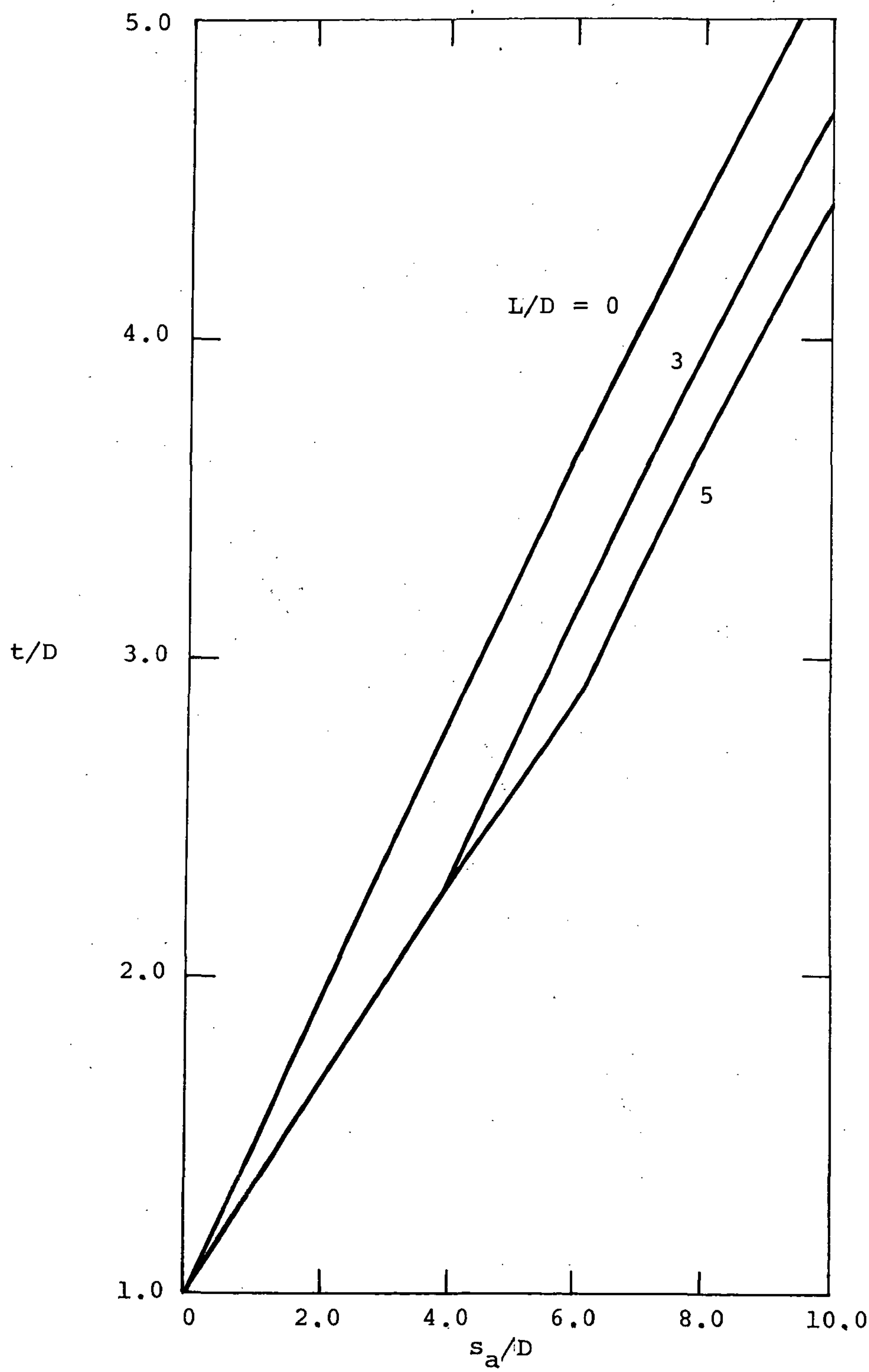

(b) $V_j/V_\infty = 8.0$.

Figure 5.- Concluded.

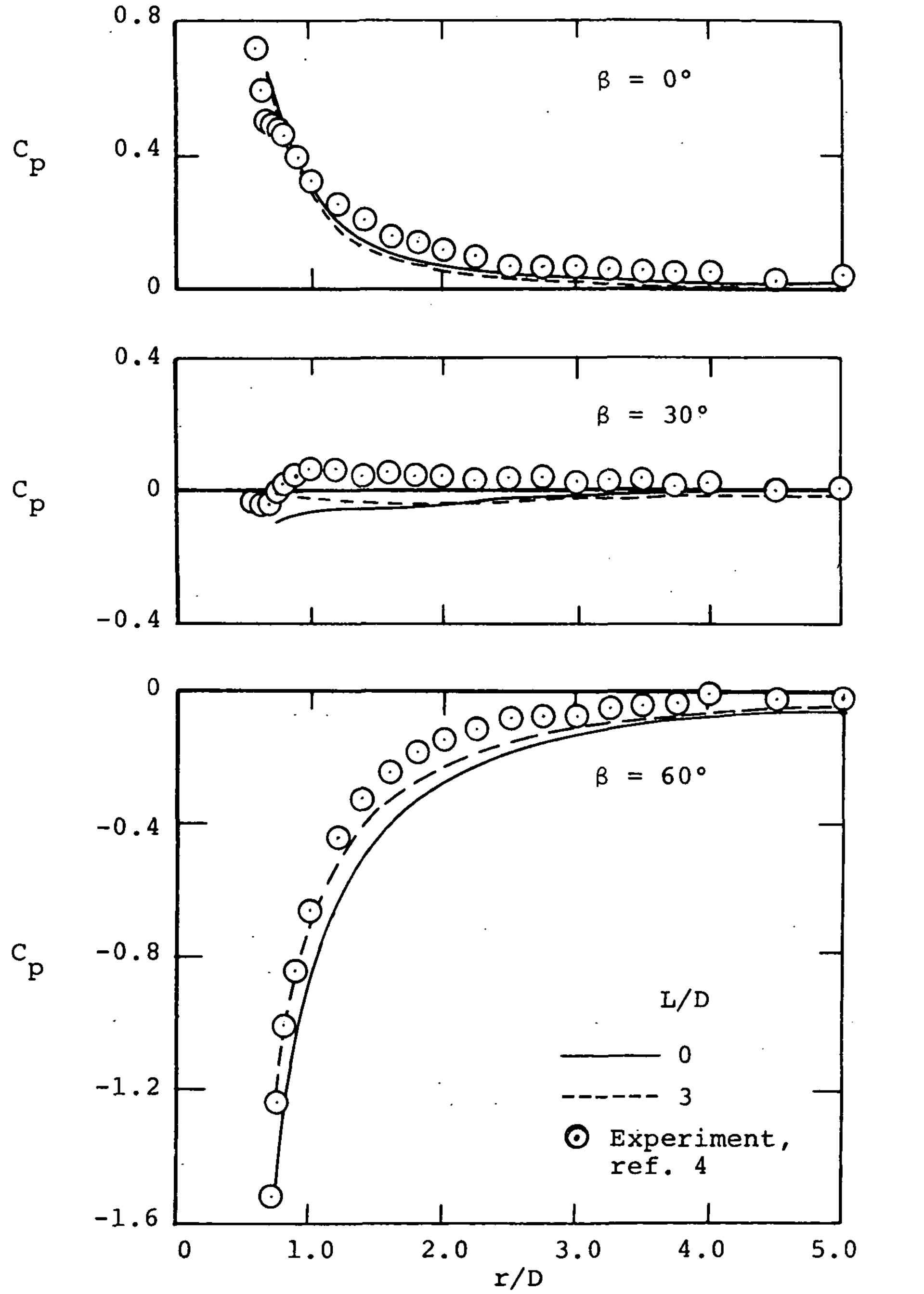

Figure 6.- Effect of initial region length on the predicted pressure distribution on a flat plate, $V_j/V_\infty \approx 4$.

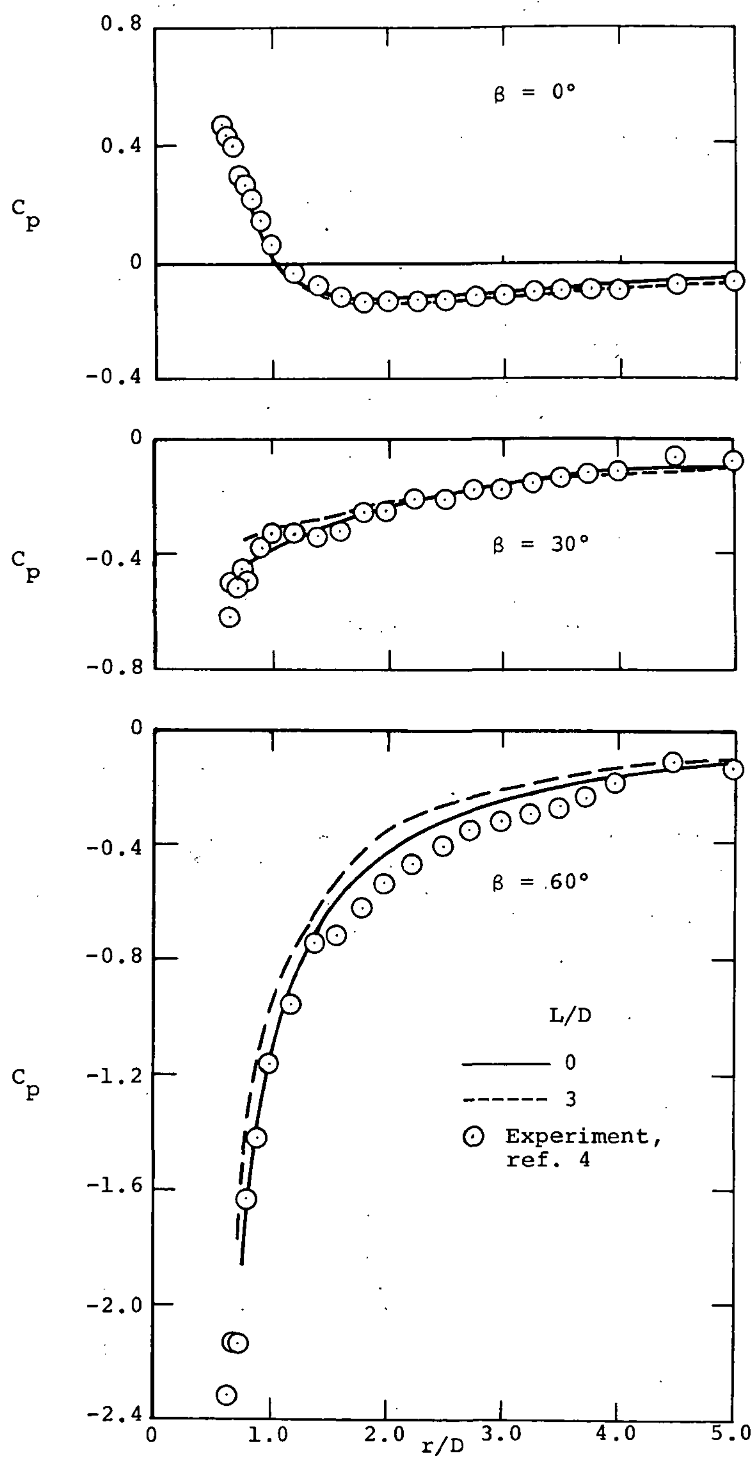

Figure 7.- Effect of initial region length on the predicted pressure distribution on a flat plate, $V_j/V_\infty = 8.0$.

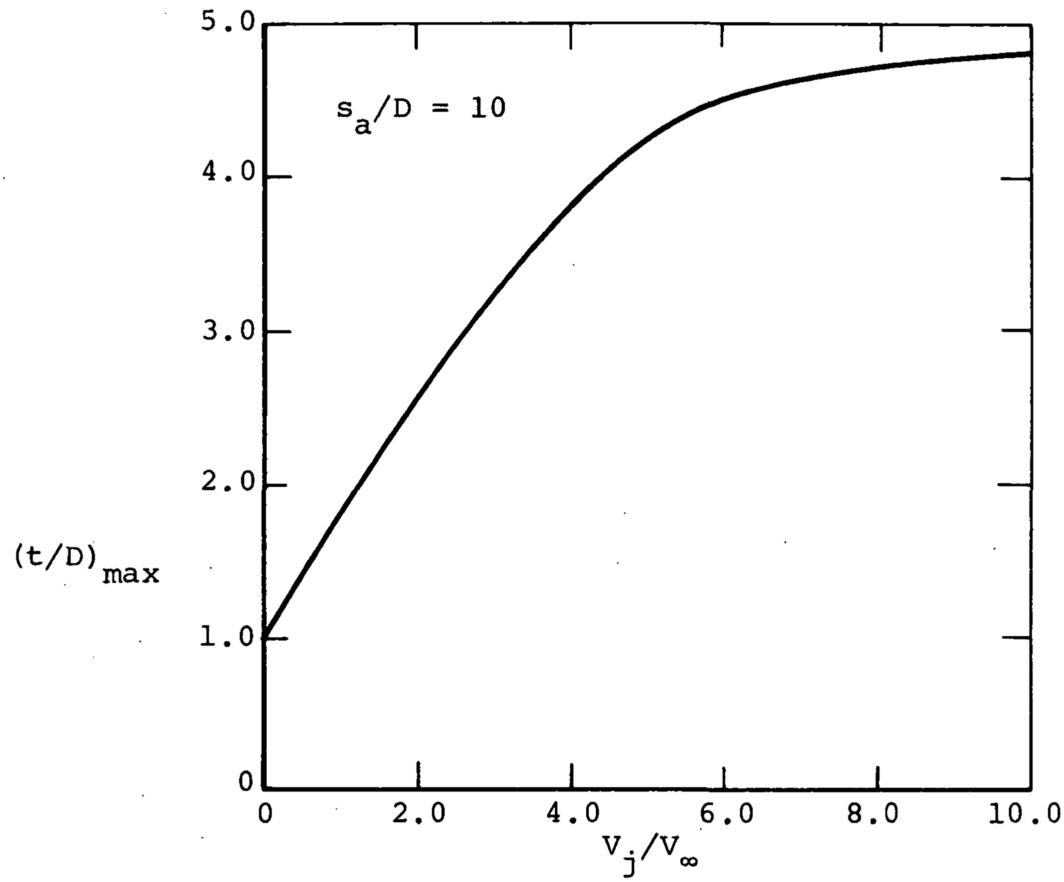

Figure 8.- Maximum jet thickness variation with jet velocity ratio.

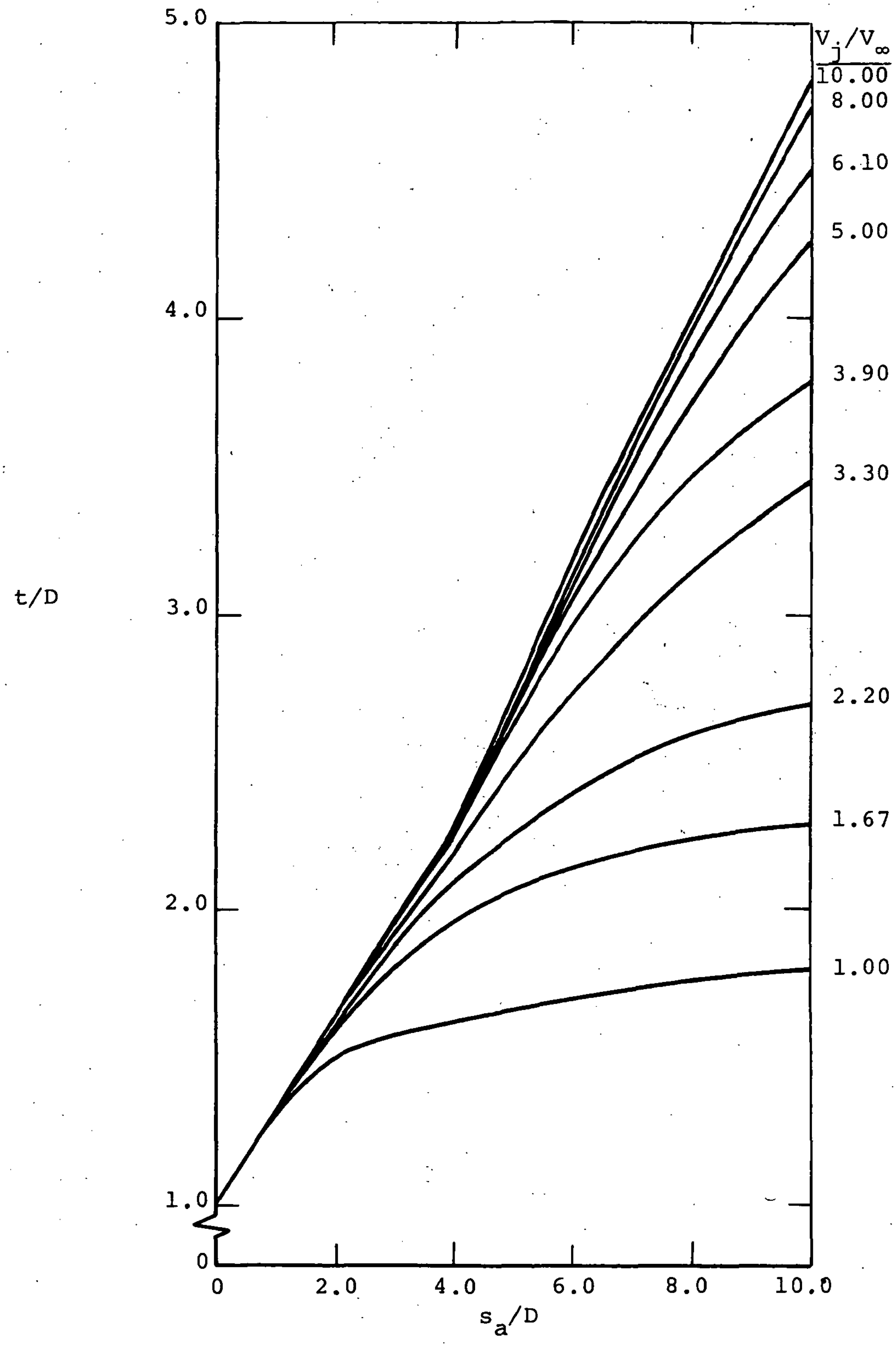

Figure 9.- Jet expansion curves.

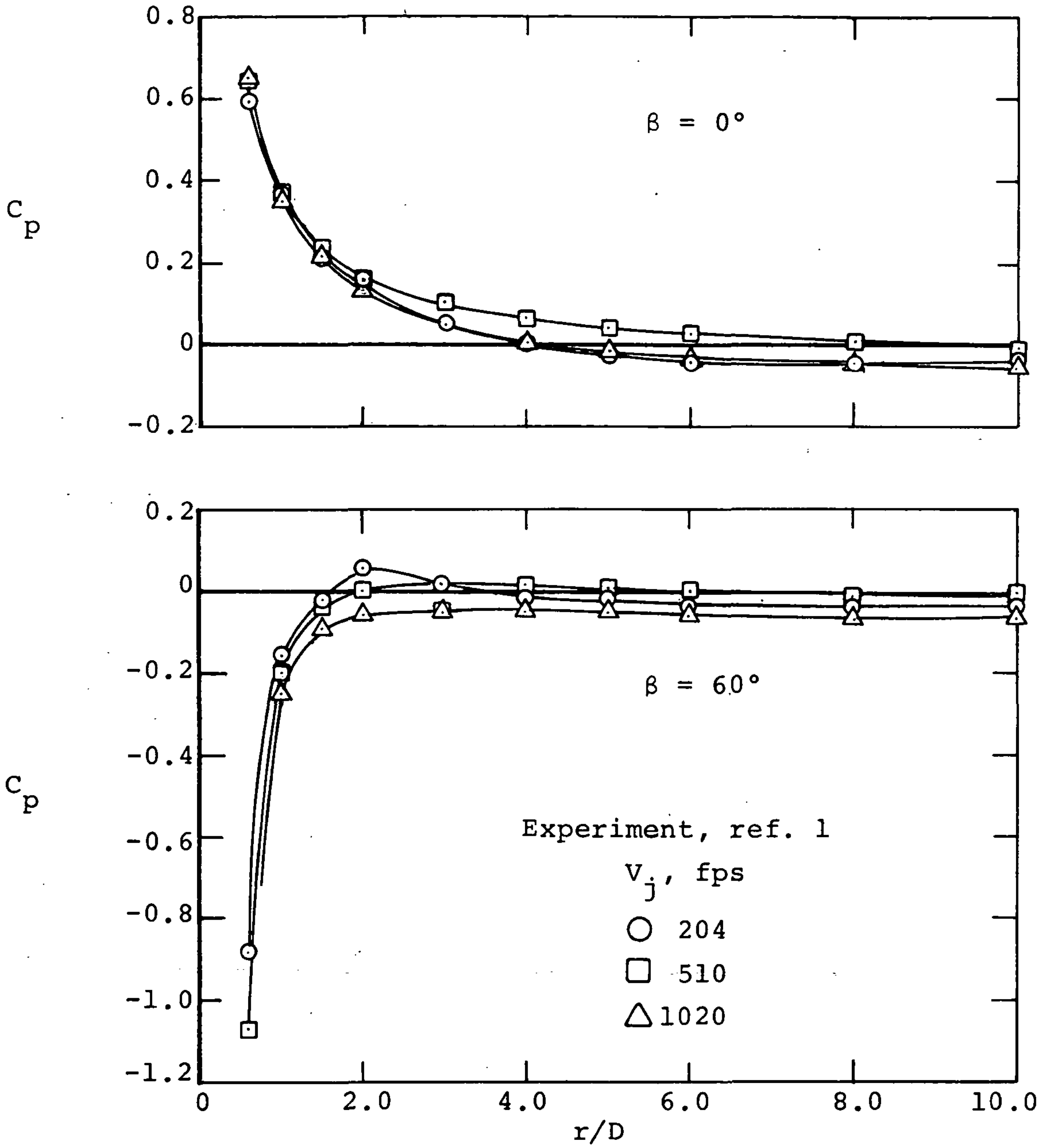

Figure 10.- Effect of free-stream velocity on the pressure distribution on a plate, $V_j/V_\infty = 2.5$.

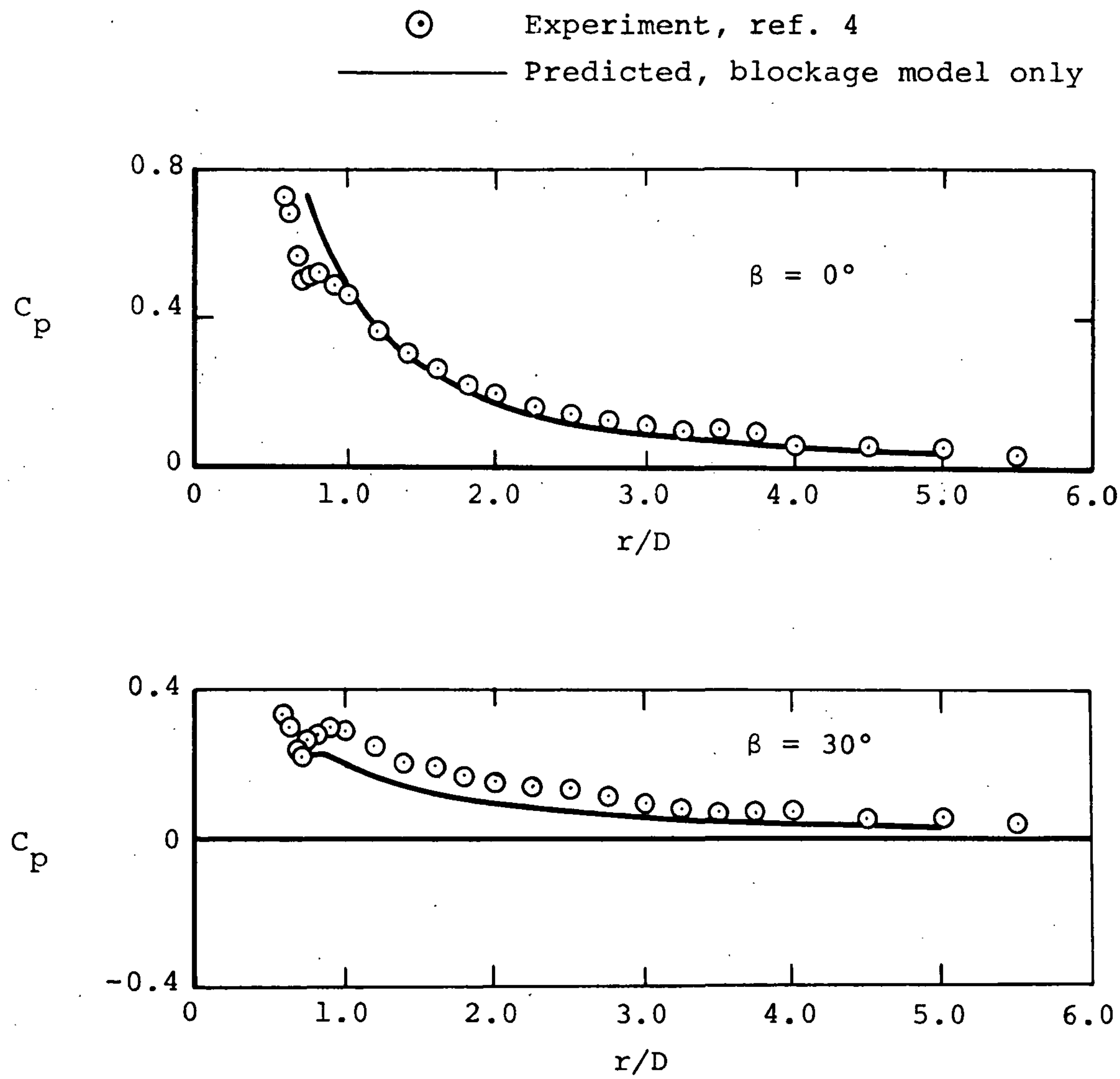

(a) $V_j/V_\infty = 2.2$

Figure 11.- Comparison of measured and predicted pressure distribution.

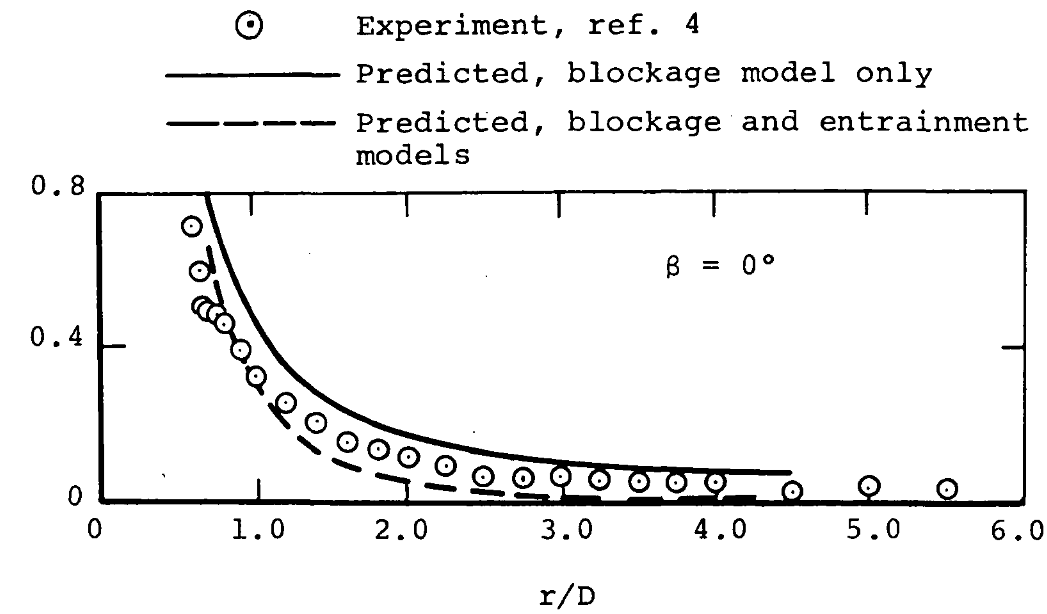

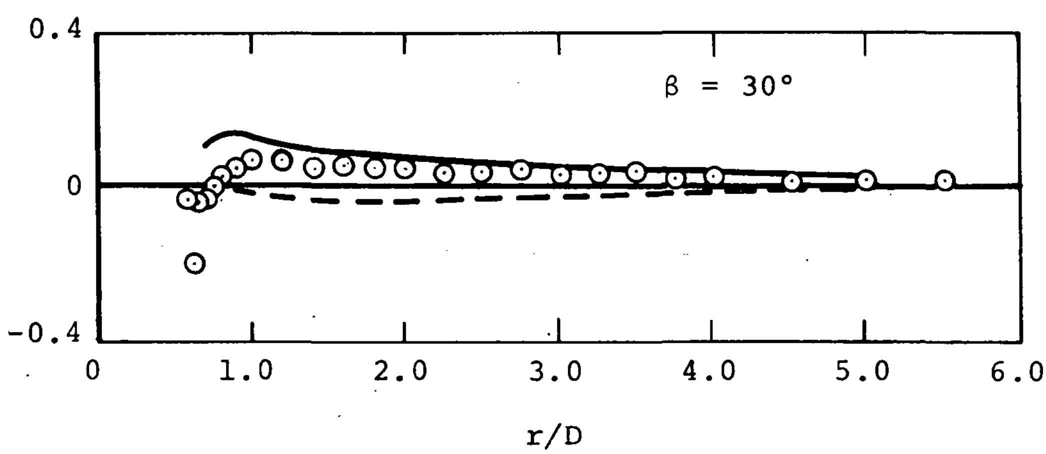

(b) $V_j/V_\infty = 3.9$

Figure 11.- Continued.

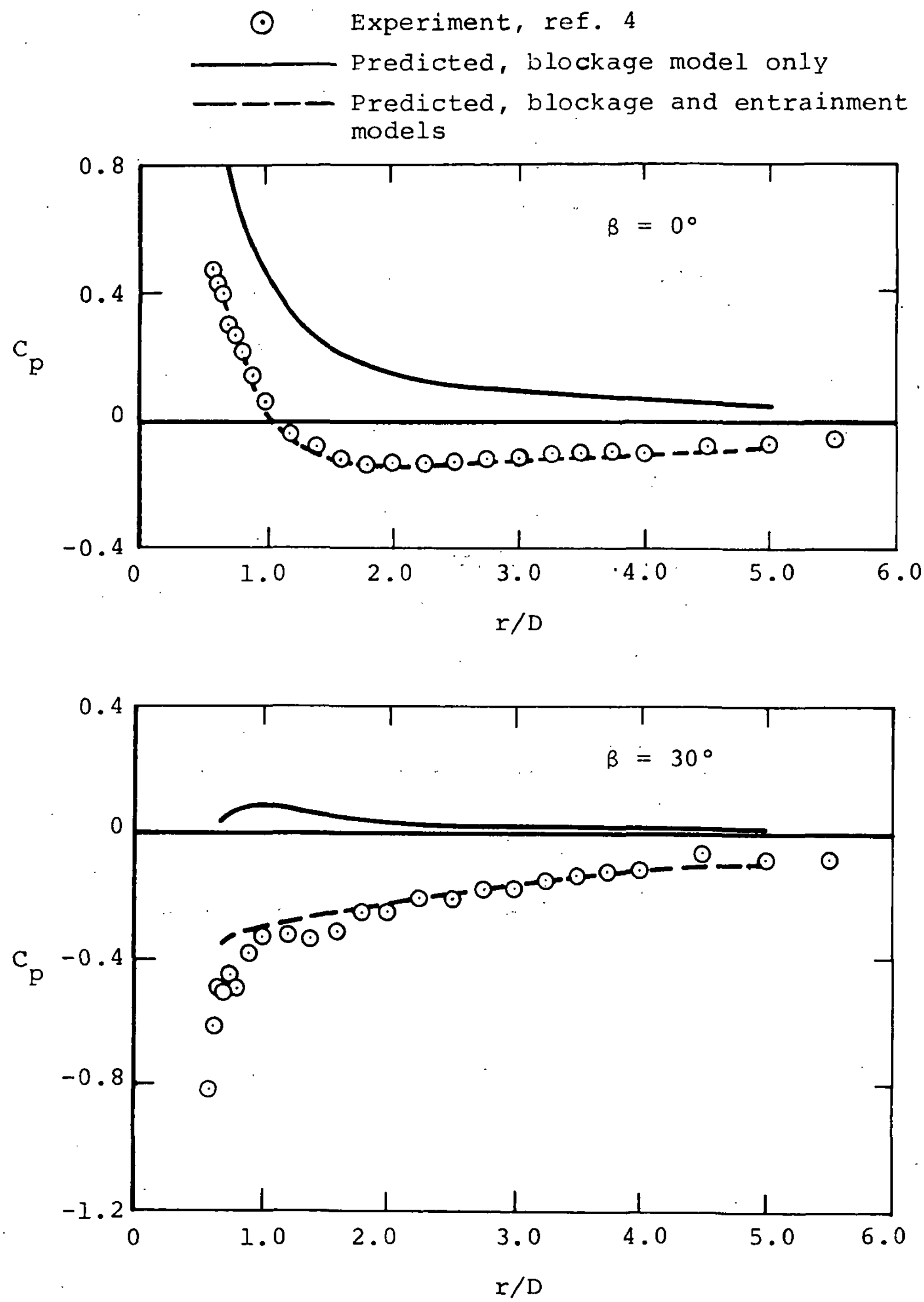

(c) $V_j/V_\infty = 8.0$

Figure 11.- Concluded.

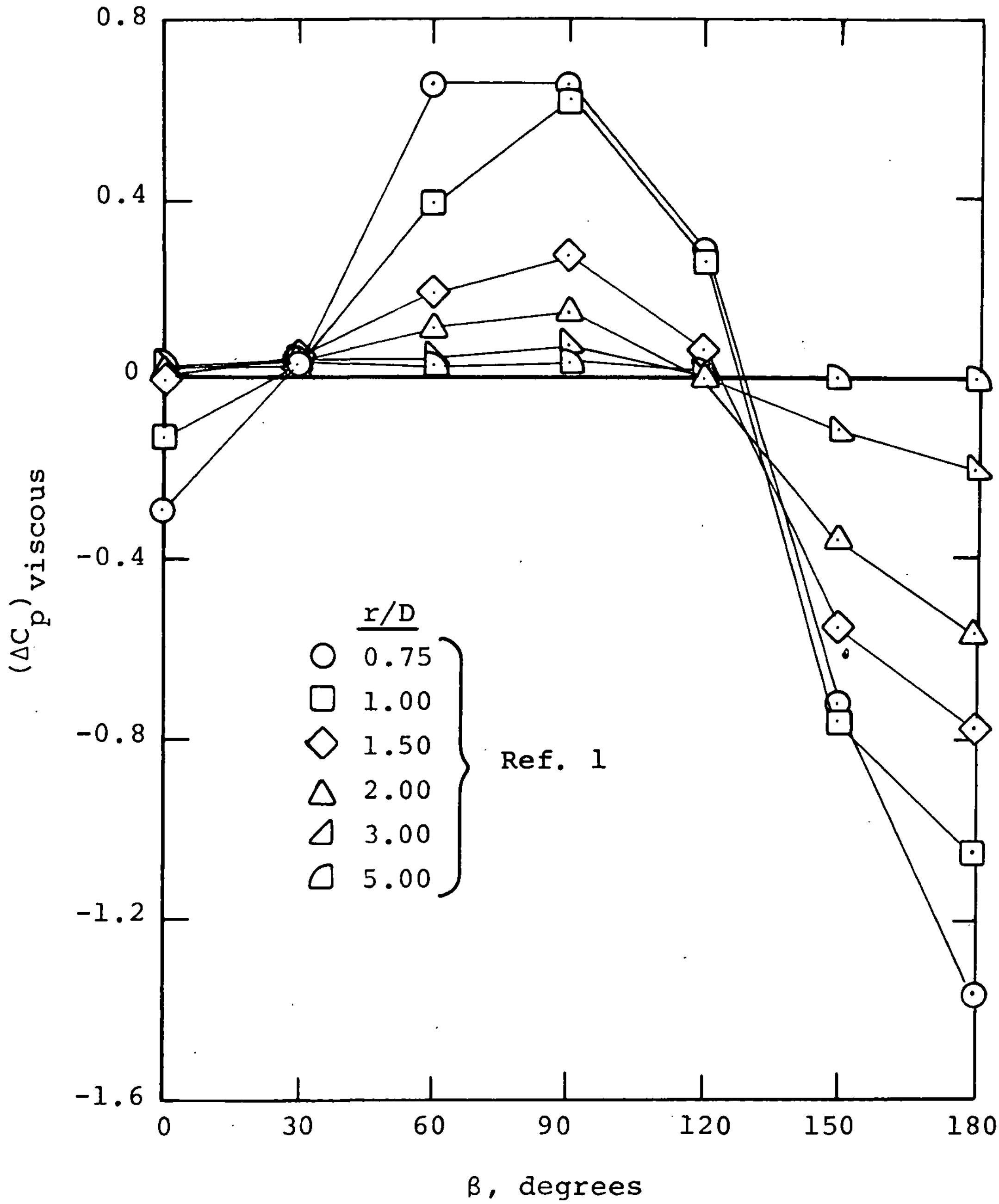

(a) $V_j/V_\infty = 1.00$

Figure 12.- Correlation factor for viscous portion of the presure coefficient induced on a flat plate by a jet exhausting into a crossflow, $\theta = 0^\circ$.

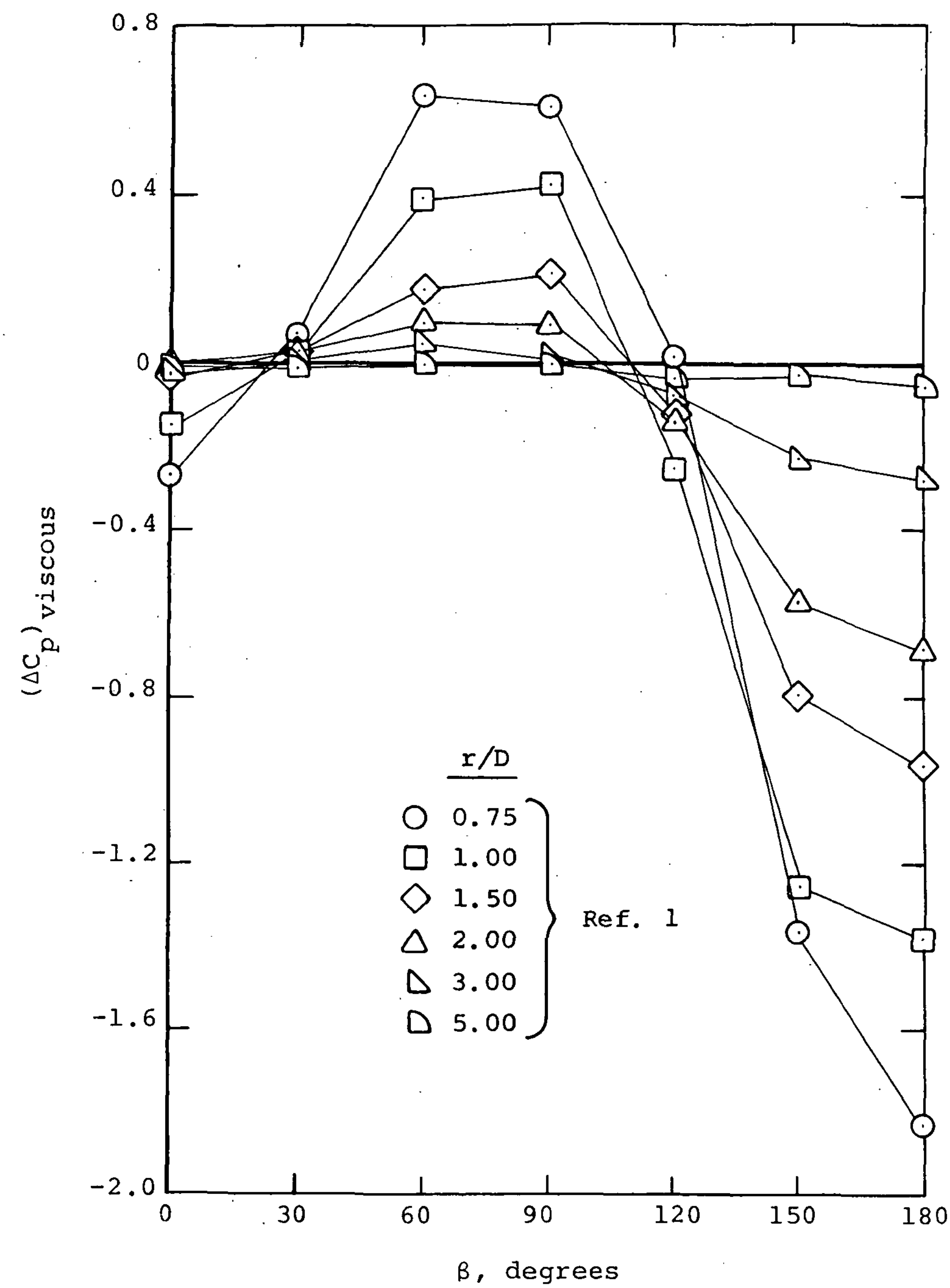

(b) $V_j/V_\infty = 1.67$

Figure 12.- Continued.

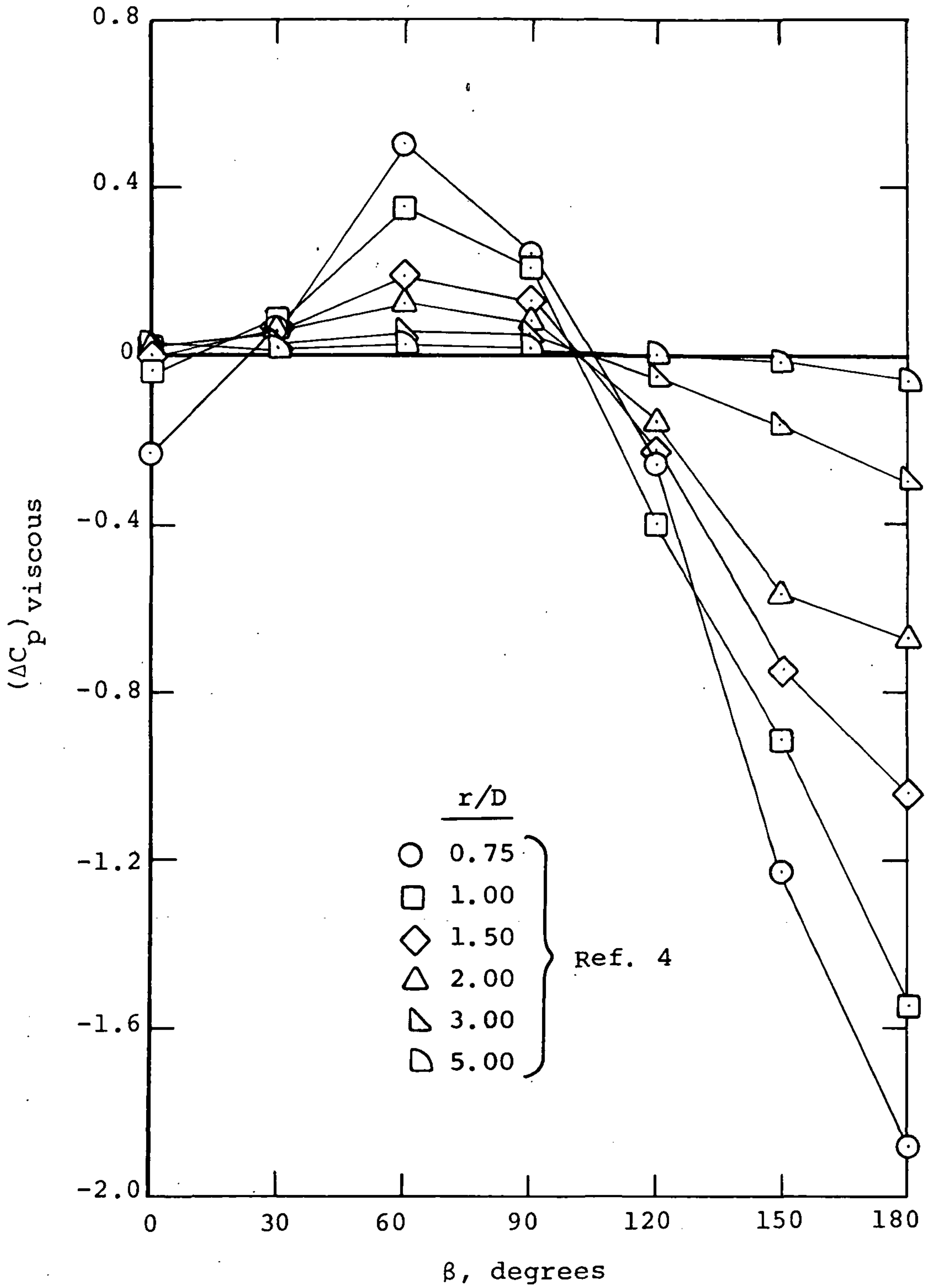

(c) $V_j/V_\infty = 2.2$

Figure 12.- Continued.

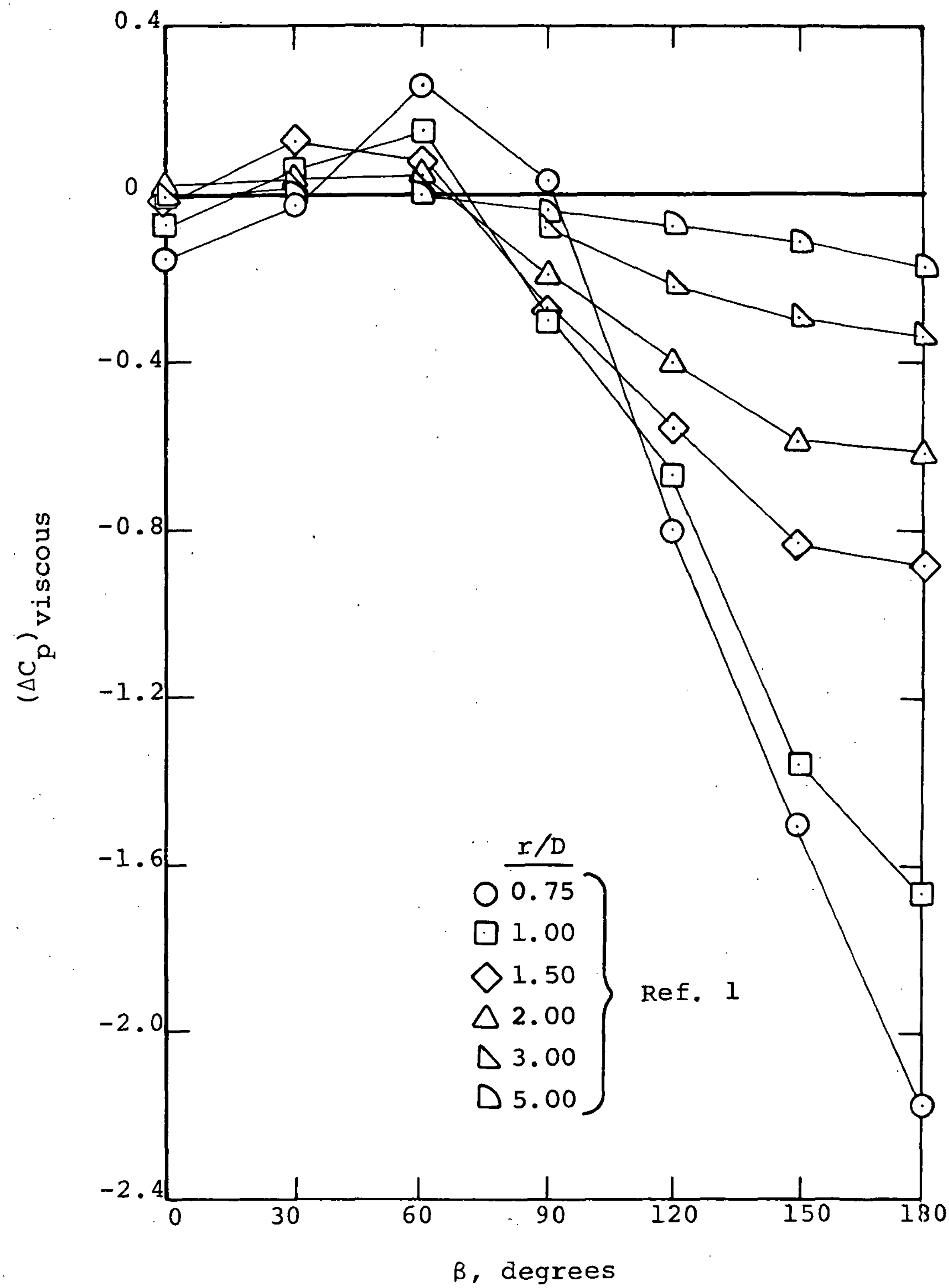

(d) $V_j/V_\infty = 3.33$

Figure 12.- Continued.

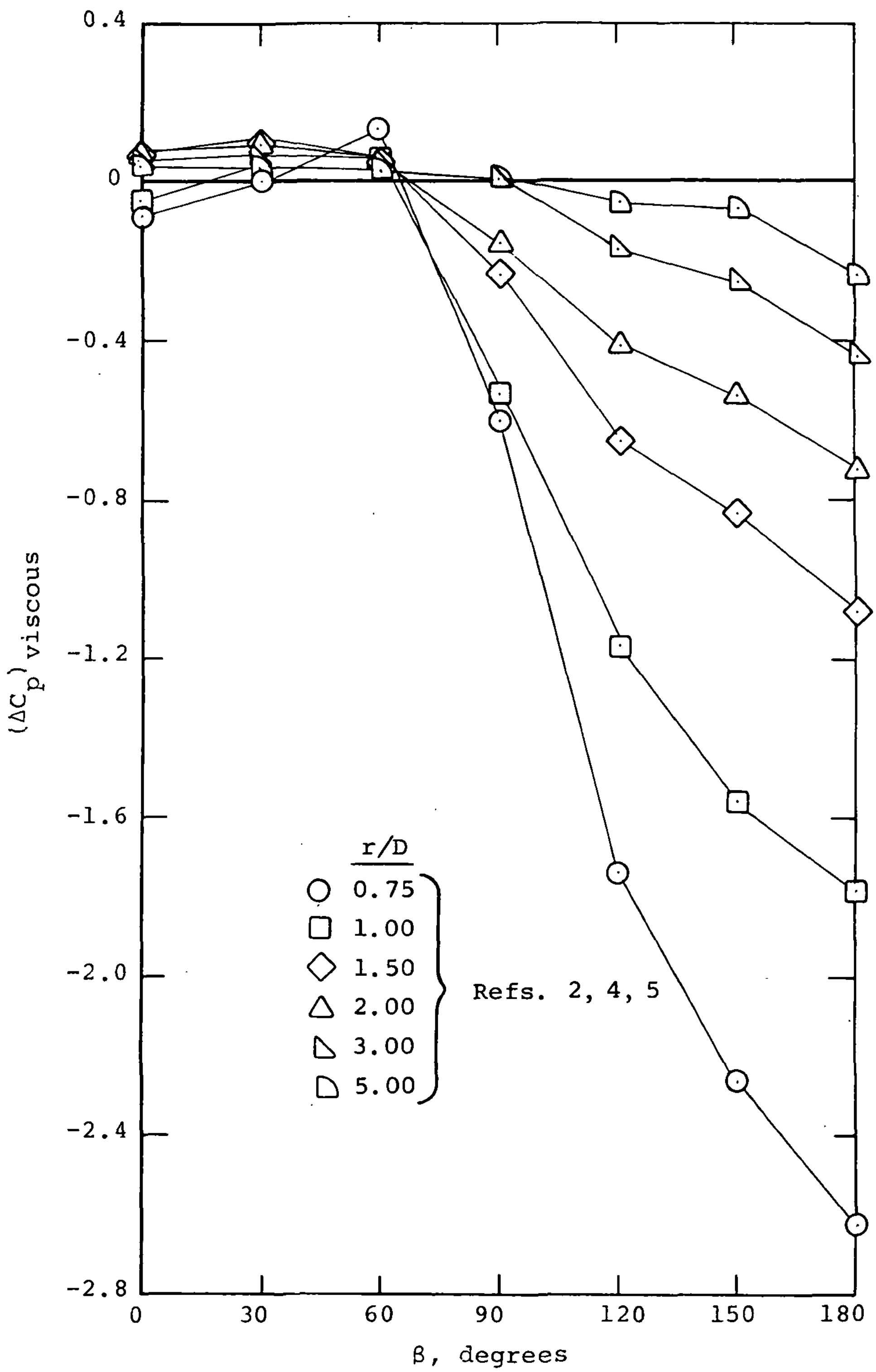

(e) $V_j/V_\infty = 3.9$

Figure 12.- Continued.

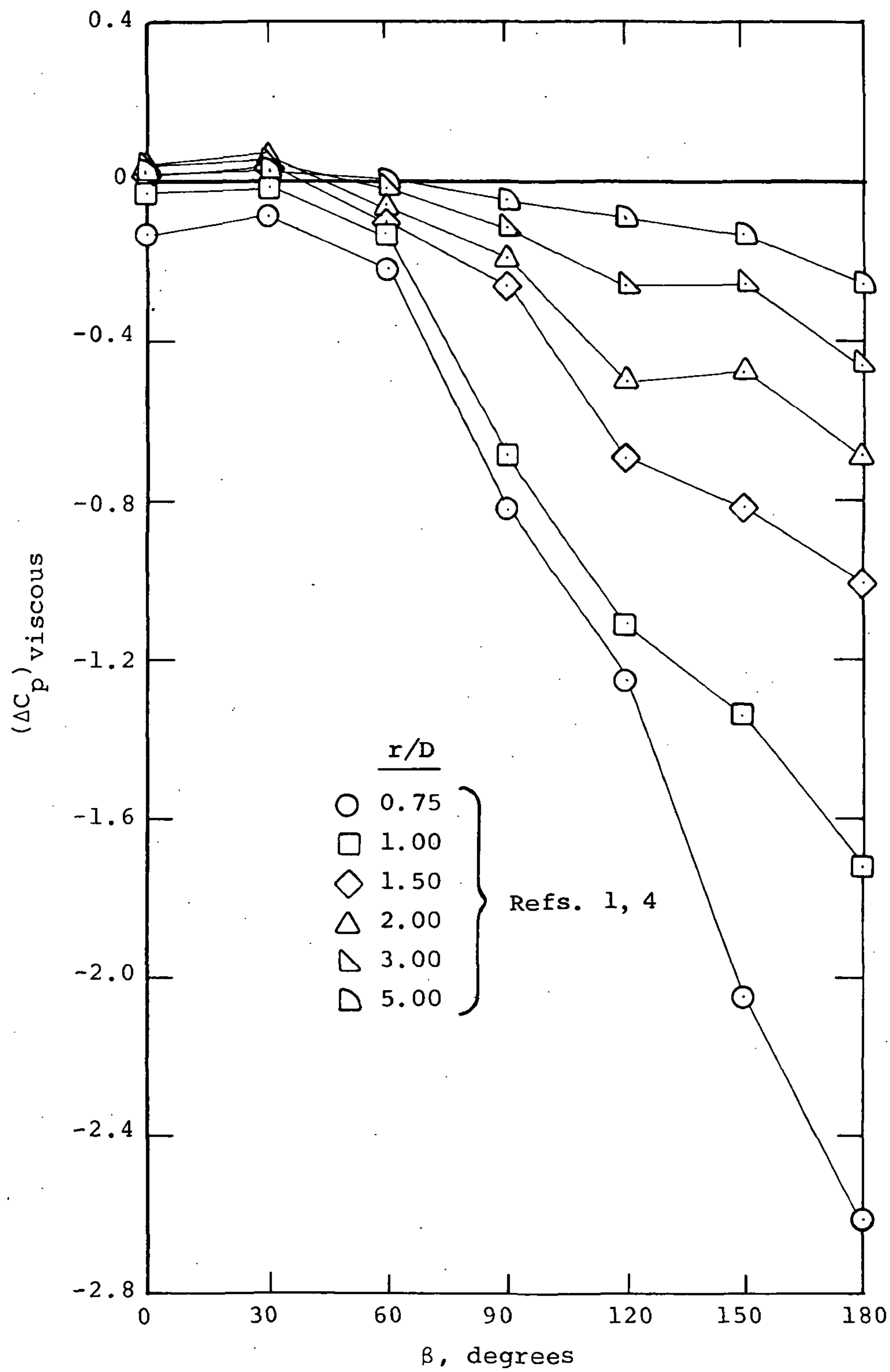

(f) $V_j/V_\infty = 5.0$

Figure 12.- Continued.

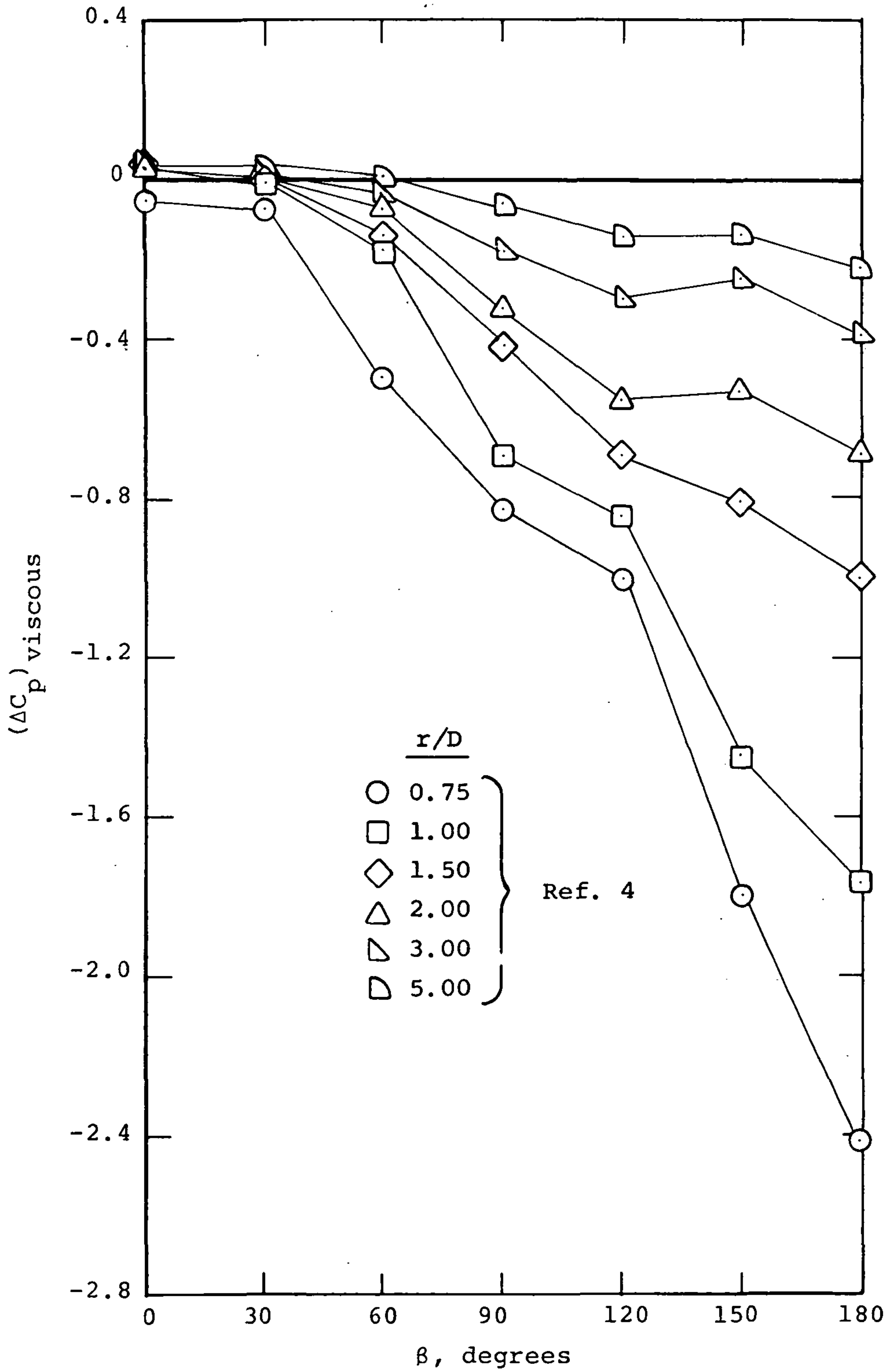

(g) $V_j/V_\infty = 6.1$

Figure 12.- Continued.

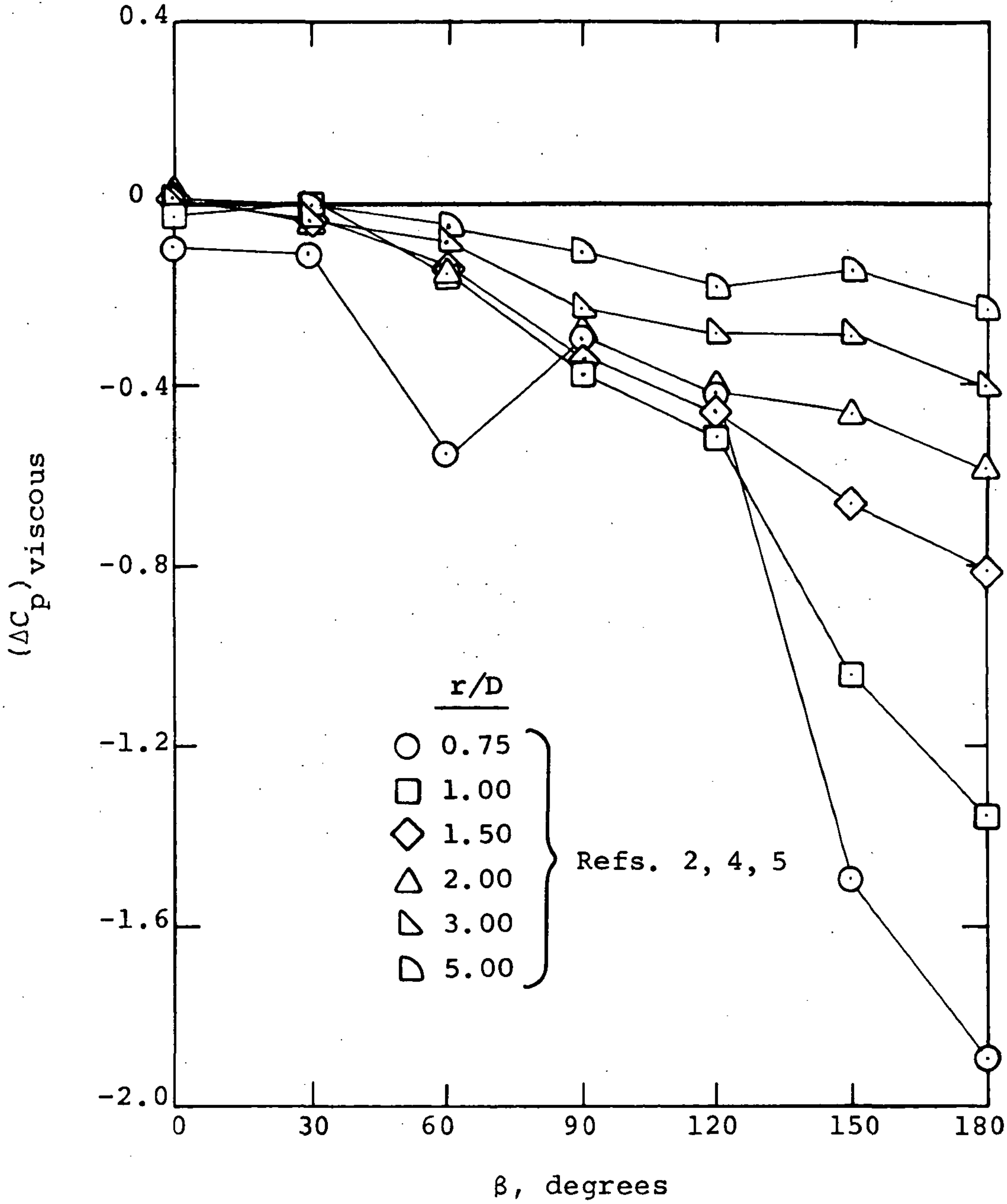

(h) $V_j/V_\infty = 8.0$

Figure 12.- Continued.

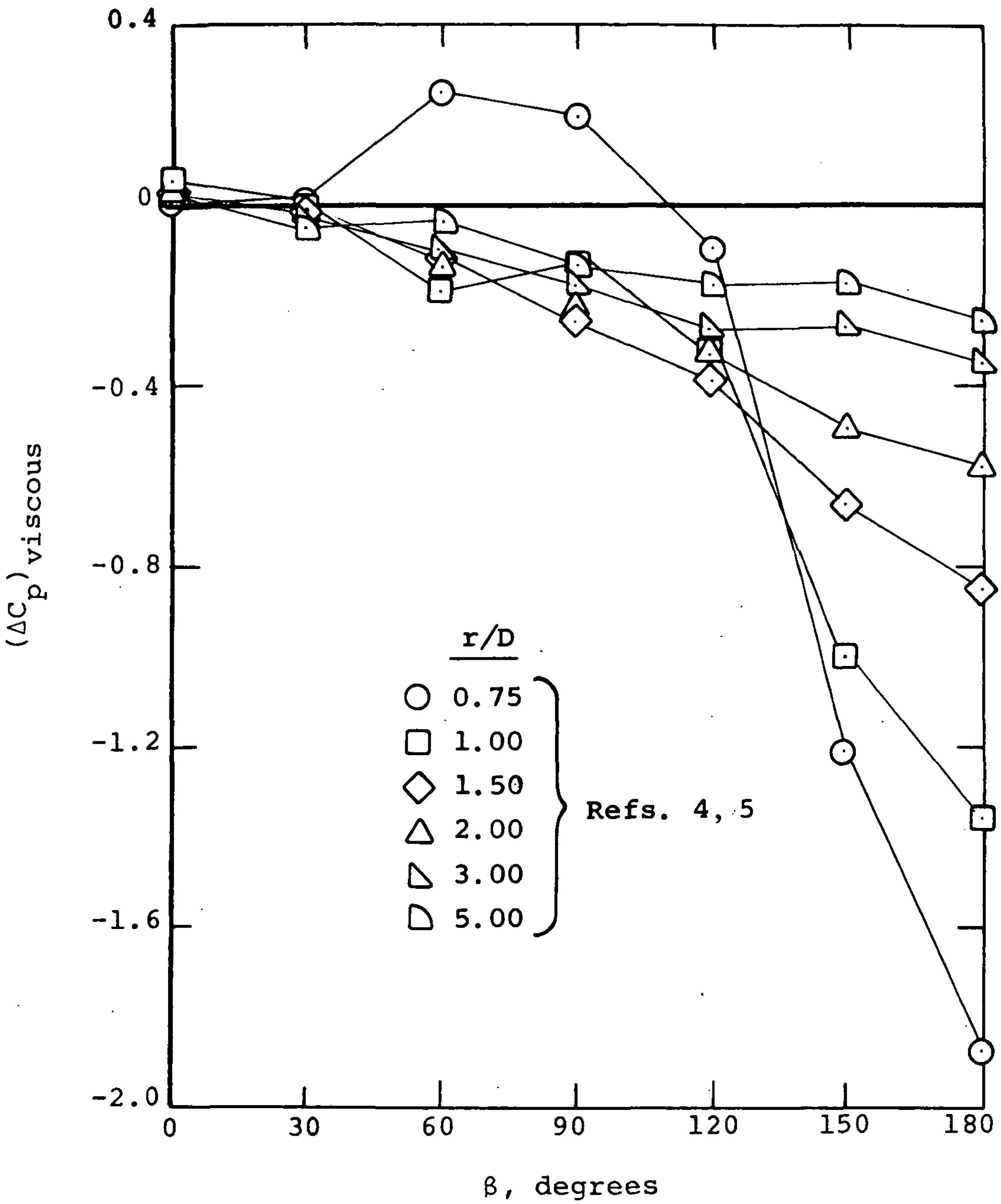

(i) $V_j/V_\infty = 10.0$

Figure 12.- Continued.

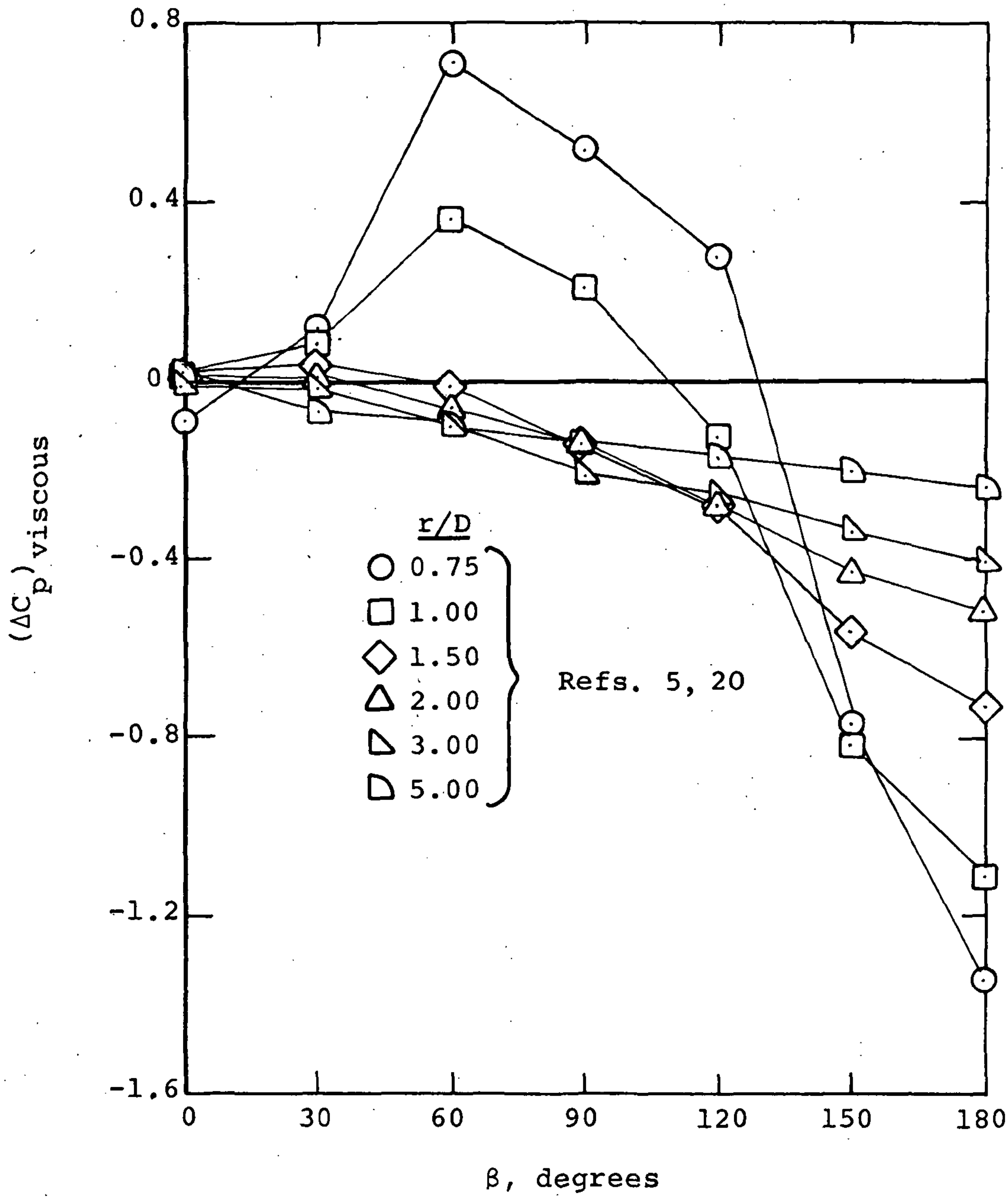

(j) $V_j/V_\infty = 12.0$

Figure 12.- Concluded.

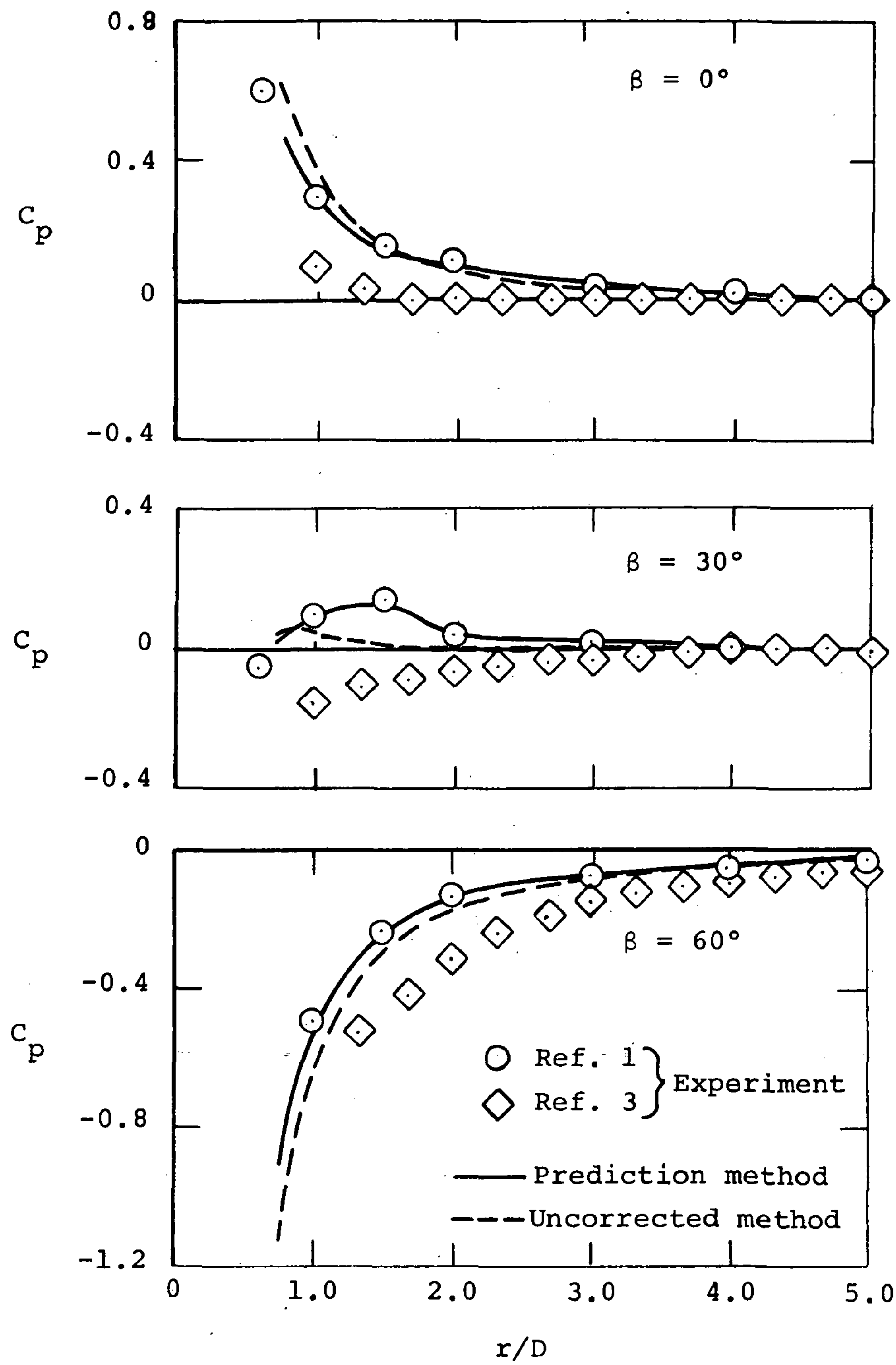

Figure 13.- Comparison of measured and predicted plate pressure distribution, $V_j/V_\infty = 3.33$.

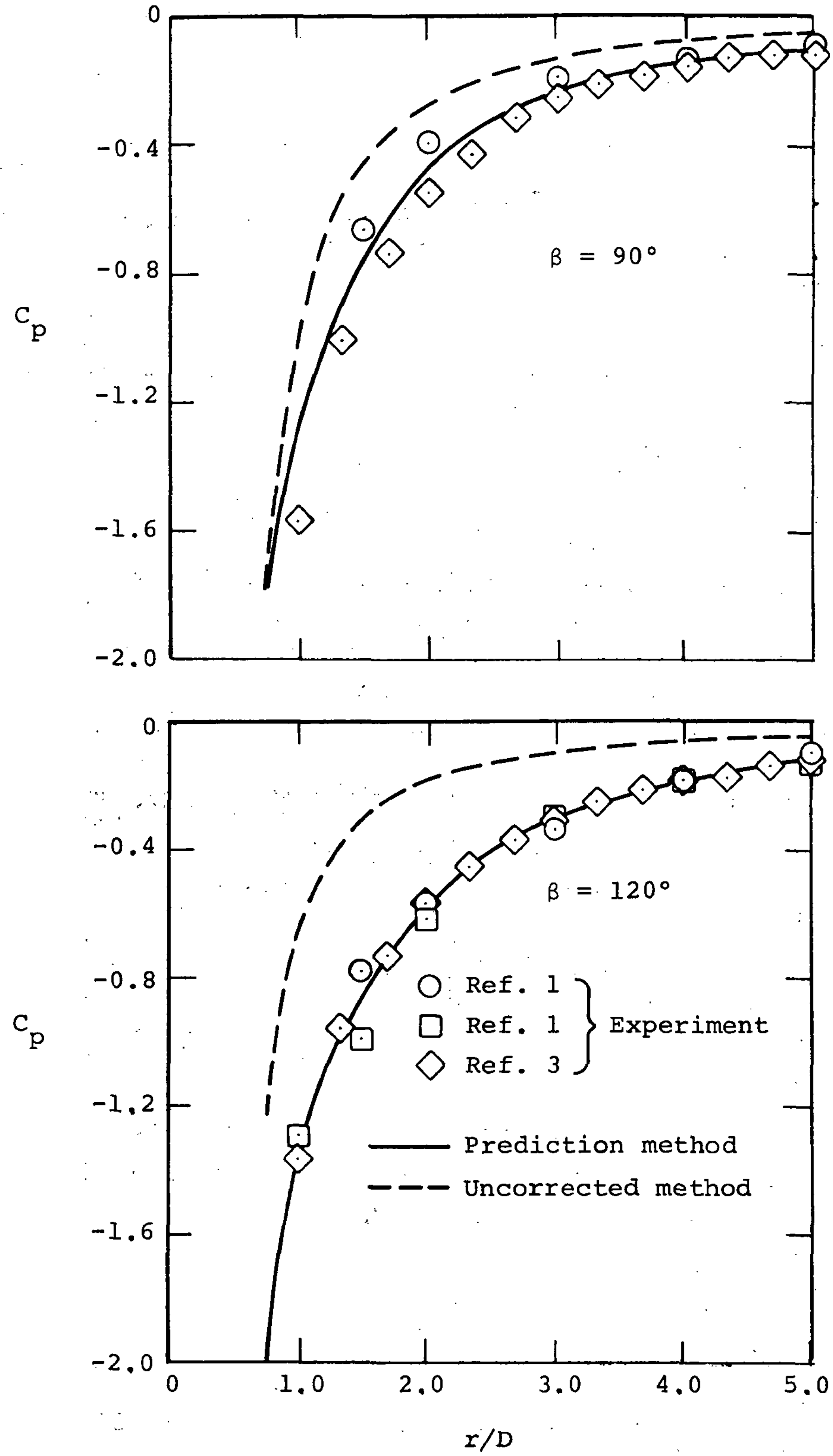

Figure 13.- Continued.

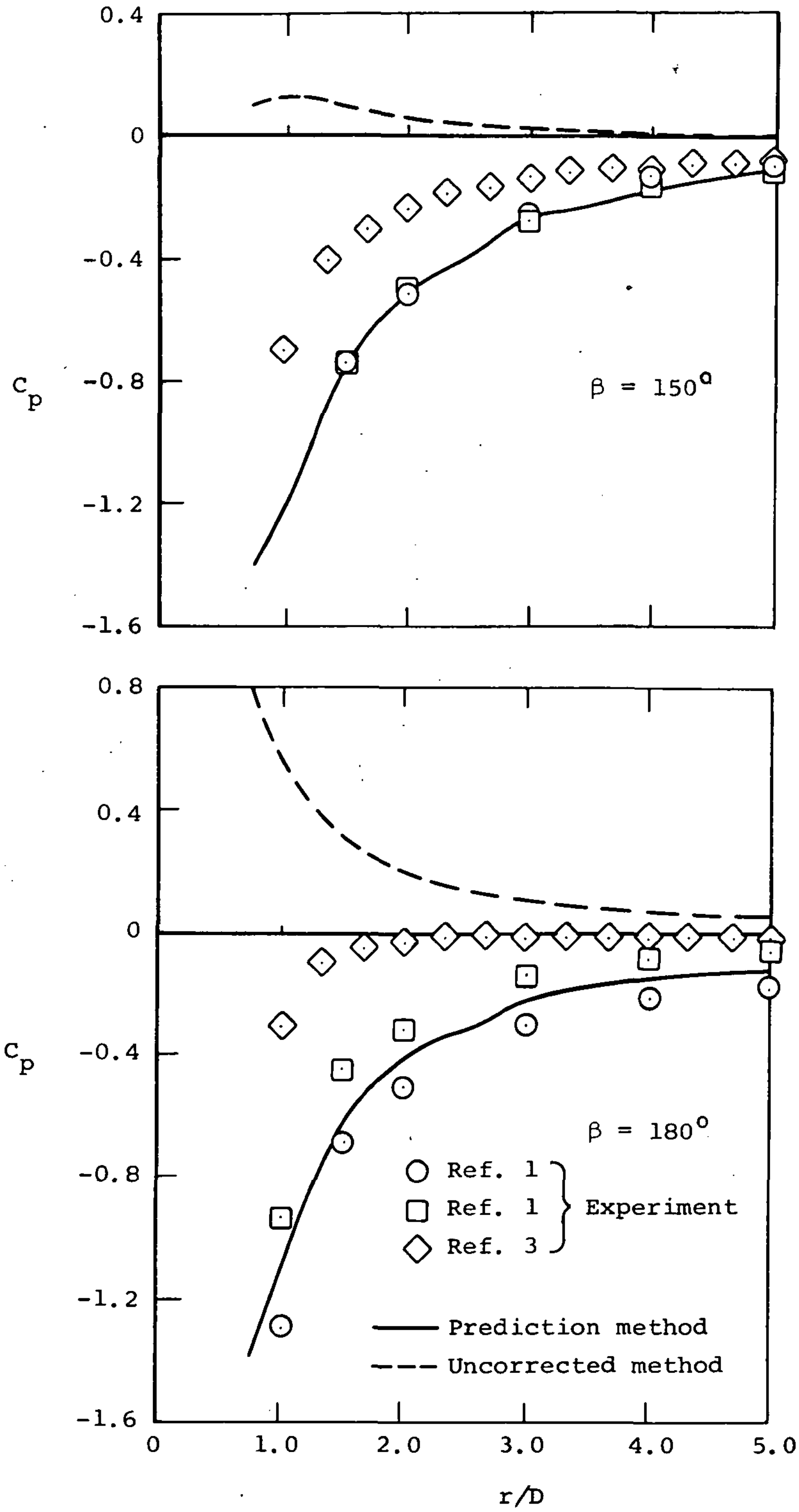

Figure 13.- Concluded

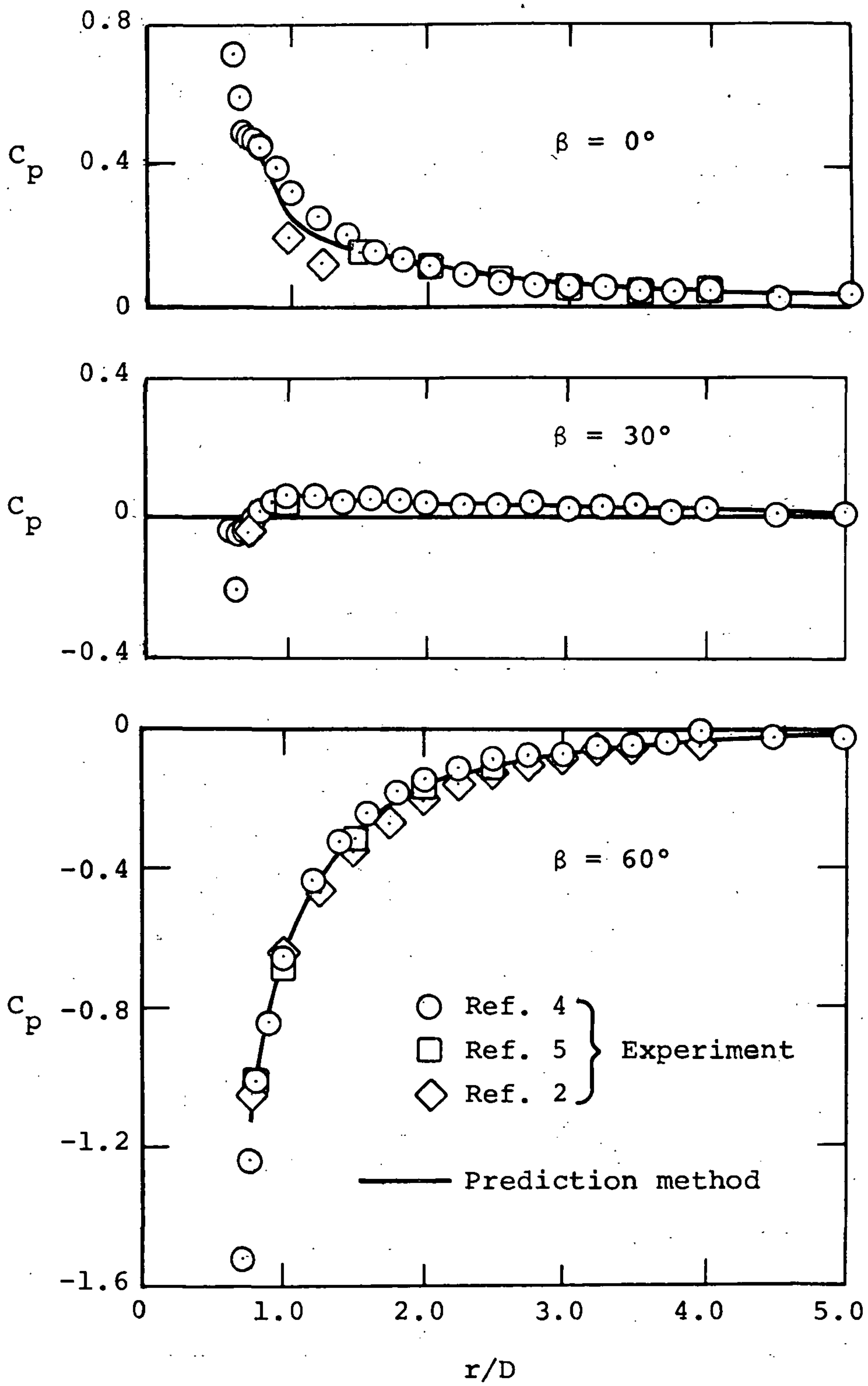

Figure 14.- Comparison of measured and predicted plate pressure distribution, $V_j/V_\infty = 3.9$.

C-2

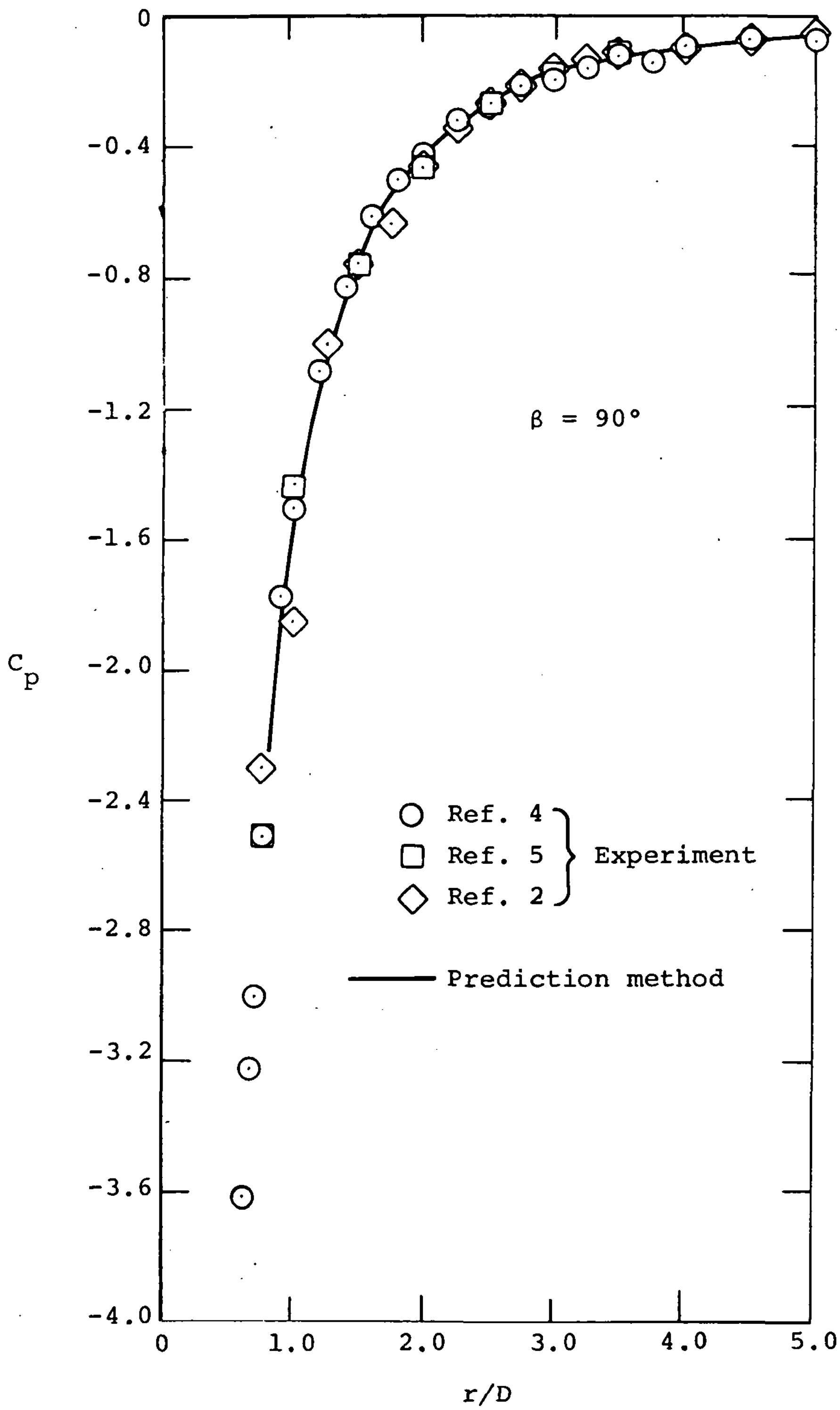

Figure 14.- Continued.

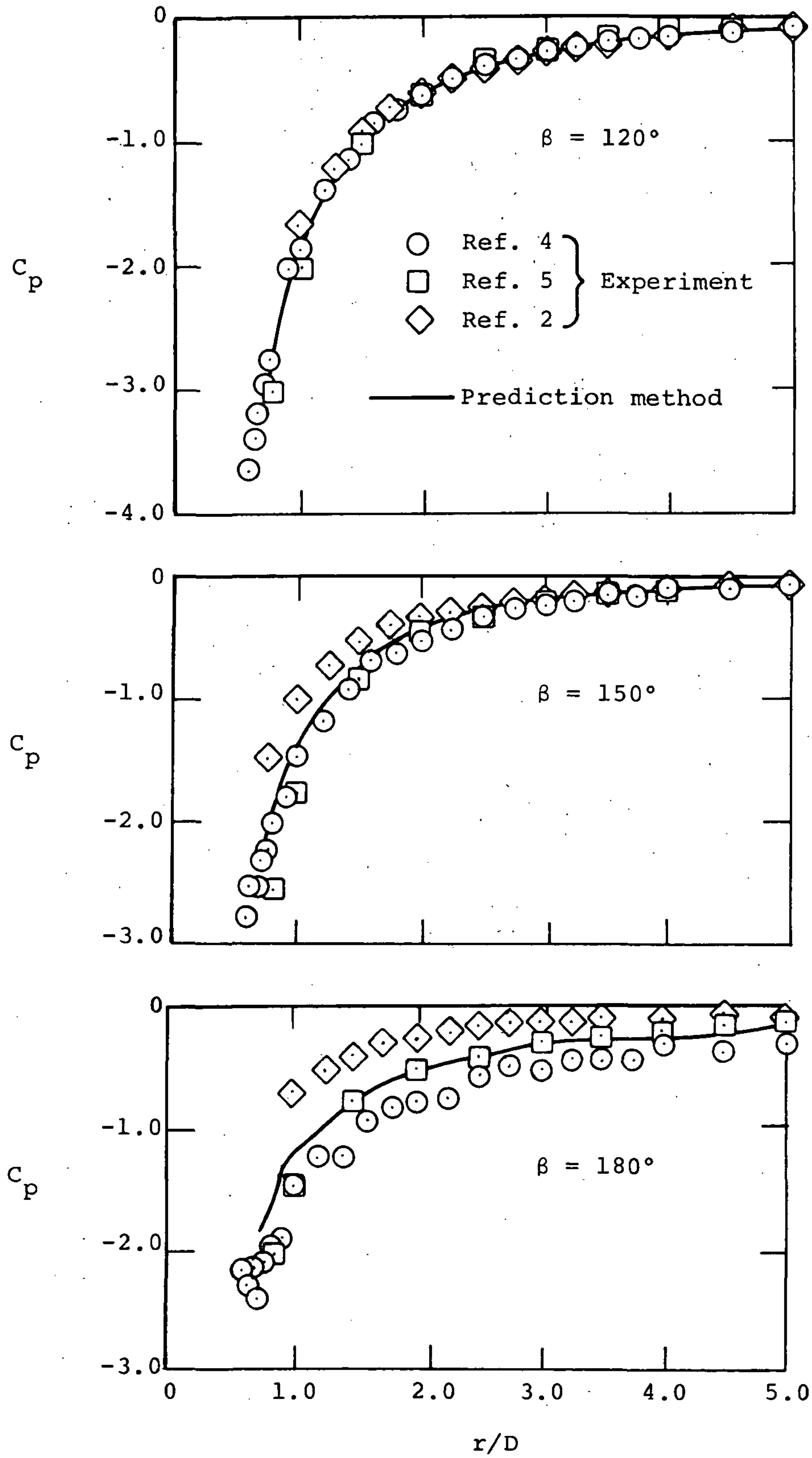

Figure 14.- Concluded.

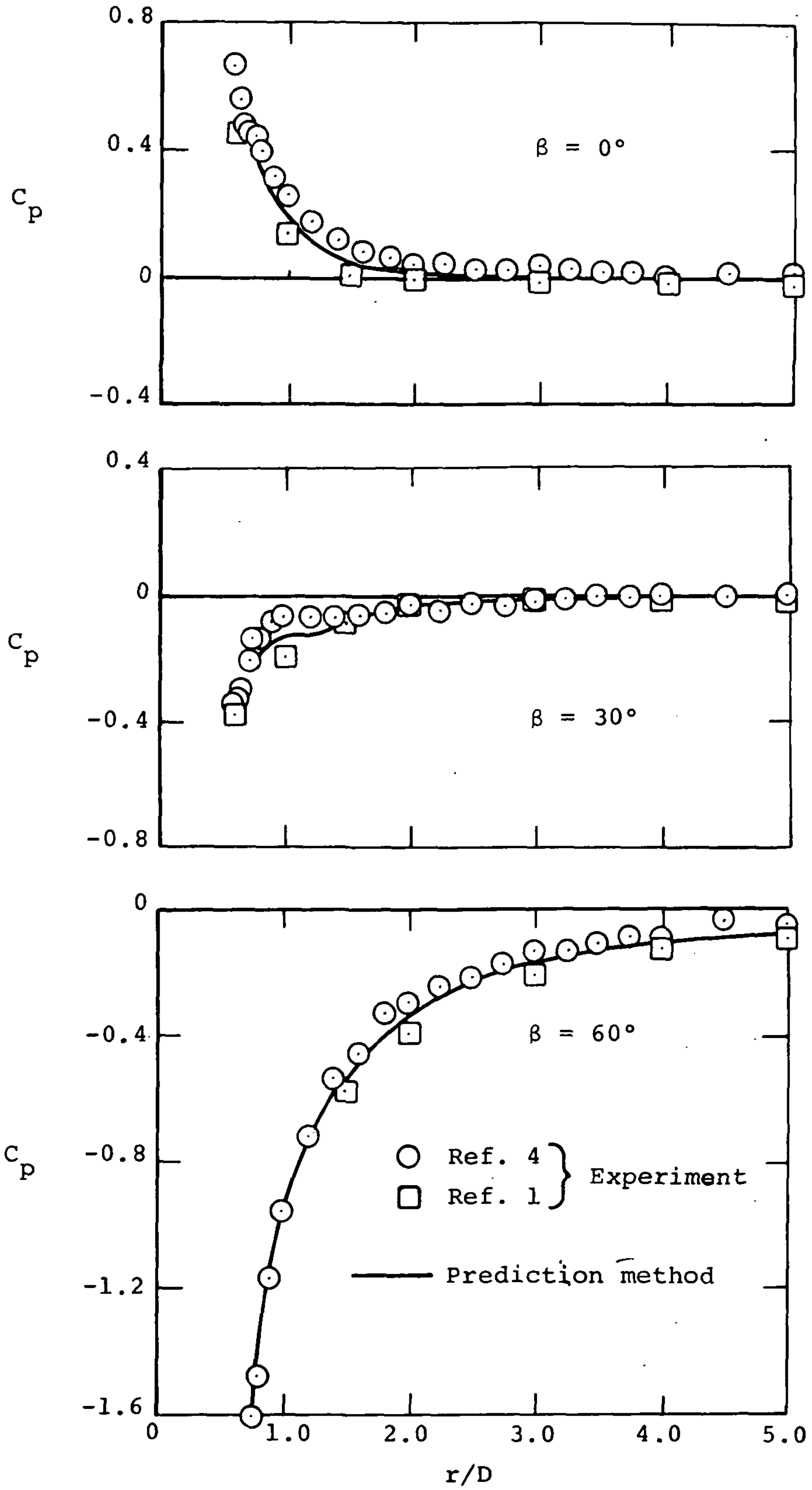

Figure 15.- Comparison of measured and predicted plate pressure distribution, $V_j/V_\infty = 5.0$.

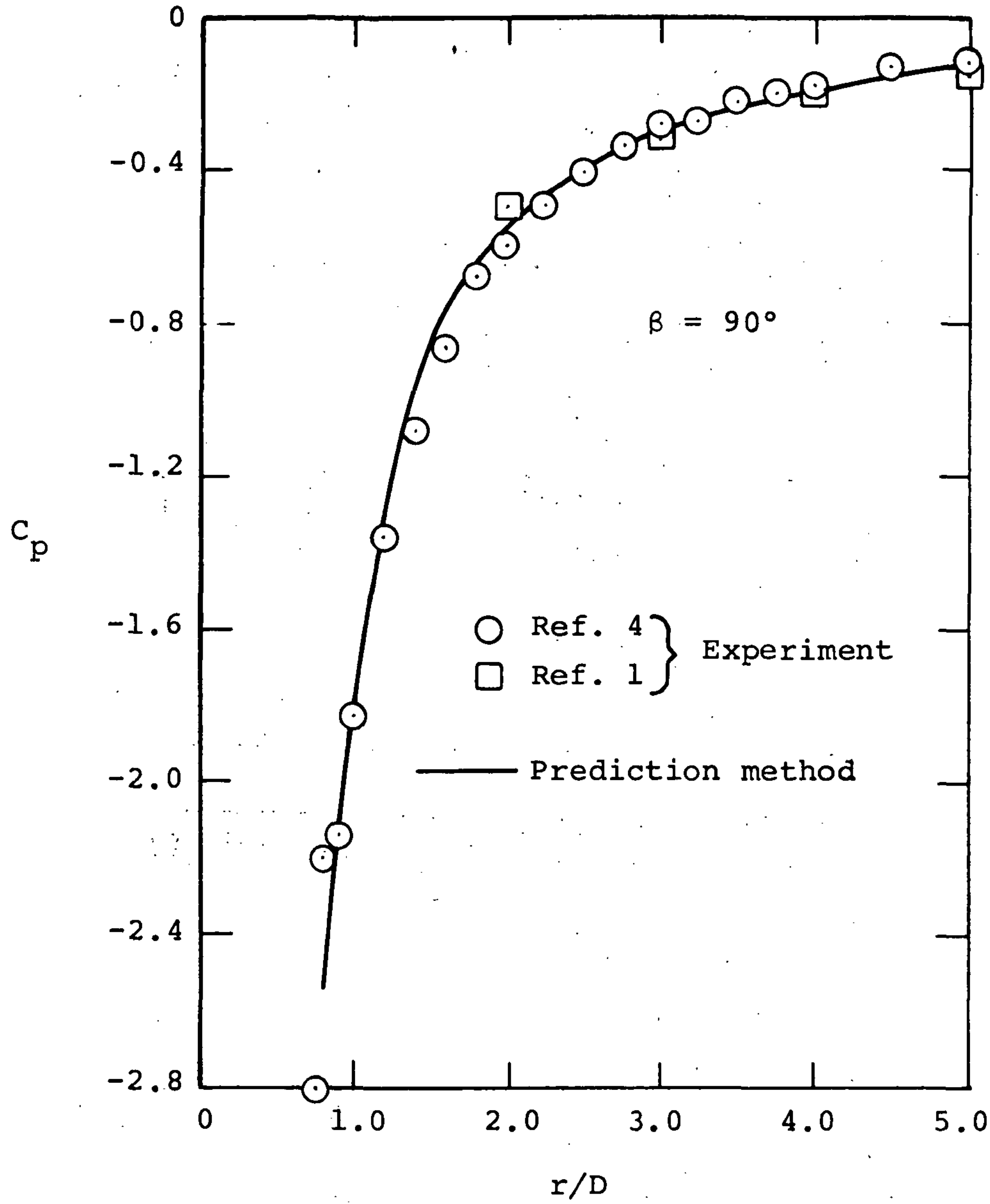

Figure 15.- Continued.

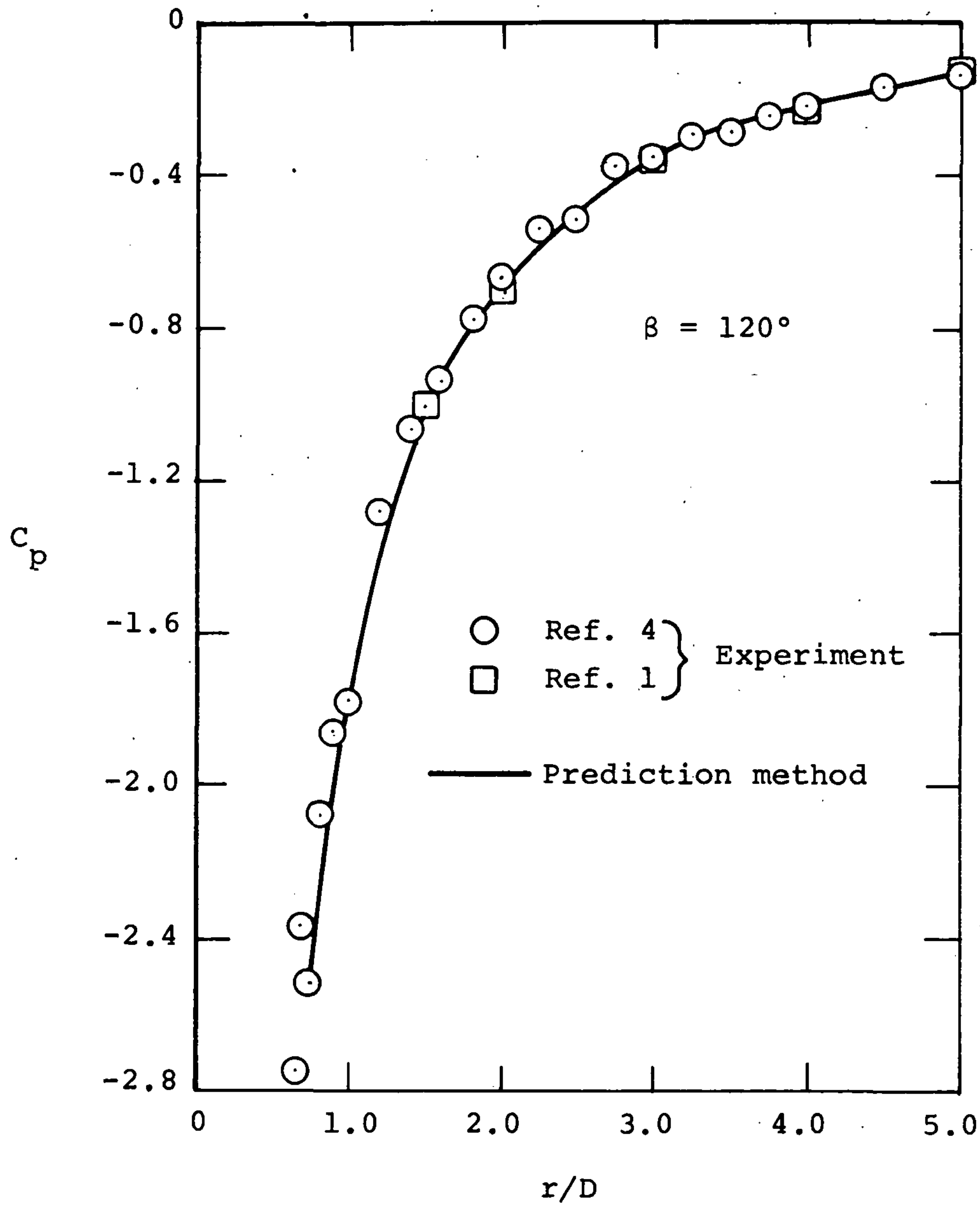

Figure 15.- Continued.

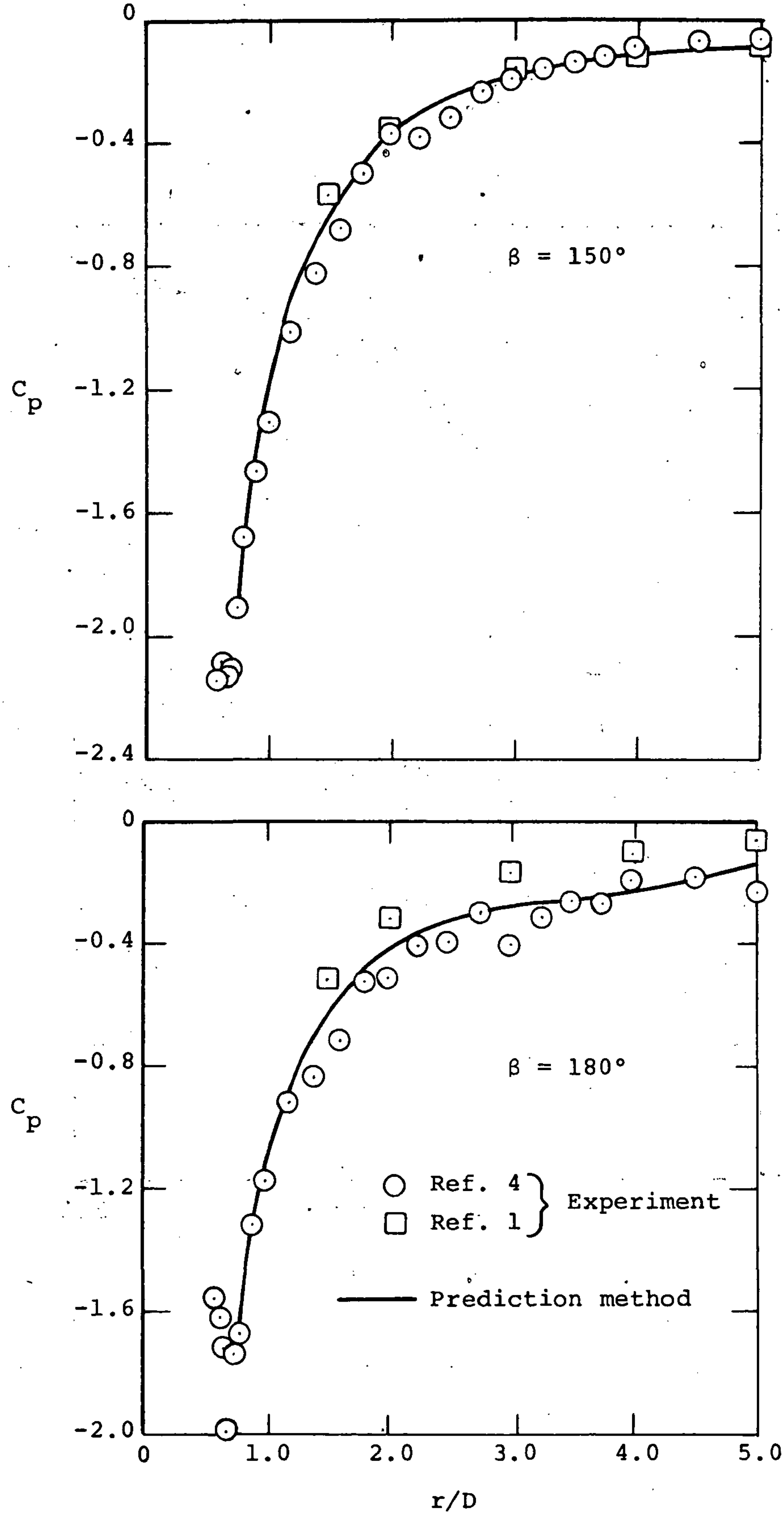

Figure 15.- Concluded.

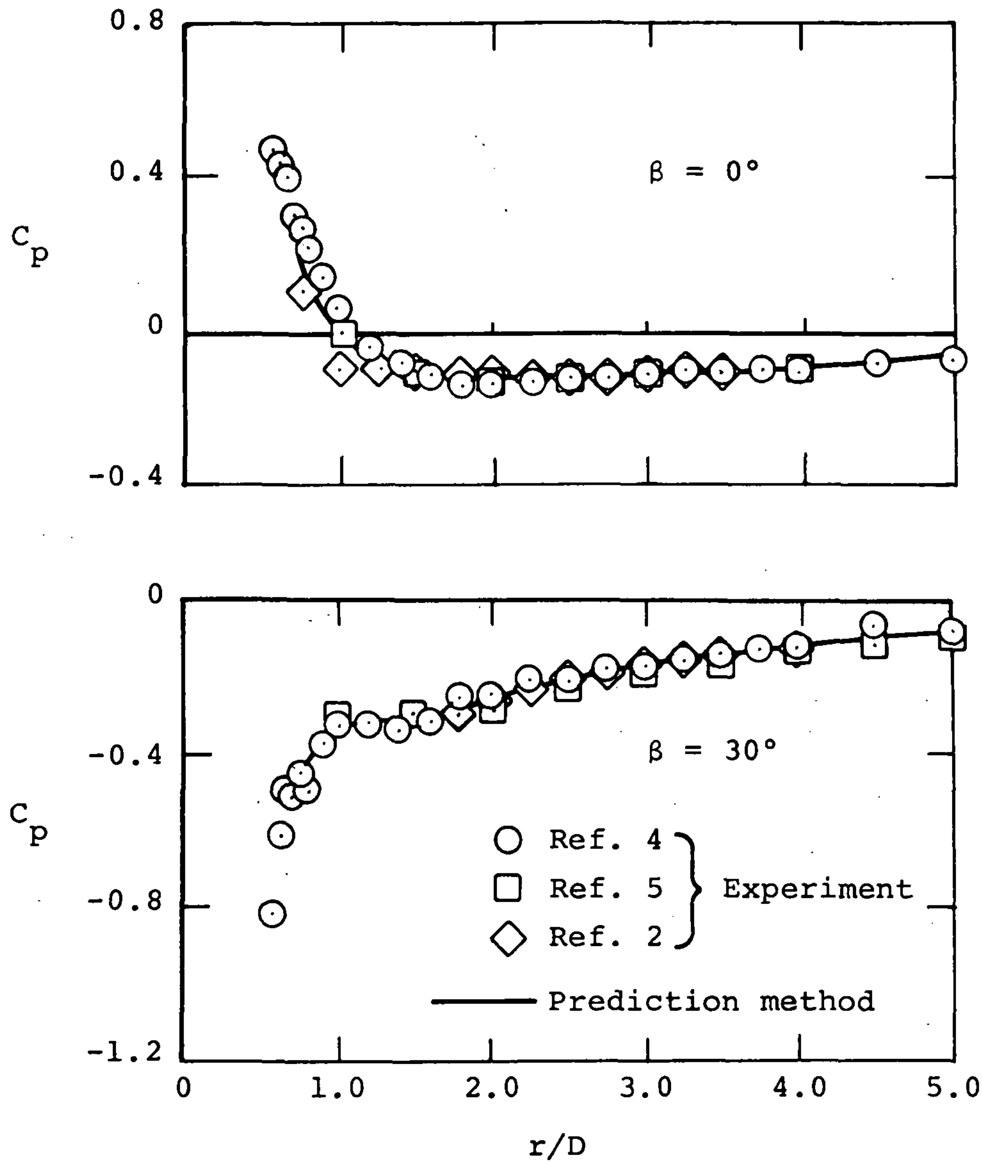

Figure 16.- Comparison of measured and predicted plate pressure distribution, $V_j/V_\infty = 8.0$.

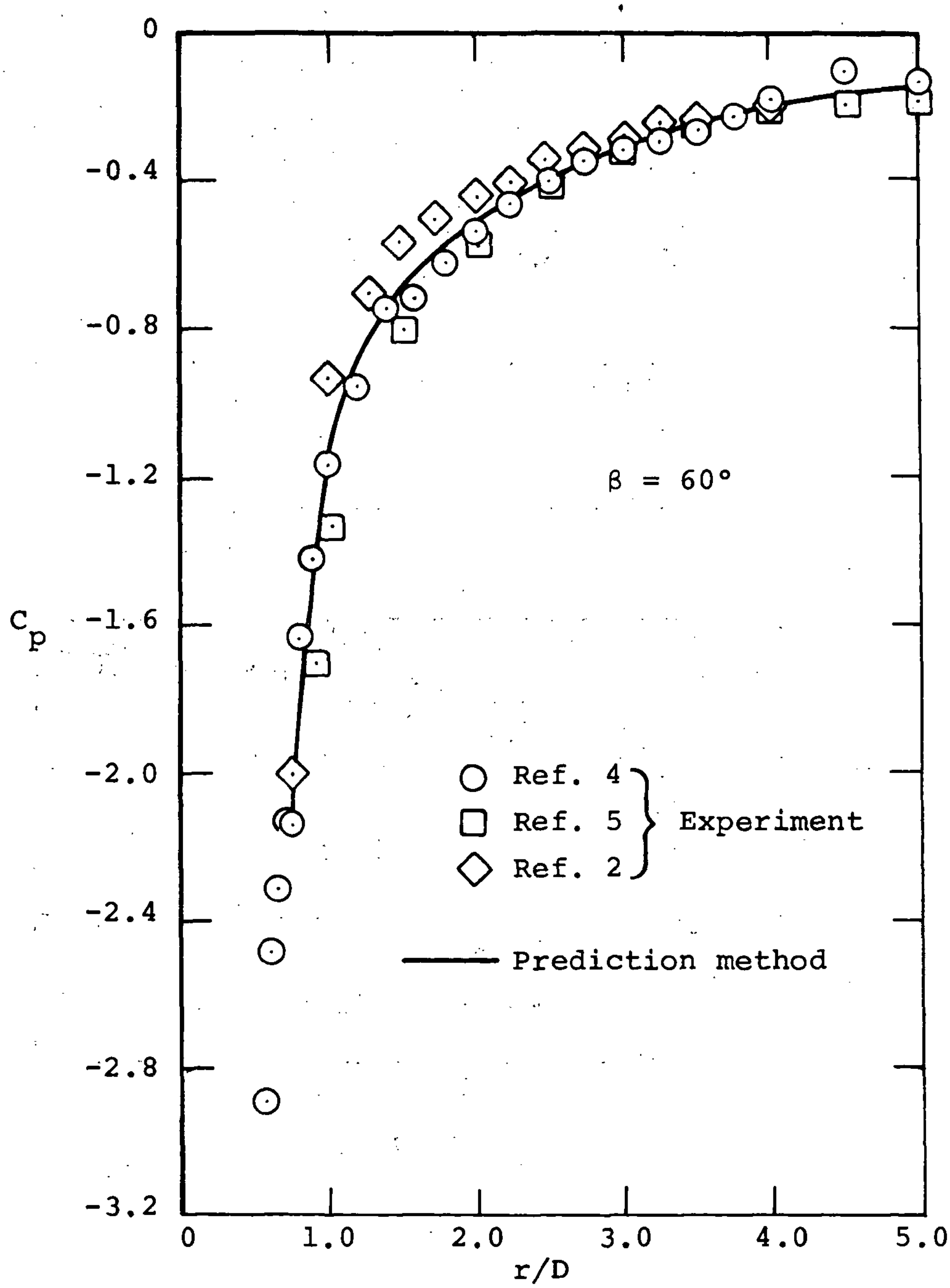

Figure 16.- Continued.

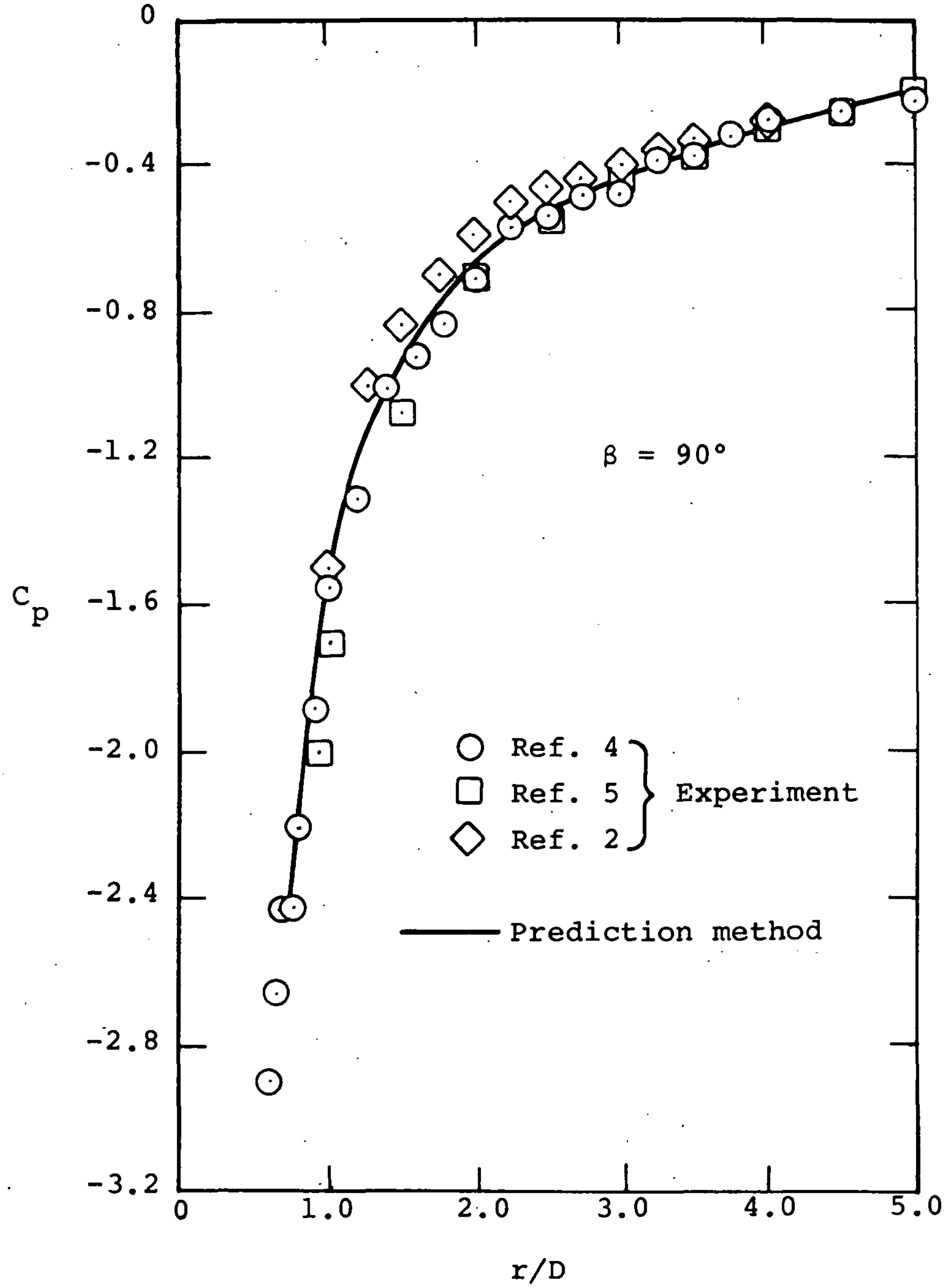

Figure 16.- Continued.

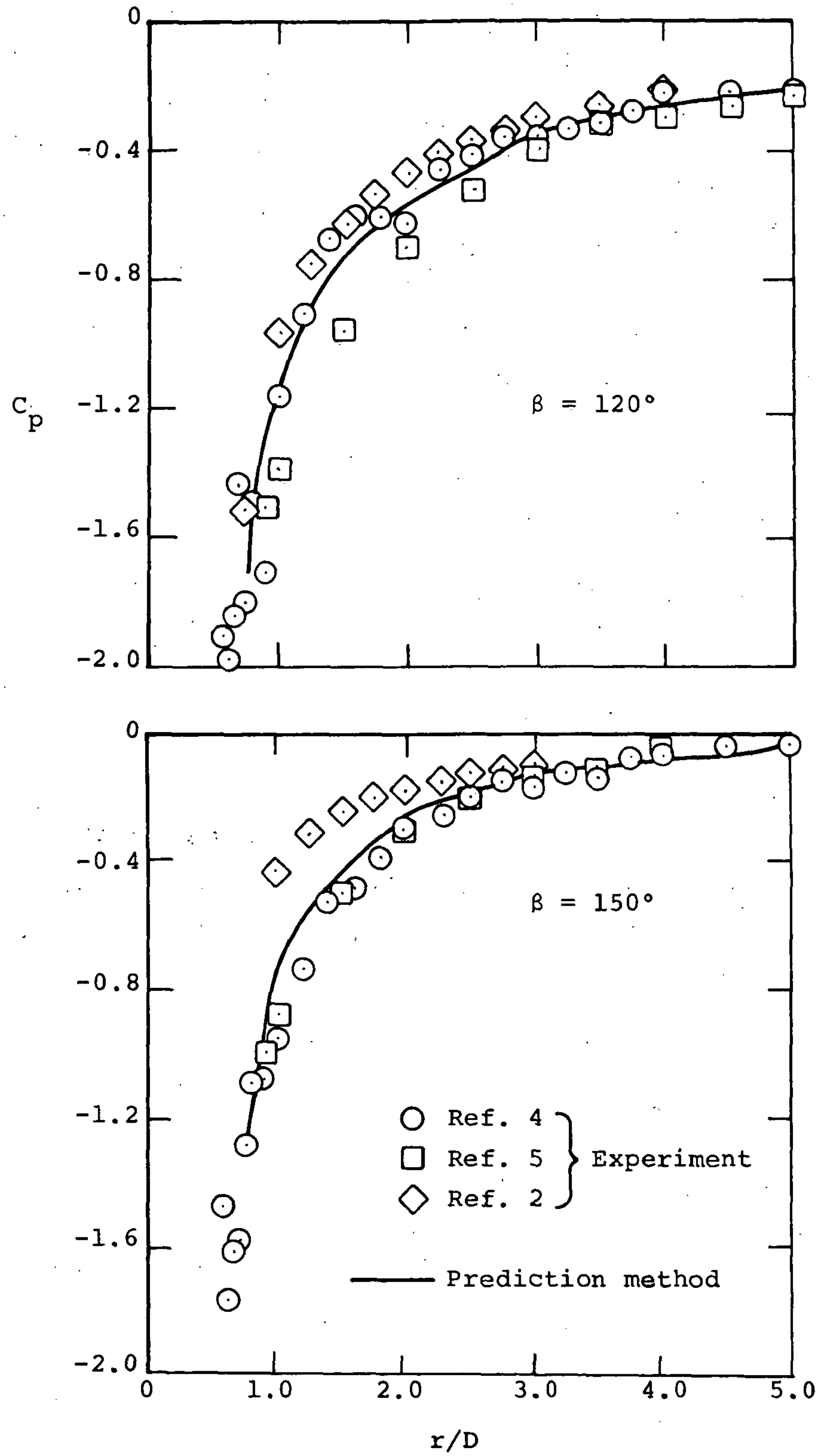

Figure 16.- Continued.

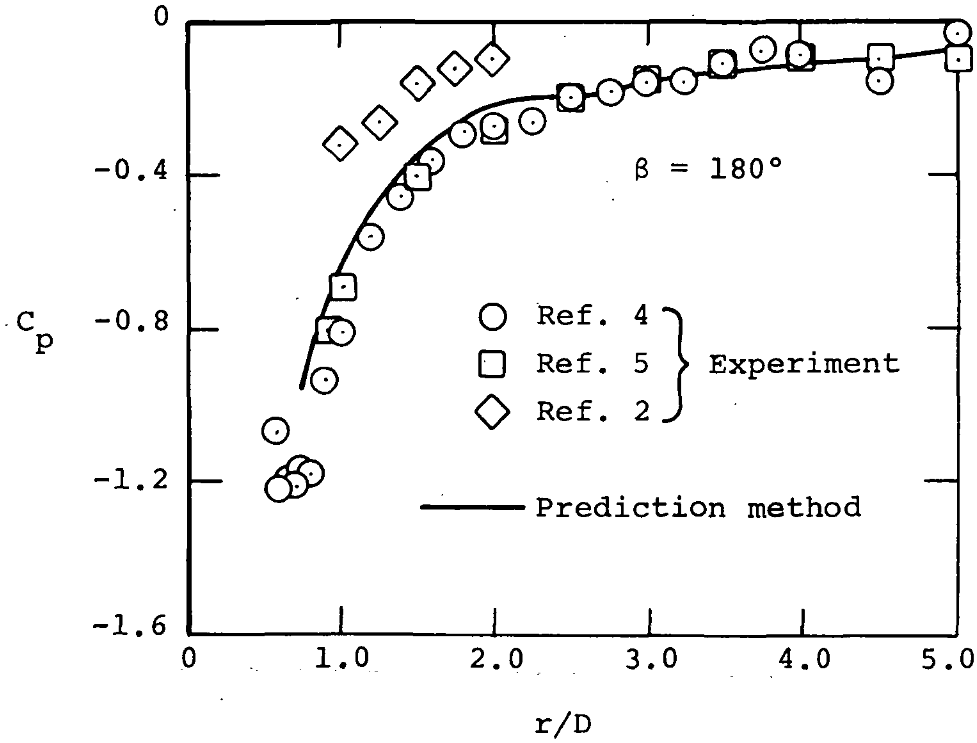

Figure 16.- Concluded.

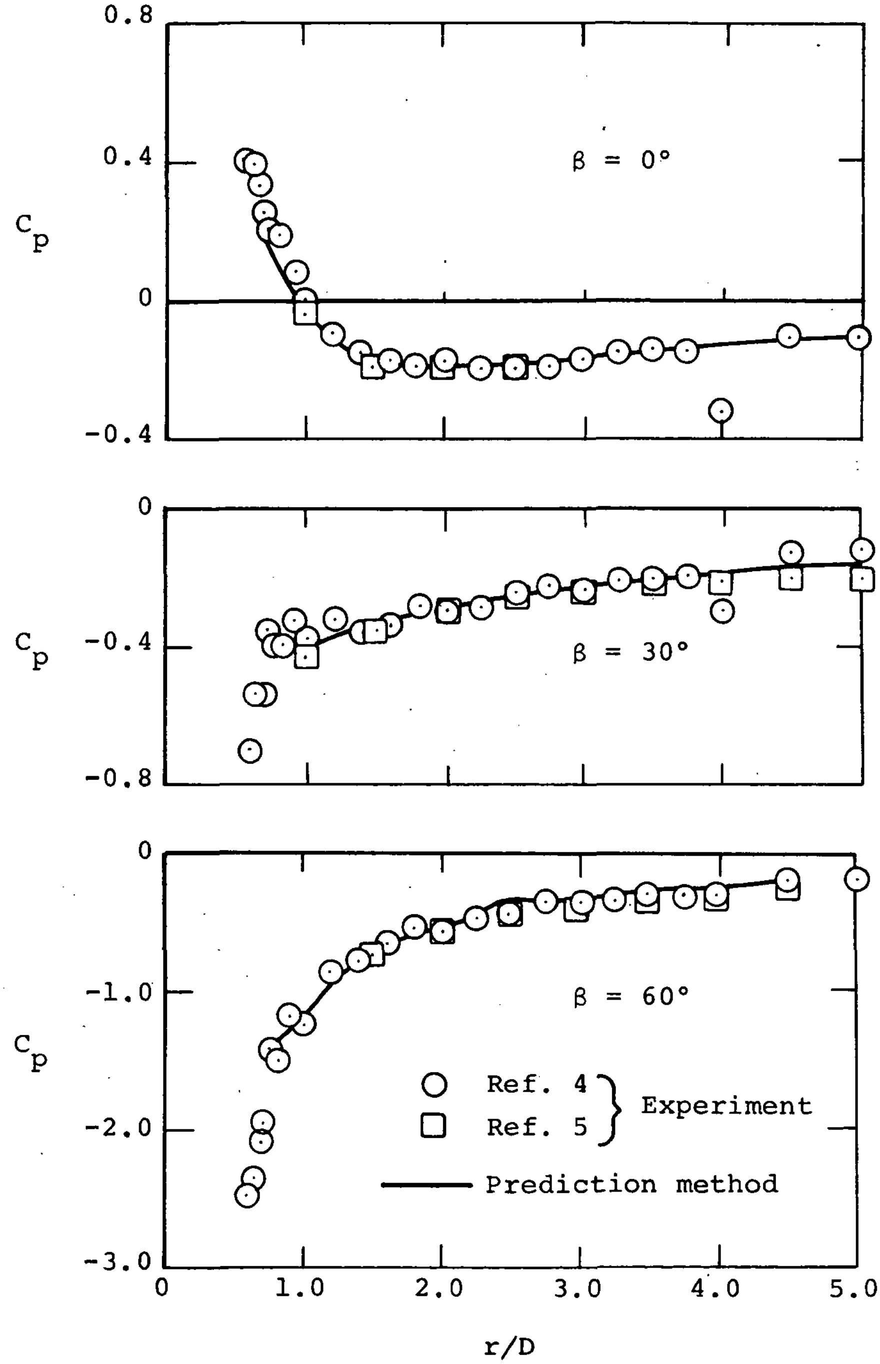

Figure 17.- Comparison of measured and predicted plate pressure distribution, $V_j/V_\infty = 10.0$.

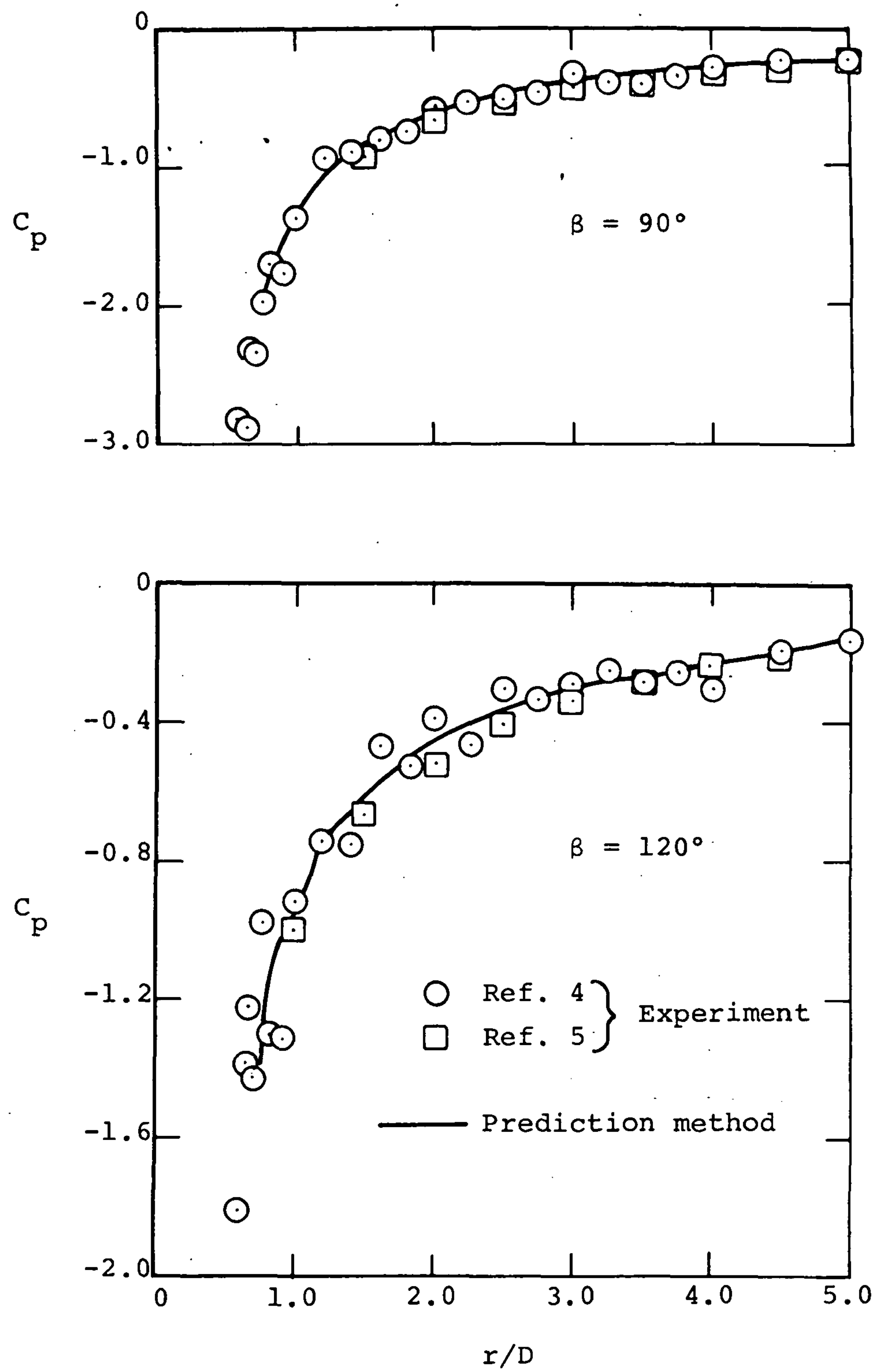

Figure 17.- Continued.

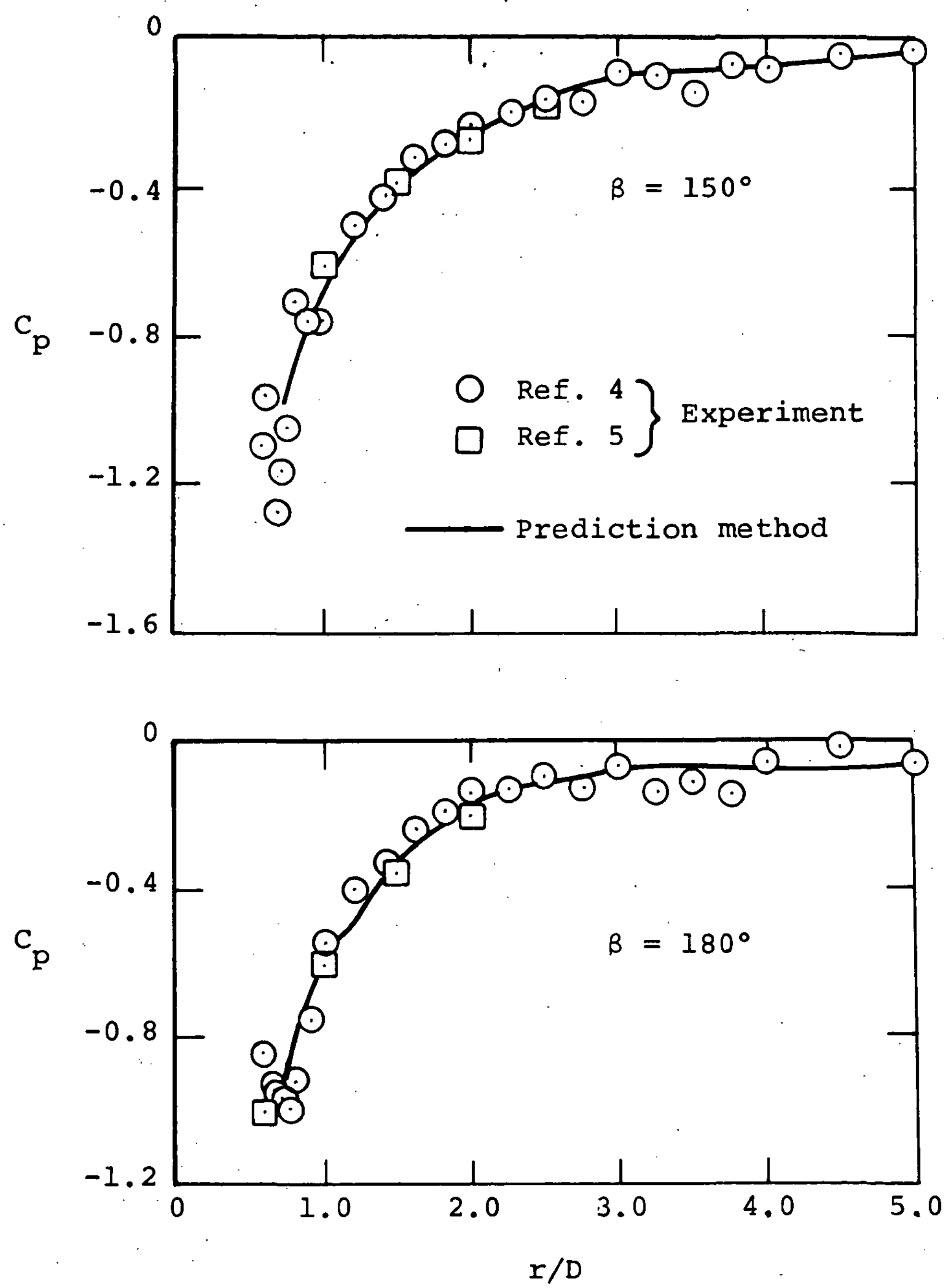

Figure 17.- Concluded.

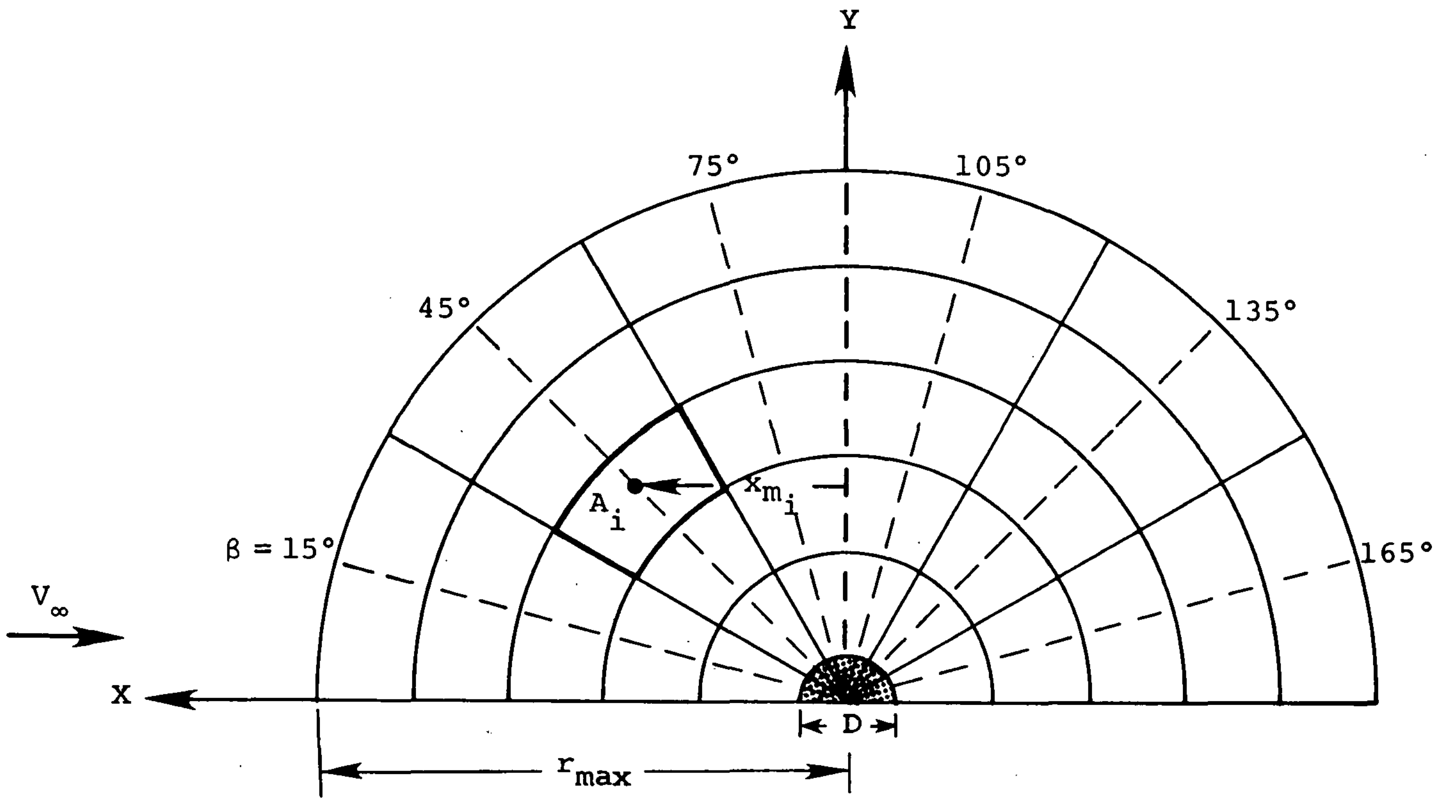

(a) Typical grid layout.

Figure 18.- Finite circular plate.

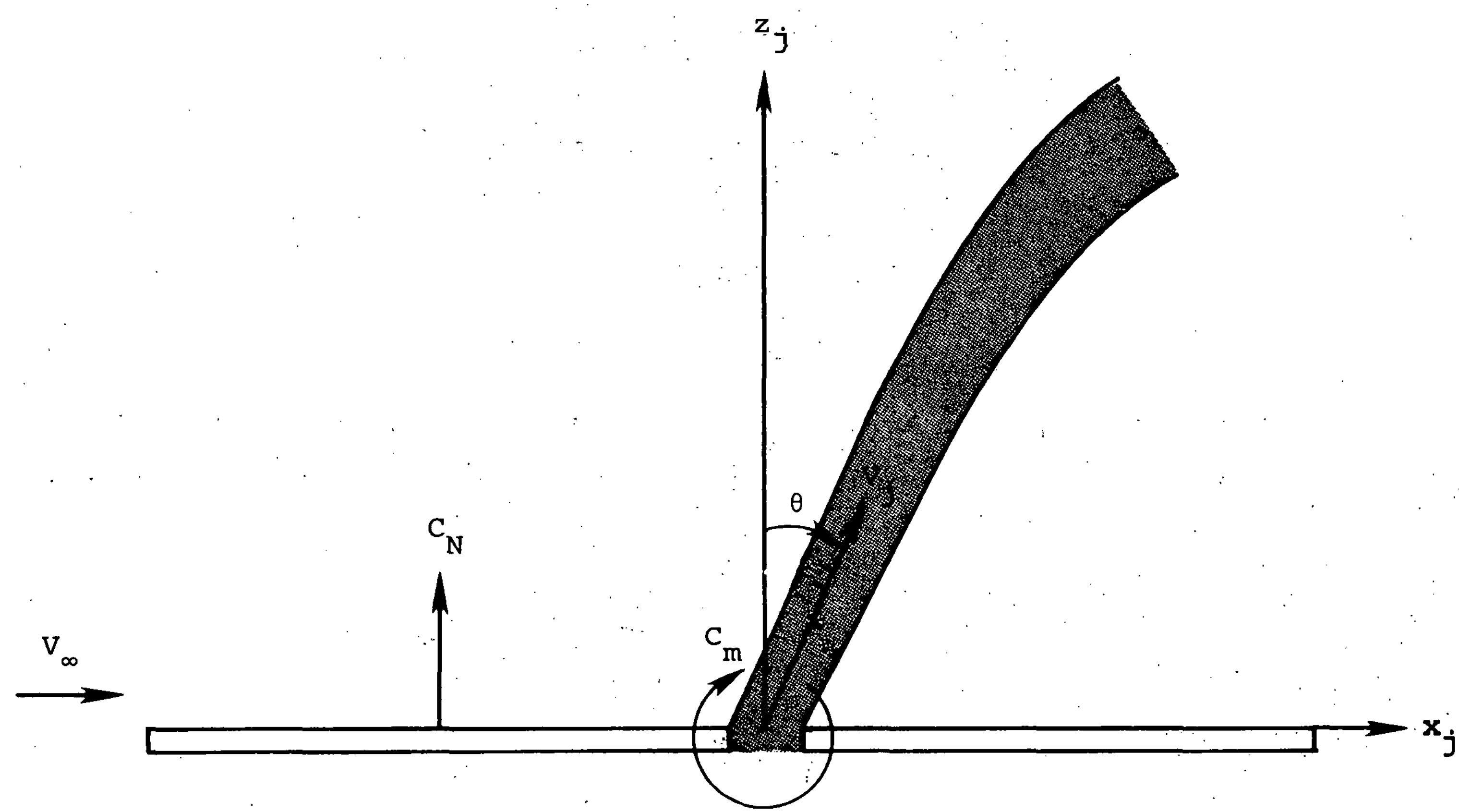

(b) Force and pitching moment nomenclature.

Figure 18.- Concluded.

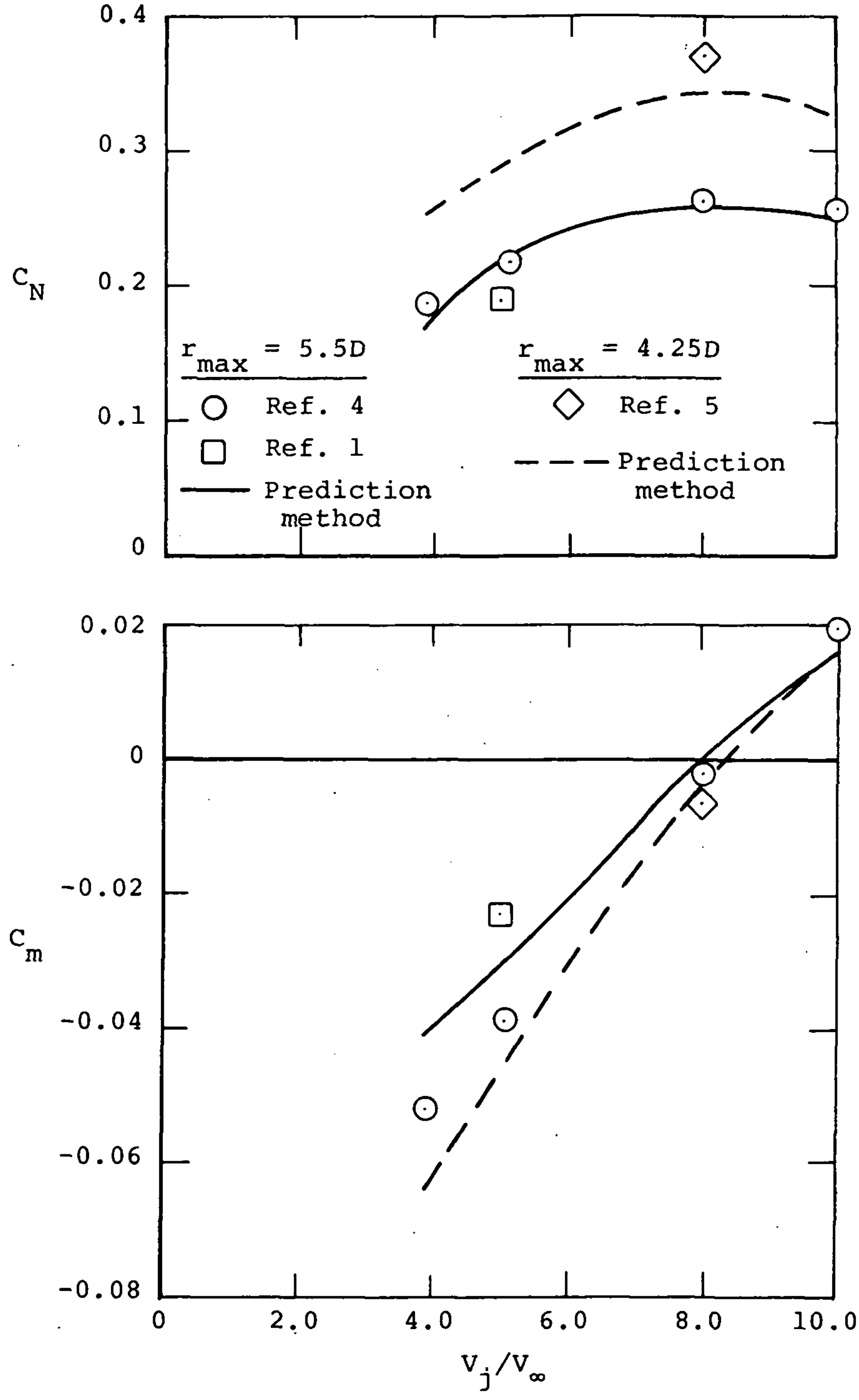

Figure 19.- Comparison of normal force and pitching moment on a plate obtained from measured and predicted pressure distributions.

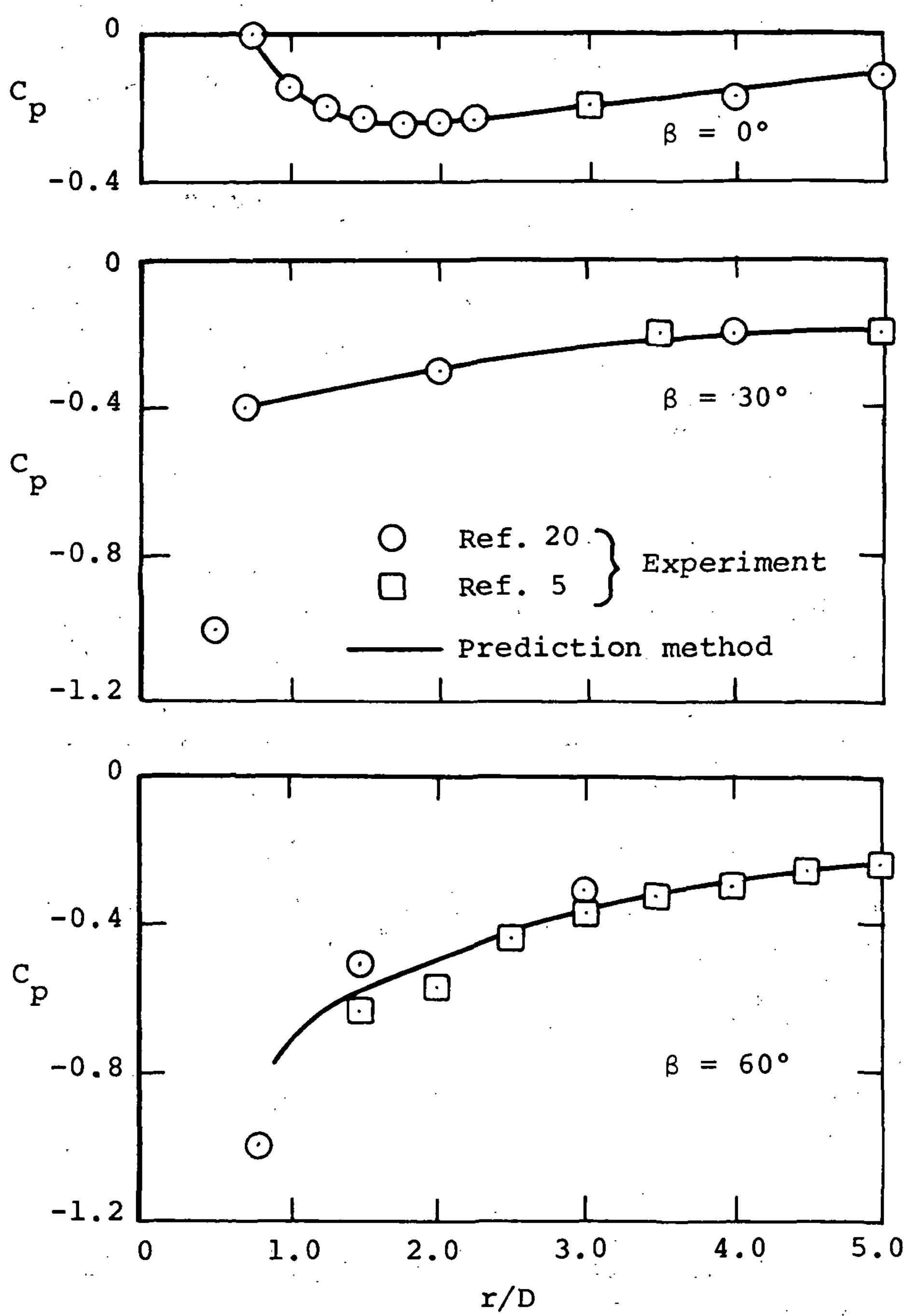

Figure 20.- Comparison of measured and predicted plate pressure distribution, $V_j/V_\infty = 12.0$, $\theta = 0°$.

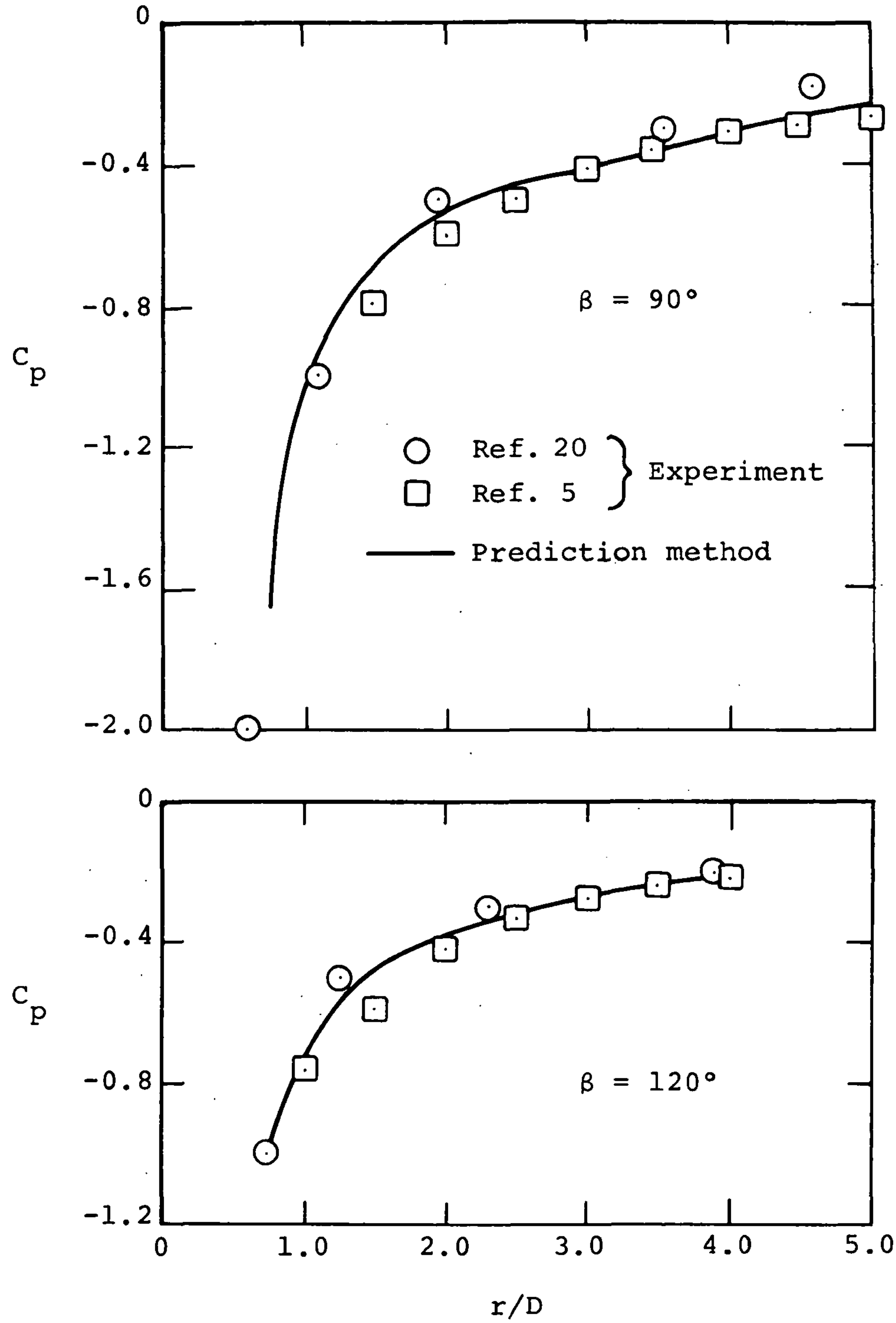

Figure 20.- Continued.

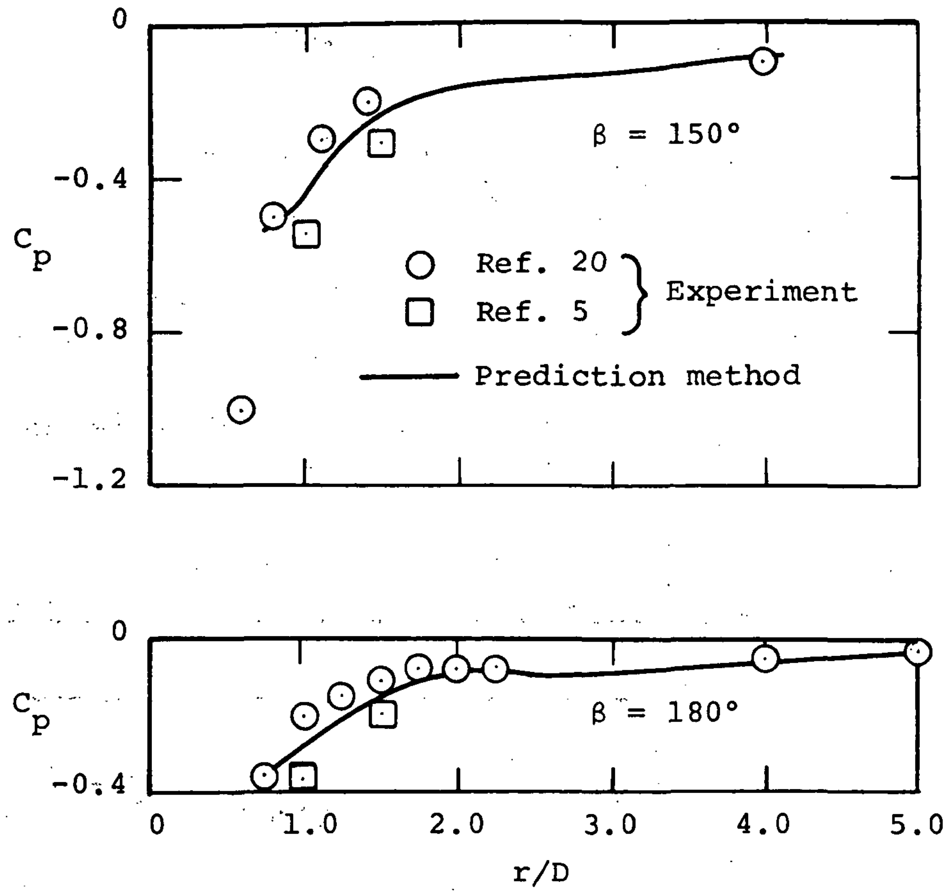

Figure 20.- Concluded.

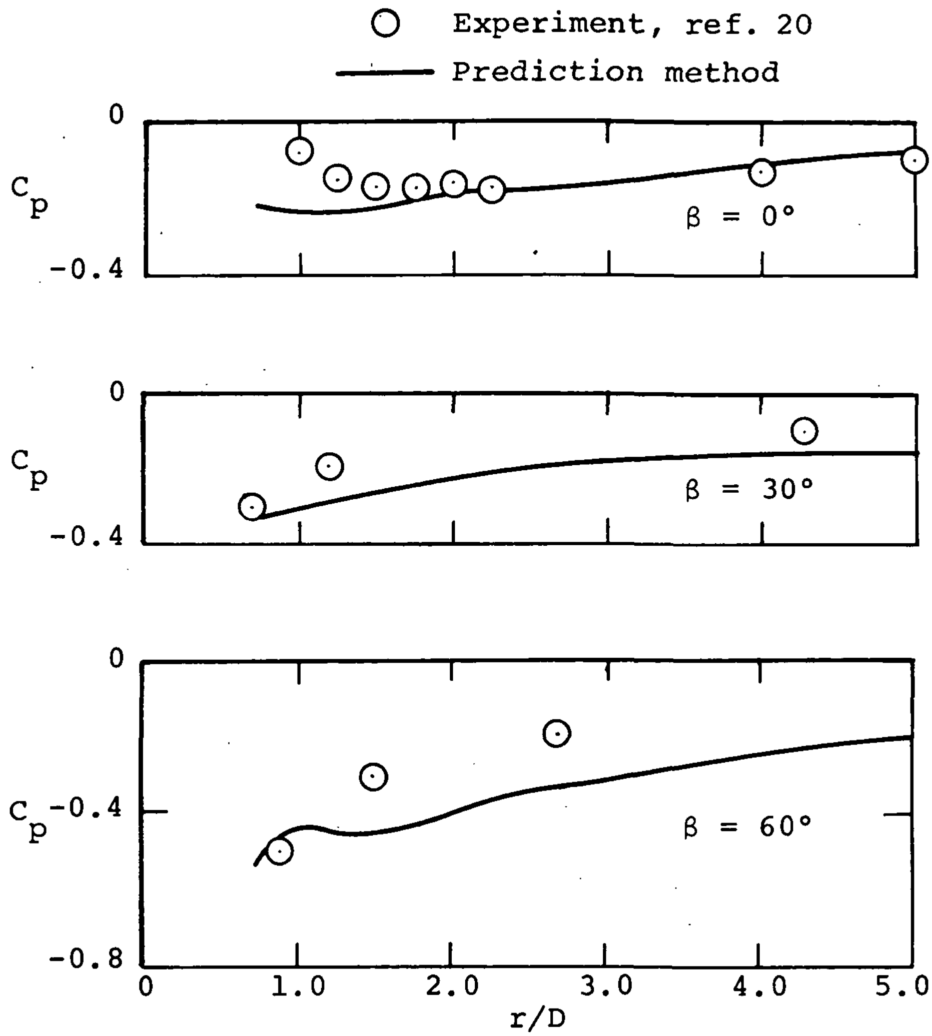

Figure 21.- Comparison of measured and predicted plate pressure distribution, $V_j/V_\infty = 12.0$, $\theta = 30°$.

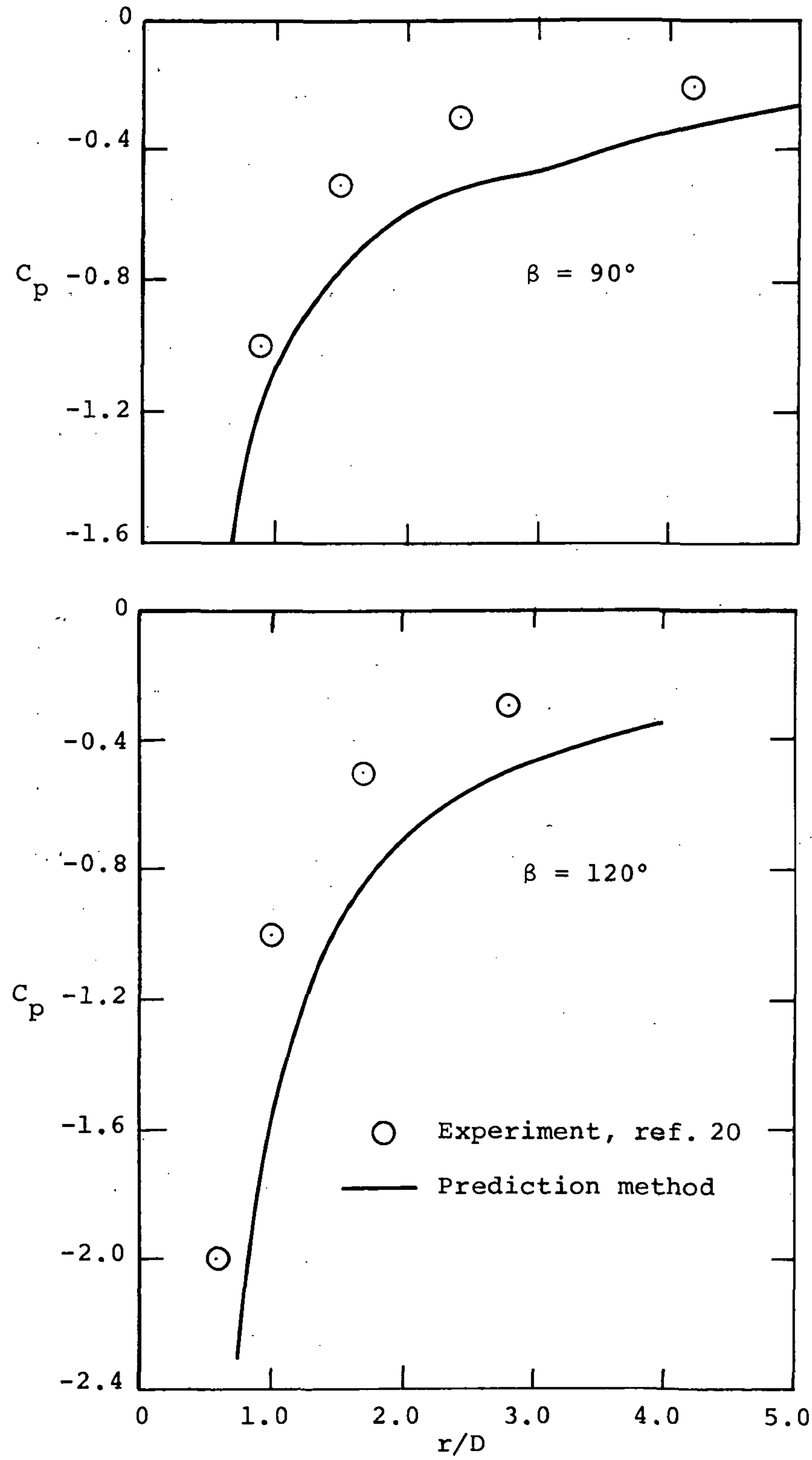

Figure 21.- Continued.

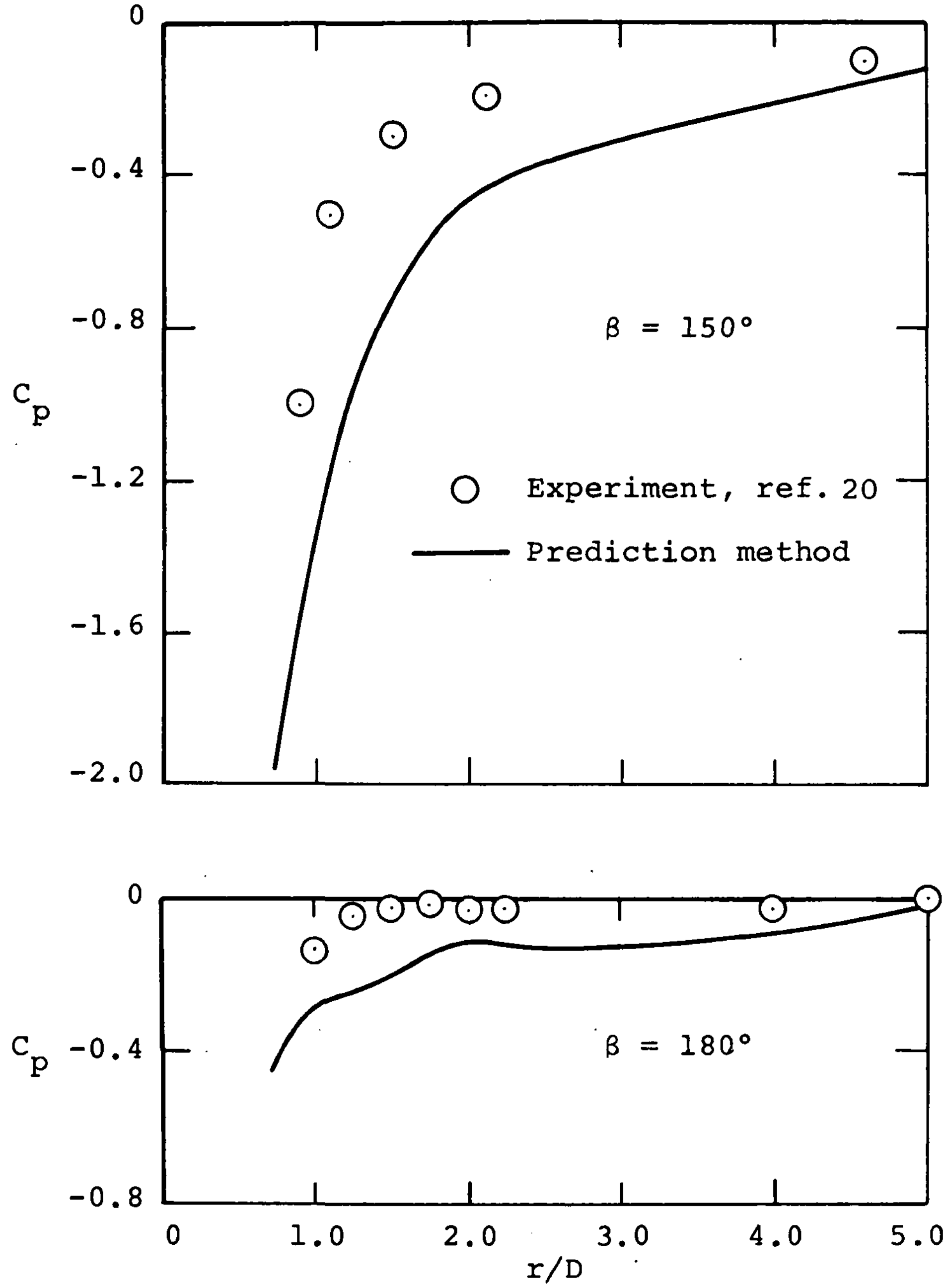

Figure 21.- Concluded.

1. Report No. NASA CR-152,160	2. Government Accession No.	3. Recipient's Catalog No.
4. Title and Subtitle A Correlation Method to Predict the Surface Pressure Distribution on an Infinite Plate from which a Jet is Issuing		5. Report Date May 1978
		6. Performing Organization Code 409/C
7. Author(s) Stanley C. Perkins, Jr. and Michael R. Mendenhall		8. Performing Organization Report No. NEAR TR-160
9. Performing Organization Name and Address Nielsen Engineering & Research, Inc. 510 Clyde Avenue Mountain View, California 94043		10. Work Unit No.
		11. Contract or Grant No. NAS2-9509
12. Sponsoring Agency Name and Address NASA Ames Research Center Moffett Field, California 94035		13. Type of Report and Period Covered Contractor Report
		14. Sponsoring Agency Code

15. Supplementary Notes

Ames Technical Monitors, David G. Koenig and Donald L. Ciffone

16. Abstract

A correlation method to predict pressures induced on an infinite plate by a jet issuing from the plate into a subsonic free stream has been developed. The complete method consists of an analytical method which models the blockage and entrainment properties of the jet and a correlation which accounts for the effects of separation. The method has been developed for jet velocity ratios up to ten and for radial distances up to five diameters from the jet. Correlation curves and data comparisons are presented for jets issuing normally from a flat plate with velocity ratios one to twelve. Also, a list of references which deal with jets in a crossflow is presented in the Appendix.

17. Key Words (Suggested by Author(s)) Subsonic crossflow; Jet in a crossflow; Pressure distribution; V/STOL	18. Distribution Statement Unclassified-Unlimited

19. Security Classif. (of this report) Unclassified	20. Security Classif. (of this page) Unclassified	21. No. of Pages 117	22. Price*

*For sale by the National Technical Information Service, Springfield, Virginia 22161